

é p í t ő a n y a g

A Szilikátipari Tudományos Egyesület lapja

Journal of Silicate Based and Composite Materials

A TARTALOMBÓL:

- Rheology of plasticized polymer solutions
- The effect of VIATOP® plus FEP on the stiffness and low temperature behaviour of hot mix asphalts
- Effect of Additives on the Rheological Properties of Fast Curing Epoxy Resins
- Towards the development of self-compacting no-slump concrete mixtures
- Wettability of particles and its effect on liquid bridges in wet granular materials
- Methods and equipment for the investigation of rheological properties of complex materials like convectional brick clays and ceramic reinforced composites
- Microrheology of Mucin: Tracking Particles and Helicobacter Pylori Bacteria
- Rheology and porosity effect on mechanical properties of zirconia ceramics

2015/4



TELJESKÖRŰ KÍNÁLAT

- Berendezések építőipari nyersanyagok feldolgozására és újrahasznosításra
- Betonkeverő berendezések gyári és kiszállított beton előállítására



GAZDASÁGOS
BERUHÁZÁS

MFL Hungária Kft. | 1103 Budapest, Gergely utca 81/e. | Tel. +36 1 433 2004
mfl@t-online.hu | www.sbm-mp.at



THE EUROPEAN SOCIETY OF RHEOLOGY

Everything for the Rheologist

The European Society of Rheology is open for everyone interested in rheology in all countries of Europe. Rheology is defined as the science of the deformation and flow of matter which means that rheology in some form enters almost every study of material properties. The ESR involves rheologists engaged in both industrial and academic research and development and is therefore a common meeting ground for engineers, physicists, chemists and biologists with a common interest in rheology.

Mission: To promote rheology throughout Europe.

[HTTP://RHEOLOGY-ESR.NET](http://rheology-esr.net)

TARTALOM

- 119** Képlékenyített polimer oldatok reológiája
Saide O. UMEROVA ■ Iryna O. DULINA ■ Andrey V. RAGULYA
- 126** VIATOP® plus FEP adalék hatása az aszfaltok merevségére és viselkedésükre alacsony hőmérsékleten
TÓTH Csaba ■ SOÓS Zoltán
- 132** Adalékok hatása gyors kötésű epoxigyanták reológiai jellemzőire
Youjiang WANG ■ Dildar Ali LAKHO ■ Donggang YAO
- 135** Roskadásmentes öntömörödő betonkeverékek fejlesztése
Hooman HOORNAHAD ■ Eduardus A. B. KOENDERS ■ Klaas van BREUGEL
- 139** Szemcsék nedvesíthetősége és ennek hatása a folyadékhidak kialakulására a nedves szemcsehalmozokban
Hooman HOORNAHAD ■ Eduardus A. B. KOENDERS ■ Klaas van BREUGEL
- 143** Módszerek és berendezések olyan komplex anyagok reológiai vizsgálatára mint a hagyományos téglalaanyagok és a kerámia erősítésű kompozitok
GÖMZE A. László ■ GÖMZE N. Ludmila ■ Sergey N. KULKOV ■ Igor SHABALIN ■ Irena GOTMAN ■ Fernando PEDRAZA ■ Gisèle LECOMTE-NANA ■ Tatiana MAYOROVA ■ KUROVICS Emese ■ HAMZA Alexandra
- 150** A mucin mikroreológiája: részecskék és H. Pylori baktériumok mozgásának követése
Rama BANSIL ■ Joseph HARDCASTLE ■ Maira CONSTANTINO
- 155** Reológiai és porozitási hatások a cirkonkerámiák mechanikai jellemzőire
Sergey N. KULKOV ■ Svetlana P. BUYAKOVA ■ Maria CHATZINIKOLAIDOU ■ István KOCSERHA
- 159** Fázis-kémiai átalakulások termodinamikai modellezése anyagok reológiai tulajdonságainak vizsgálatára
Alexander SLOBODOV ■ Andrey USPENSKIY ■ Ricardas RALYS ■ Dmitry KREMNEV
- 164** Fázis-kémiai összetétel termodinamikai modellezésének és reológiai jellemzőknek használhatósága több komponensű természetes és mesterséges objektumoknál
Alexander SLOBODOV ■ Alexander USPENSKIY ■ Sergey YAVSHITS ■ Alexey MISCHENKO

CONTENT

- 119** Rheology of plasticized polymer solutions
Saide O. UMEROVA ■ Iryna O. DULINA ■ Andrey V. RAGULYA
- 126** The effect of VIATOP® plus FEP on the stiffness and low temperature behaviour of hot mix asphalts
Csaba TÓTH ■ Zoltán SOÓS
- 132** Effect of Additives on the Rheological Properties of Fast Curing Epoxy Resins
Youjiang WANG ■ Dildar Ali LAKHO ■ Donggang YAO
- 135** Towards the development of self-compacting no-slump concrete mixtures
Hooman HOORNAHAD ■ Eduardus A. B. KOENDERS ■ Klaas van BREUGEL
- 139** Wettability of particles and its effect on liquid bridges in wet granular materials
Hooman HOORNAHAD ■ Eduardus A. B. KOENDERS ■ Klaas van BREUGEL
- 143** Methods and equipment for the investigation of rheological properties of complex materials like convectional brick clays and ceramic reinforced composites
László A. GÖMZE ■ Ludmila N. GÖMZE ■ Sergey N. KULKOV ■ Igor SHABALIN ■ Irena GOTMAN ■ Fernando PEDRAZA ■ Gisèle LECOMTE-NANA ■ Tatiana MAYOROVA ■ Emese KUROVICS ■ Alexandra HAMZA
- 150** Microrheology of Mucin: Tracking Particles and Helicobacter Pylori Bacteria
Rama BANSIL ■ Joseph HARDCASTLE ■ Maira CONSTANTINO
- 155** Rheology and porosity effect on mechanical properties of zirconia ceramics
Sergey N. KULKOV ■ Svetlana P. BUYAKOVA ■ Maria CHATZINIKOLAIDOU ■ István KOCSERHA
- 159** Thermodynamic modelling of phase-chemical transformations as the method for study of rheological properties of substances
Alexander SLOBODOV ■ Andrey USPENSKIY ■ Ricardas RALYS ■ Dmitry KREMNEV
- 164** Applicability of thermodynamic modelling of phase-chemical composition and rheological properties for multi-component natural and technological objects
Alexander SLOBODOV ■ Alexander USPENSKIY ■ Sergey YAVSHITS ■ Alexey MISCHENKO

A finomkerámia-, üveg-, cement-, mész-, beton-, tégl- és cserép-, kő- és kavics-, tűzállóanyag-, szigetelőanyag-iparágak szakmai lapja
Scientific journal of ceramics, glass, cement, concrete, clay products, stone and gravel, insulating and fireproof materials and composites

SZERKESZTŐBIZOTTSÁG • EDITORIAL BOARD

Prof. Dr. GÖMZE A. László – elnök/president
Dr. BOROSNYÓI Adorján – főszerkesztő/editor-in-chief
WOJNÁROVITSNÉ Dr. HRAPKA Ilona – örökös
tiszteltbellei felelős szerkesztő/senior editor-in-chief
TÓTH-ASZTALOS Réka – tervezőszervező/design editor

TAGOK • MEMBERS

Prof. Dr. Parvin ALIZADEH, BOCSKAY Balázs,
Prof. Dr. CSÖKE Barnabás, Prof. Dr. Katherine T. FABER,
Prof. Dr. Saverio FIORE, Prof. Dr. David HUI,
Prof. Dr. GÁLOS Miklós, Dr. Viktor GRIBNIAK,
Prof. Dr. Kozo ISHIZAKI, Dr. JÓZSA Zsuzsanna,
KÁRPÁTI László, Dr. KOCSERHA István,
Dr. KOVÁCS Kristóf, Prof. Dr. Sergey N. KULKOV,
MATTYASOVSZKY ZSOLNAY Eszter, Dr. MUCSI Gábor,
Dr. PÁLVÖLGYI Tamás, Dr. RÉVAY Miklós,
Prof. Dr. Tomasz SADOWSKI, Prof. Dr. Tohru SEKINO,
Prof. Dr. David S. SMITH, Prof. Dr. Bojja SREEDHAR,
Prof. Dr. SZÉPVÖLGYI János, Prof. Dr. SZÜCS István

TANÁCSADÓ TESTÜLET • ADVISORY BOARD

FINTA Ferenc, KISS Róbert, Dr. MIZSER János

A folyóiratot referálja • The journal is referred by:



ProQuest



A folyóiratban lektorált cikkek jelennek meg.

All published papers are peer-reviewed.

Kiadó • Publisher: Szilikátipari Tudományos Egyesület (SZTE)

Elnök • President: ASZTALOS István

1034 Budapest, Bécsi út 122-124.

Tel./fax: +36-1/201-9360, E-mail: epitoanyag@szte.org.hu

Tördelőszerkesztő • Layout editor: NÉMETH Hajnalka

Címlapfotó • Cover photo: KÓSA Luca Kornélia

HIRDETÉSI ÁRAK 2015 • ADVERTISING RATES 2015:

B2 borító színes • cover colour	76 000 Ft	304 EUR
B3 borító színes • cover colour	70 000 Ft	280 EUR
B4 borító színes • cover colour	85 000 Ft	340 EUR
1/1 oldal színes • page colour	64 000 Ft	256 EUR
1/1 oldal fekete-fehér • page b&w	32 000 Ft	128 EUR
1/2 oldal színes • page colour	32 000 Ft	128 EUR
1/2 oldal fekete-fehér • page b&w	16 000 Ft	64 EUR
1/4 oldal színes • page colour	16 000 Ft	64 EUR
1/4 oldal fekete-fehér • page b&w	8 000 Ft	32 EUR

Az árak az áfát nem tartalmazzák. • Without VAT.

A hirdetés megrendelő letölthető a folyóirat honlapjáról.

Order-form for advertisement is available on the website of the journal.

AZ SZTE TÁMOGATÓ TAGVÁLLALATAI

SUPPORTING COMPANIES OF SZTE

3B Hungária Kft. • Air Liquide Kft. • Anzo Kft.
Baranya Téglá Kft. • Beériyi Téglaiipari Kft. • Budai Téglá Zrt.
Budapest Kerámia Kft. • Cerlux Kft. • Colas-Északkő Kft.
Electro-Coord Kft. • Fátálylőveg Kft. • G&B Elastomer Kft.
GE Hungary Zrt. • Geoteam Kft. • Guardian Orosháza Kft.
Hunext Kft. • Interkerám Kft. • KK Kavics Beton Kft.
KÓKA Kft. • Kötés Kft. • KTI Kft. • Kvarc-Ásvány Kft.
Lambda Systeme Kft. • Libál Lajos • Lighttech Kft.
Maltha Hungary Kft. • Messer Hungarogáz Kft.
MFL Hungária Kft. • Mineralholding Kft.
MTA KK AKI O-I Manufacturing Magyarország Kft.
OMYA Kft. • Pápateszéri Tégl. Kft. • Perlit-92 Kft. • Q&L Kft.
RATH Hungária Kft. • Rockwool Hungary Kft.
Speciál Bau Kft. • Szema Makó Kft. • SZIKKTI Labor Kft.
WITEG Kőpor Kft. • Zalakerámia Zrt.

WWW.EPITOANYAG.ORG.HU

Online ISSN: 2064-4477 • Print ISSN: 0013-970x
INDEX: 2 52 50 • 67 (2015) 117-168

Editorial note

ADORJÁN BOROSNYÓI • Editor-in-Chief

It is an honour to welcome readers of *Építőanyag – Journal of Silicate based and Composite Materials* and to announce our 2015/4 issue as Special Edition dedicated to **icrmm2**, the 2nd International Conference on Rheology and Modeling of Materials, October 5–9, 2015, Lillafüred, Hungary.



Two years ago **icrmm1**, the 1st International Conference on Rheology and Modeling of Materials was organized in Lillafüred, Hungary, with the participation of more than 150 scientists and researchers arrived from more than 40 countries. The very successful event have demonstrated that rheologists – engineers, geologists, chemists, physicists, mathematicians, biologists, physicians – need to have a possibility to regularly meet each other in the heart of Europe.

Rheology – as a scientific discipline – studies the deformation of bodies under the effect of stresses. In this context bodies are considered generalised and they can be either solids, or fluids, or gases; rheology universally studies the deformation and flow of any matter. Rheology was preceded by theories describing ideal materials like Robert Hooke's ideal elastic solids (Hooke, 1678), Blaise Pascal's inviscid fluids (Pascal, 1663) or Isaac Newton's ideal fluids (Newton, 1687). Real materials are neither ideal solids nor ideal fluids. Real materials usually exhibit both elastic and viscous behaviour and are called viscoelastic. Complicated deformations are formed under mechanical stresses due to the internal structure of real materials and the relationships between stress and strain can not be defined by elastic and viscous constants alone; the behaviour depends on time, direction and intensity of stress or extent of deformation.

Rheology is a relatively young and highly multidisciplinary field and is one of the very few scientific disciplines which appearance can be tied to a precise date: 29 April, 1929. The first committee meeting of The Society of Rheology was organized on 29 April, 1929 at Columbus, Ohio, USA, where the term *rheology* was proposed by Eugene C. Bingham and Markus Reiner to describe “the study of the flow and deformation of all forms of matter”. The term *rheology* was inspired by the aphorism of *Simplicius* (often attributed to *Heraclitus*), πάντα ρεῖ: everything flows. With his own words, Reiner recalls (Reiner, 1964): “Rheology has become a well-known branch of physics, but most typists think it is a misprint for theology” (i.e. the letter *R* and the letter *T* are next to each other on the QWERTY keyboard and rheology is easy to be mistyped as theology). “This seems ridiculous, but there is some relation between rheology and theology, and on this I want to say a few words... Prophetess Deborah, even before Heraclitus, in her famous song after the victory over the Philistines, she sang, “The mountains flowed before the Lord.” ... Deborah knew two things. First, that the mountains flow, as everything flows. But, secondly, that they flowed before the Lord, and not before man, for the simple reason that man in his short lifetime cannot see them flowing, while the time of observation of God is infinite. We may therefore well define as a nondimensional number the Deborah number $D = \text{time of relaxation}/\text{time of observation}$... If your time of observation is very large, or, conversely, if the time of relaxation of the material under

observation is very small, you see the material flowing.” Everything flows if you wait long enough, even solid rock.

The aphorism πάντα ρεῖ also holds a hidden message to challenge the non-professional for unleashing his fantasy. There is a popular worldwide myth about stained glass windows in cathedrals, according to which noticeable change in thickness (=flow) is formed by gravity forces over hundreds of years, and stained glass cathedral windows are thicker at the bottom than the top due to this effect. One famous example is the glass windows of the Cathedral of Chartres in France that are said to have flown since they were produced centuries ago: it is claimed that the glass panes originally had a uniform thickness from top to bottom in mediaeval times, but today the thickness at the top is paper-thin while the pane thickness has more than doubled at the bottom due to the flow induced by gravity. Main reason for this misconception can be most probably attributed to the idea that glass cannot be classed simply as fluid or solid, but rather glass behaves as a liquid or solid under certain conditions of stress, shear rate or time. At room temperature glass has a viscosity about 10^{40} Pa·s. Calculations made by Zanotto and Gupta (1999) have shown that the timescale over which flow of glass might be realized at room temperature is in the range of 10^{23} years, thus is well beyond the estimated age of the Universe (10^{10} years). Theory implies that the dimensional variations of the stained glass windows in cathedrals are not caused by cold flow of glass. An explanation can be speculated in connection with the manufacturing techniques of ancient glass. These techniques produced glass that was inherently not of a uniform thickness, unlike the glass made by the float glass process of today. Ancient window glasses were blown into cylinders that were split and flattened manually. Hence, the pieces were not uniform in thickness and some lower parts could be thicker than the upper parts. It is quite possible that the cathedral window makers installed the cut up windowpanes instinctively with thicker side at the bottom (Zanotto, Gupta, 1999). Professionalism of cathedral window makers - based on their instinct or experience – has given rise to the non-professional urban myth of flow of glass at room temperature, hundreds of years later.

Rheology covers different topics in the development and processing of polymers, ceramics, adhesives, mortars, concretes, asphalts, paints, inks, lubricants, surfactants, emulsions, suspensions, foams, ferrofluids, magneto-rheological materials, molten metals and glasses, cosmetics, pharmaceuticals, foods, dairies and biological systems. Applications of rheology are virtually endless and the topic would - in itself - fill several books. Thus, the Editorial Board of *Építőanyag – Journal of Silicate based and Composite Materials* decided not to give a comprehensive survey in this Special Edition (that would be simply impossible for a journal issue), but to provide a colourful collection of special topics presented at the **icrmm2** conference. Authors represent high rank institutes from different continents and show their most recent theoretical and experimental results.

References

- Hooke, R. J. (1678): De potentia restitutura
 Newton, I. S. (1687): Philosophiae Naturalis Principia Mathematica
 Pascal, B. (1663): Traités de l'équilibre des liqueurs et de la pesanteur de la masse de l'air
 Reiner, M. (1964): The Deborah Number, *Physics Today*, January 1964, p. 62.
 Zanotto, E. D. – Gupta, P. K. (1999): Do cathedral glasses flow?—Additional remarks, *American Journal of Physics*, Vol. 67, No. 3, pp. 260-262.

Source of illustration – <https://inspirationlog.files.wordpress.com>

Rheology of plasticized polymer solutions

SAIDE O. UMEROVA ■ Frantsevich Institute for Problems of Materials Science of NASU
 ■ SaideshaShine@mail.ru

IRYNA O. DULINA ■ Frantsevich Institute for Problems of Materials Science of NASU ■ i_risha@online.ua

ANDREY V. RAGULYA ■ Frantsevich Institute for Problems of Materials Science of NASU
 ■ ragulya@ipms.kiev.ua

Érkezett: 2015. 07. 08. ■ Received: 08. 07. 2015. ■ <http://dx.doi.org/10.14382/epitoanyag-jsbcm.2015.19>

Abstract

This paper is about rheological properties of plasticized polymer solutions with different concentration of plasticizer. It was established that the investigated polymer solutions were three-dimensionally structured systems which were shear thickened at low shear rates and maintained the thixotropic structural state under high shear rates. However, addition of different amount of plasticizer had an ambiguous influence on rheology of solutions and led to formation of transient polymer network with a complicated character of structuration because of the features of interaction in the polymer - plasticizer system. It was found that the plasticization results in changing of EC molecules conformation and simultaneous breaking of the polymer continuity due to DBP adsorption on EC macromolecule. Herewith, the formation of smaller crystallites took place. Besides, the investigated solutions showed causal link between structural states.

Keywords: rheology, polymer, rheopexy, pseudoplasticity, thixotropy

Kulcsszavak: reológia, polimer, reopexia, pszeudoképlékenység, tixotrópia

Saide Oleksandrivna UMEROVA
 postgraduate student. Leading engineer
 of Department of Physics, Chemistry and
 Technology of Nanotextured Ceramics and
 Nanocomposite Materials of Frantsevich Institute
 for Problems of Materials Science of NASU;

Iryna Oleksiivna DULINA
 junior researcher of department of Physics,
 Chemistry and Technology of Nanotextured
 Ceramics and Nanocomposite Materials of
 Frantsevich Institute for Problems of Materials
 Science of NASU

Andrey Vladimirovich RAGULYA
 doctor of technical sciences, professor,
 corresponding member of NASU, Deputy Director
 Frantsevich Institute for Problems of Materials
 Science of NASU, Head of Department of Physics,
 Chemistry and Technology of Nanotextured
 Ceramics and Nanocomposite Materials of
 Frantsevich Institute for Problems of Materials
 Science of NASU

1. Introduction

Rheological behavior of concentrated suspensions is an important area of research because it provides rich information, concerning flow and storage of relevant materials under operation conditions. There are many publications focusing on rheology of polymer concentrated suspensions filled with metal oxide powders of various particle diameters. The rheological properties depend on the solid phase concentration [1-3], particle size [2, 4-6], concentration and molecular weight of polymer [1-3, 5-7] and also interaction between particles, solvent and polymer molecules [2, 5, 9]. Because of rapid development of microelectronics, the suspensions based on nanopowders represent the most promising objects for rheological investigations. Herewith, nanosized particles allow obtaining green ceramic layers with thickness of 700 to 800 nm and surface parameter Ra commensurable with size of nanoparticle [10].

It is known that screen printing pastes based on micron powders are generally required to be shear thinning, thixotropic over definite time scale and shear rate, stable for screen/shelf-life and low solvent evaporation [11-13]. Therefore, terpeneol [14-21] and its derivatives [17, 20, 22-25, 26-29] are used as a solvent, ethylcellulose as an organic binder [14, 15-21, 30-42] because of their ability to form thixotropic systems with suspensions of particles of various origination [43]. However, there is almost no information about rheology of ethyl cellulose solutions in terpeneol with the exception of [44]. In turn, it is the main factor that reflects structural features of polymer and determines degree of interaction with surface of solid particles.

In this work, the dependence of the rheological properties of ethyl cellulose (EC) solutions in terpeneol (Terp) on plasticizer dibutyl phthalate (DBP) content has been studied to improve elastic properties of polymer, pastes and films based on them [45-53]. In general, the plasticization leads to decreasing the glass transition temperature, fluidity and improving the

mechanical properties due to reduced interaction between macromolecules and mobility of enhanced segments [54-58]. Normally, plasticization implies great change of structural-mechanical properties [55, 58, 59] due to interaction features in polymer - plasticizer system. The polymer macromolecule conformation and flow character of the appropriate solution are changing. Plasticizer influence, however, is not limited by rearrangement inside the EC molecule. EC is a rigid-chain polymer peculiar to polymorphism [60-62] – it forms individual crystallites in the form of packed antiparallel separate segments of macromolecule [63-65]. According to that, the DBP concentration should affect the polymer crystallization rate due to molecule re-conformation.

Therefore, this paper is about the features of viscosity and rheological behavior in the EC-DBP polymer systems depending on DBP concentration.

2. Materials and methods

Investigated solutions were prepared under heating and permanent stirring conditions. Terpeneol was used as a solvent (mixture of α - and β -terpeneol isomers, Merck GmbH) forethyl cellulose (10 cP, Merck GmbH) as an organic binder and dibutyl phthalate (Merck GmbH) as a plasticizer.

The rheological tests of the solutions has been carried out using rotary rheometer Rheotest RN4.1, Medingen at shear stresses from 1 to 1000 Pa and gap between coaxial cylinders of 1.48 mm. All measurements were carried out at $20 \pm 0.5^\circ\text{C}$. Herewith, the variable was DBP concentration in the solutions (changing from 0 to 40 m%).

Thixotropy and rheopexy degrees were determined from the hysteresis loop areas between up- and down-curves. In turn, the hysteresis loop area has a dimensionality of energy, correlated to sheared volume and determines the value of energy consumed for disrupting of thixotropic (rheopexic) structure [66].

A criterion of equilibrium degree of structure destruction (EDSD) for effective viscosity is determined as follows:

$$\text{EDSD} = \frac{\eta_{\text{max}} - \eta_{\tau}}{\eta_{\text{max}} - \eta_{\infty}}$$

where η_{τ} – is the effective viscosity at given shear stress; η_{max} – is a maximal viscosity corresponding to nonvolatile initial structure; η_{∞} – is the less viscosity, corresponding to breaking point [67]. When $\text{EDSD} < 1$ the recovery processes prevail destruction processes and vice-versa when $\text{EDSD} > 1$.

Dilatancy degree D is characterized by the strength of sheared initial structure [68] and determined as:

$$D = \frac{\eta_{\text{max}} - \eta_{\tau}}{\eta_{\tau}}$$

where η_{max} – is the maximal viscosity corresponding to nonvolatile initial structure; η_{τ} – is the effective viscosity at given shear stress.

3. Results and discussion

3.1 Rheology of initial polymer solution EC+Terp

Fig. 1 shows viscosity profiles of EC+Terp solution PP1. Significant difference between up-curve and down-curve suggests PP1 as structured polymer system with complicated flow due to the presence of two hysteresis loops. According to the hysteresis loop in Fig. 1 a rheopexic structure is undergone destruction at shear stresses 0.1 – 407 Pa. Further shearing has led to pseudoplastic flow region reflected in superposition of up-curve and down-curve. Above 483 Pa the system becomes thixotropic. Herewith, the thixotropy degree T is almost equal to the rheopexy degree R (Table 1). In turn, such a structural transition could be explained as follows. It is known that polymer solution represents three-dimension amorphous-crystalline system with high elastic properties [66, 69-71]. But individual molecules, their segments and microfibrils look spherical-shape coils and are in Brownian motion. When the system is undergone to low shearing, the elastic deformation of the initial network takes place: the coils partially overlap and form molecular linkage. This process is manifested in shear thickening region on viscosity profile (Fig. 1) and corresponds to dilatant properties of the system. Thus, the shear rate region where the viscosity increases is named an interval of structure reinforcement and formation; and V_d value corresponds to yield stress of initial structure. Herewith, the system shears like individual unit. According to the flow curves (Fig. 1), the beginning of initial structure damage is expressed in the rheopexic hysteresis loop. Further shearing above V_d led to pseudoplastic flow region due to disrupting of cross links and transition to the regime of layered flow [72]. In the pseudoplastic region, the system is in equilibrium state because of balance between recovery and destruction processes. Further increased shear deformation leads to difference in shear rates between longitudinal molecular layers and the regions of intermolecular bonds appear. Co-existing of molecular associates with multiple bonds which can deform elastically so that the instantaneous local bonding is possible. Besides viscosity decreasing takes place due to thixotropy.

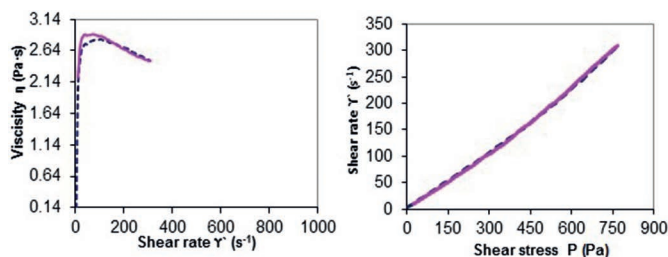


Fig. 1 Viscosity profiles and flow curves of PP1 sample
1. ábra Vízkozitási profilok és folyási görbék a PP1 jelű mintánál

3.2 Rheology of plasticized polymer solutions

In general, different concentration of DBP has an ambiguous influence on rheological properties of plasticized solutions and leads to various character of structuration. It was found that all solutions have thixotropic structural state and were shear thickened at low shear rates (Table 1).

Addition of 3.75, 5, 8.75, 17.5, 18.75, 20.8, 22.5, 25 and 30 m% of DBP resulted information of system structuring similarly to PP1. Fig. 2 shows that the solutions PP3, PP4, PP6, PP11, PP12, PP14, PP16, PP17 and PP18 were successively in three structural states – rheopexic, pseudoplastic and thixotropic. The presence of plasticizer has led to viscosity η_r decreasing. At the same time, for the sample PP14, increase of the viscosity value from 2.11 to 2.13 Pa·s was observed. Moreover, the DBP gives the V_d mean value of 25 – 30 s^{-1} (Table 1). It was also found that for the plasticized solutions with three structural states, the strength can be determined by thixotropy degree (Fig. 3). The increasing of T from 0.000001 to 0.0016 MPa/s almost does not affect the systems strength but further T rising to 0.006 MPa/s has led to abrupt lowering of strength and decreasing of viscosity η_r almost by four times (PP16, 22.5 m% of DBP).

Discussed structural features could be explained as follows. The polymer systems with three structural states are disrupted thixotropic after passing through the previous states because of lower linearity and bigger size of polymer molecule and its similarity to a coil. Therefore, for the rheopexic and pseudoplastic states the orientation and layer-wise structural elements appear to be transformed to the thixotropic state.

It was established that addition of 2.5, 10, 11.25, 12.5, 20, 21.7 and 40 m% of DBP resulted in thixotropic solutions (Fig. 4). The decrease of viscosity η_r was observed as well. However, the presence of 10 m% of plasticizer (PP7) increases viscosity η_r from 2.11 up to 2.20 Pa·s. In general, the plasticizing leads to V_d value growth in average 20 – 25 s^{-1} (Table 1). This structural state could be explained as follows. The thixotropy phenomenon means disrupting of initial three-dimensional network structure under increased shearing accompanied with viscosity decrease for entire range of applied shear rates [66]. In the case of PP2, PP7, PP8, PP9, PP13, PP15 and PP19 solutions, the disrupting of initial structure begins from V_d shear rate: i.e. the initial three-dimensional structure after hardening within shear thickening region followed by two-dimensional layering in the Newtonian flow region ΔV_n , gradually transforms to the one-dimensional structure. The absence of rheopexy and pseudoplasticity can be explained by polymer texture originating from linearity of EC macromolecule adsorbing the DBP. Thus, the orientation of initial layered structure takes place due to shearing.

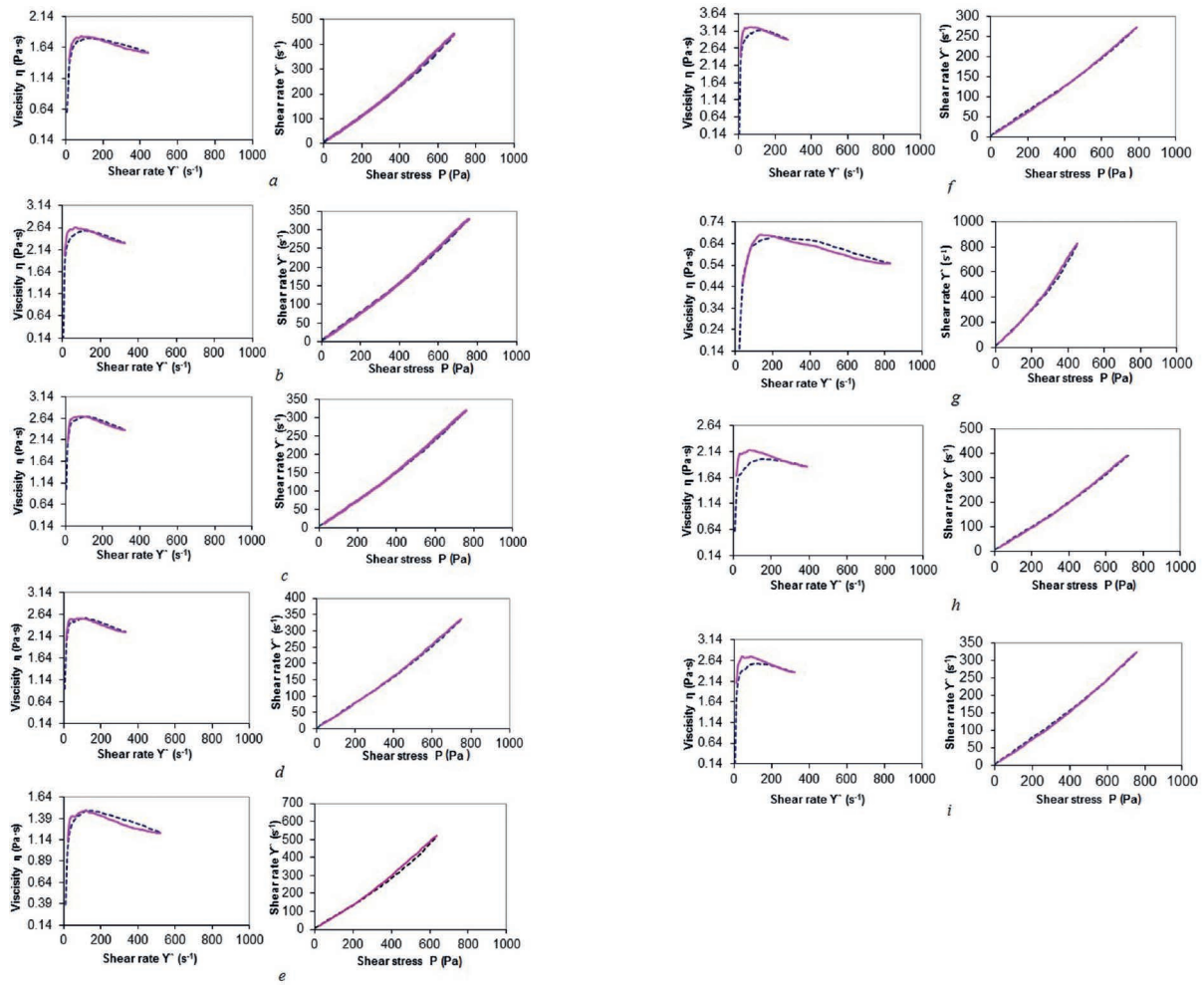


Fig. 2 Viscosity profiles and flow curves of plasticized solutions with three structural states (rheopectic, pseudoplastic and thixotropic)
 2. ábra Viskozitási profilok és folyási görbék a képlékenyített oldatok három szerkezeti állapotára vonatkozóan (reopexikus, pszeudoplasztikus és tixotróp)

Solution	DBP content, wt. %	Viscosity η_t , Pa·s	Strenght stress, Pa	Dilatent flow Vd, s ⁻¹	Maximal viscosity η_{max} , Pa·c	Newtonian flow end Vn_t , s ⁻¹	Length of Newtonian region, ΔVn , s ⁻¹	Thixotropy degree T, MPa/s	Dilatancy degree R, r.u.	Rheoexy degree R, MPa/s	EDSD, r.u.	Pseudoplastic flow start, Pa
PP1	0	2.11	766	78	2.81	108	30	0.001	0.33	0.001	2.12	407
PP2	2.5	1.44	694	108	1.96	129	21	0.006	0.36	0	1.58	0
PP3	3.75	1.33	686	117	1.79	139	22	0.003	0.35	0.001	2.00	305
PP4	5	1.83	753	109	2.58	130	21	0.001	0.41	0.001	2.68	363
PP5	7.5	1.53	717	121	2.12	148	28	0.004	0.39	0	2.19	25
PP6	8.75	2.07	759	106	2.68	144	38	0.002	0.29	0.000	2.03	242
PP7	10	2.20	784	103	3.19	117	14	0.004	0.45	0	2.54	0
PP8	11.25	1.05	595	116	1.40	130	14	0.012	0.33	0	0.92	0
PP9	12.5	1.29	649	99	1.68	123	24	0.011	0.30	0	1.05	0
PP10	15	1.46	732	172	2.18	189	17	0.000	0.49	0.003	4.50	0
PP11	17.5	1.91	750	86	2.54	127	41	0	0.33	0.000	2.17	261
PP12	18.75	1.08	636	136	1.46	162	26	0.006	0.35	0.000	1.65	164
PP13	20	1.59	709	108	2.15	127	19	0.010	0.35	0	1.40	0
PP14	20.8	2.13	789	130	3.18	0	0	0.001	0.49	0.001	3.75	435
PP15	21.7	1.05	684	100	1.92	132	33	0.010	0.83	0	2.35	0
PP16	22.5	0.46	453	198	0.67	0	0	0.006	0.48	0.000	1.75	134
PP17	25	1.40	718	146	2.00	165	19	0.000	0.43	0.004	4.00	538
PP18	30	1.82	757	109	2.57	133	25	0.000	0.41	0.002	3.41	535
PP19	40	1.88	744	77	2.53	110	33	0.004	0.35	0	1.86	0

Table 1 Composition and rheological properties of two- and three-component polymer solutions
 1. táblázat Két- és háromkomponensű polimer oldatok összetétele és reológiai jellemzői

The solution PP5 (7.5 m% of DBP) was the polymer system with two structural states: in the range of shear strain of 25 – 173 Pa the pseudoplastic flow has been observed and further shearing led the system to transform into thixotropic one (Fig. 5). In this case the plasticizer addition also led to viscosity η_r decreasing from 2.11 to 1.53 Pa·s and Vd increasing up to 121 s⁻¹ (Table 1).

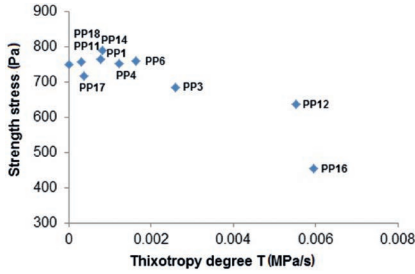


Fig. 3 Strength dependence of thixotropy degree for plasticized solutions with three structural states (rheopexic, pseudoplastic and thixotropic)
 3. ábra Szilárdság függése a tixotrópia fokától a képlékenyített oldatok három szerkezeti állapotára vonatkozóan (reopexikus, pszeudoplasztikus és tixotróp)

Addition of 15 m% of DBP (PP10) corresponds to formation of two structural states in the system. In the shear stress range 25 – 520 Pa the solution was rheopexic but the further shearing up to 732 Pa forced the systems transform into thixotropic one and abide the pseudoplastic structural state (Fig. 6). The viscosity η_r decreasing from 2.11 to 1.46 Pa·s and Vd increasing from 78 to 172 s⁻¹ were observed (Table 1).

Understanding of whether the plasticizer provides one or several structural states during shearing needs to establish what the dissolved polymer is. It is known that polymer chains have some flexibility because of which macromolecules are folded [55, 73]. Thus, polymer has loosen structure with large intermolecular voids (Fig. 7, 1st stage). On the first stage of dissolving the swelling of polymer takes place – solvent molecules diffuse into the polymer and fill the intermolecular voids. Further increasing of solvent volume leads to macromolecules moving apart because of changed gyration radius and distance between the centers of mass. Herewith, the continuity of polymer body is retained. However, an intensification of swelling leads to appearance of antiparallel separate segments of macromolecule referred as crystallites [74]. At the same time the crystallites exist in large quantities and alternating with amorphous regions form the center of elementary fibril [54] (Fig. 7, 3rd stage). The external part of elementary fibril is paracrystalline zone with large surface energy. Thus, elementary fibrils are prone to lateral aggregation with formation of fibrils (Fig. 7, 4th stage). But further stirring and, therefore, exceeding the optimal swelling time results in destruction of polymer continuity and molecules begin to tear off passing into the solution.

However, if plasticizer would be added before the final transition of polymer to the solution, the molecule conformation changes simultaneously with segments moving apart due to DBP adsorption on EC molecule [58] (Fig. 8, 2nd stage). Herewith the smaller crystallites are formed because of reducing the number of antiparallel macromolecule segments. Thus, the achieved plasticized solution will be predominantly

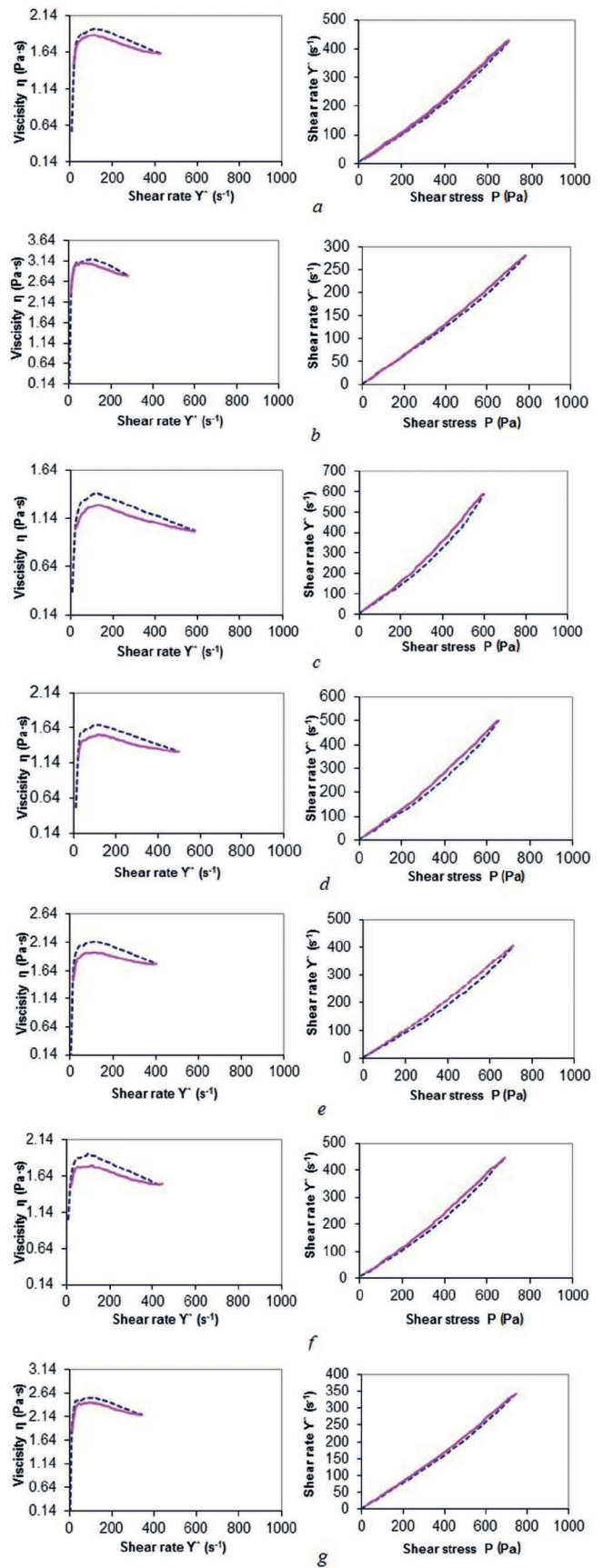


Fig. 4 Viscosity profiles and flow curves of plasticized solutions with thixotropic structural state
 4. ábra Viskozitási profilok és folyási görbék a képlékenyített oldatok tixotróp szerkezeti állapotára vonatkozóan

amorphous system with some concentration of crystallites. But plasticizer addition does not exclude the possibility of EC macromolecule disrupting to smaller parts (Fig. 8, 3rd stage) on dissolving. The EC macromolecule has so-called weak points (authors of [55] assume the presence of leisure chains without hemiacetal bond $C_{(1)} \rightarrow C_{(5)}$ together with closed pyranose cycles).

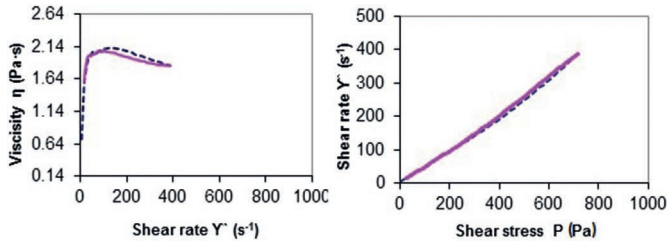


Fig. 5 Viscosity profile and flow curves of plasticized solution PP5 with pseudoplastic and thixotropic structural states

5. ábra Viskozitási profil és folyási görbék a PP5 jelű képlékenyített oldat pszeudoplasztikus és tixotróp szerkezeti állapotára vonatkozóan

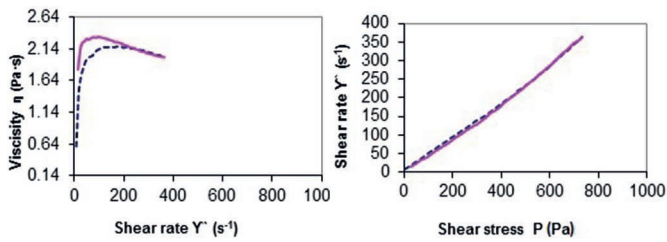


Fig. 6 Viscosity profile and flow curves of plasticized solution PP10 with rheopectic and thixotropic structural states

6. ábra Viskozitási profil és folyási görbék a PP10 jelű képlékenyített oldat reoepexikus és tixotróp szerkezeti állapotára vonatkozóan

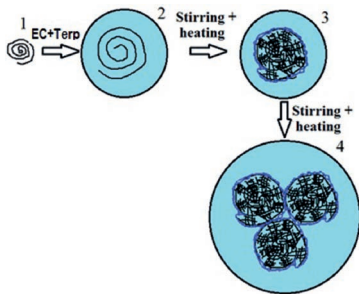


Fig. 7 Stages of interaction in the initial solution EC+Terp

7. ábra A kölcsönhatások szakaszai a kezdeti EC+Terp oldatban

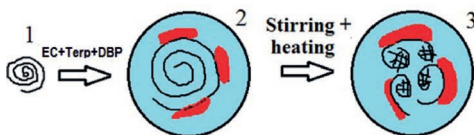


Fig. 8 Stages of interaction in plasticized solution EC+Terp+DBP

8. ábra A kölcsönhatások szakaszai a képlékenyített EC+Terp+DBP oldatban

So, plasticizer addition leads to formation of three-dimensional structure with certain physical-mechanical properties as a result of plasticized EC macromolecule conformation. In general, the specific change of some rheological characteristics is comprehensive. In particular, V_d increases and η_r decreases that is entirely consistent with features of structure formation during plasticizing. Formed small crystallites affect as particulate-reinforcing phase. The viscosity η_r decreases due

to lowering of strength stress of structure (Fig. 9). However, for PP16 (22.5 m% of DBP) the viscosity η_r decreases in almost 4 times because of the lowest strength value and possible bimodal distribution of crystallites [75].

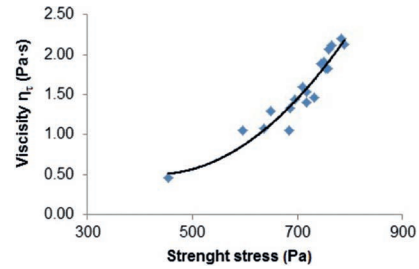


Fig. 9 Viscosity η_r dependence on strength

9. ábra Viskozitás η_r szilárdsághoz viszonyított függése

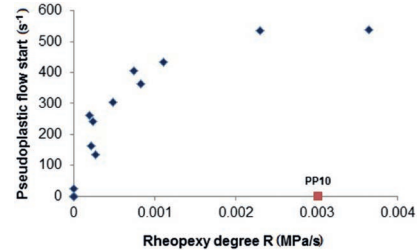


Fig. 10 Rheopecty degree versus pseudoplastic flow start

10. ábra Reoepexikusság foka és pszeudoplasztikus folyás kezdete

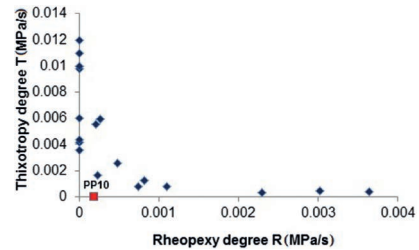


Fig. 11 Rheopecty degree versus thixotropy degree

11. ábra Reoepexikusság foka és tixotrópia foka

It was established that the investigated solutions demonstrate causal link between structural states formed. In particular, the rheopecty degree R determines the start of pseudoplastic flow and thixotropy degree T . Fig. 10 shows that the R increasing from 0 to 0.0015 MPa/s leads to pseudoplastic flow start at higher shear rates ($\sim 500 \text{ s}^{-1}$). But further increase in R does not effect on system transforming into two-dimensional state. Such a tendency was observed almost for all solutions (the PP10 was exception only because of absence of pseudoplastic flow region). In turn, the R value grows up to 0.0015 Mpa/s and leads to abrupt decrease in T . Further increase in R does not affect the system transforming into one-dimensional state. The only exception concerns the PP10 similarly to dependence shown in Fig. 10. In both cases, the PP10 exception can be explained as follows. Due to the fact that the initial structure of all the solutions is disrupted and restored under increased shear rates, it seems to be true that the thixotropy degree T decreases with increasing of the rheopecty degree R (Fig. 11). Besides, Table 1 shows that for the PP10 the EDS criteria value is the highest one. Thus, in the PP10 case the destruction processes dominate over recovery processes without equilibrium state.

4. Conclusions

The investigated polymer solutions were three-dimensional structured systems which were shear thickened at low shear rates and maintained the thixotropic structural state under high shear rates. It was found that the initial polymer solution EC+Terp was successively in three structural states: rheopexic, pseudoplastic and thixotropic. Herewith, the R was almost equal to T because of equal recovery and destruction processes. However, addition of different amount of plasticizer had an ambiguous influence on rheology of solutions and led to formation of transient polymer network with a complicated character of structuration because of the features of interaction in the polymer - plasticizer system. It was established that the plasticization results in changing of EC molecules conformation and simultaneous breaking of the polymer continuity due to DBP adsorption on EC macromolecule. Herewith, the formation of smaller crystallites took place. Besides, the investigated solutions showed causal link between structural states. In particular, the rheopexy degree R determines pseudoplastic flow start and the thixotropy degree T.

5. Acknowledgment

Authors are grateful to the State Agency on Science Innovations and Informatization of Ukraine for a financial support for the project NN352-2012.

References

- [1] Zupančič, A. – Lapasin, R. – Žumer, M. (1997): Rheological characterization of shear thickening TiO₂ suspensions in low molecular polymer solution. *Progress in organic coatings*. Vol. 30. pp. 67 – 78. [http://dx.doi.org/10.1016/S0300-9440\(96\)00670-4](http://dx.doi.org/10.1016/S0300-9440(96)00670-4)
- [2] Kamibayashi, M. – Ogura, H. – Otsubo, Y. (2008): Shear thickening flow of nanoparticle suspensions flocculated by polymer bridging. *Journal of Colloid and Interface Science*. Vol. 321. pp. 294 – 301. <http://dx.doi.org/10.1016/j.jcis.2008.02.022>
- [3] Otsubo, Y. (1990): Elastic percolation in suspensions flocculated by polymer bridging. *Langmuir*. Vol. 6. No. 1. pp. 114 – 118. <http://dx.doi.org/10.1021/la00091a016>
- [4] Fleer, G.J. – Lyklema, J. (1974): Polymer adsorption and its effect on the stability of hydrophobic colloids. *Journal of Colloid and Interface Science*. Vol. 46. No. 1. pp. 1 – 12. [http://dx.doi.org/10.1016/0021-9797\(74\)90018-6](http://dx.doi.org/10.1016/0021-9797(74)90018-6)
- [5] Kamibayashi, M. – Ogura, H. – Otsubo, Y. (2006): Rheological behavior of suspensions of silica nanoparticles in associating polymer solutions. *Ind. Eng. Chem. Res.* Vol. 45. pp. 6899 – 6905. <http://dx.doi.org/10.1021/ie0512486>
- [6] Otsubo, Y. (1986): Effect of polymer adsorption on the rheological behavior of silica suspensions. *Journal of Colloid and Interface Science*. Vol. 112. No. 2. pp. 380 – 386. [http://dx.doi.org/10.1016/0021-9797\(86\)90105-0](http://dx.doi.org/10.1016/0021-9797(86)90105-0)
- [7] Otsubo, Y. (1999): Rheological behavior of suspensions flocculated by weak bridging of polymer coils. *Journal of Colloid and Interface Science*. Vol. 215. pp. 99 – 105. <http://dx.doi.org/10.1006/jcis.1999.6252>
- [8] Otsubo, Y. (1990): Rheological studies on bridging flocculation. *Colloids and Surfaces*. Vol. 50. pp. 341 – 352. [http://dx.doi.org/10.1016/0166-6622\(90\)80274-8](http://dx.doi.org/10.1016/0166-6622(90)80274-8)
- [9] Otsubo, Y. (1994): Relation between bridging conformation and rheology of suspensions. *Advances in Colloid and Interface Science*. Vol. 53. pp. 1 – 32. [http://dx.doi.org/10.1016/0001-8686\(94\)00206-1](http://dx.doi.org/10.1016/0001-8686(94)00206-1)
- [10] Umerova, S. O. – Dulina, I. O. – Ragulya, A. V. (2014): Formation features of thin bilayer objects «conductor - dielectric» obtained by screen printing method. *International conference "Nanomaterials: Application and properties"*. Lviv. 21 – 26 of September 2014. Proceedings of Conferens. Vol. 1. pp. 01NTF04-1 - 01 NTF04-6.
- [11] Lin, H.-W. – Chang, C.-P. – Hwu, W.-H. – Ger, M.-D. (2008): The rheological behaviors of screen-printing pastes. *J. Mater. Process. Technol.* Vol. 197. pp. 284 – 291. <http://dx.doi.org/10.1016/j.jmatprotec.2007.06.067>
- [12] Vijatovic, M. M. – Bobic, J. D. – Stojanovic, B. D. – Malic, B. (2010): Barium titanate thick films prepared by screen printing technique. *Process. Appl. Ceram.* Vol. 4. No. 2. pp. 53 – 58. <http://dx.doi.org/10.2298/PAC1002053V>
- [13] Phair, J. (2008): Rheological analysis of concentrated zirconia pastes with ethyl cellulose for screen printing SOFC electrolyte films. *J. Am. Ceram. Soc.* Vol. 91. pp. 2130 – 2137. <http://dx.doi.org/10.1111/j.1551-2916.2008.02443.x>
- [14] Wagiran, R. – Wan Zaki, W. S. – Mohd Noor, S. D. B. – Shaari, A. Y. – Ahmad, I. (2005): Characterization of screen printed BaTiO₃ thick film humidity sensor. *Int. J. Eng. Technol.* Vol. 2. No. 1. pp. 22 – 26.
- [15] Chen, Y. – Gong, S.-P. – Li, H. – Wang, F.-J. – Yu, S.-J. – Xu, L.-F. (2007): Ni-BaTiO₃ interface phenomenon of Co-fired PTCR by aqueous tape casting. *J. Nonferr. Metal. Soc.* Vol. 17. pp. 1391-1395. [http://dx.doi.org/10.1016/S1003-6326\(07\)60283-0](http://dx.doi.org/10.1016/S1003-6326(07)60283-0)
- [16] Pat. 6.454.830 B1 US. Int. Cl. B22F 1/00. Nickel powder for multilayer ceramic capacitors / T. Ito (JP). H. Takatori (JP); assignee Toho Titanium Co., Ltd. (JP). – Appl. No. 09/786.032; filed 09.04.2001; published 24.09.2002. – 8 p.
- [17] Pat. 2002/0189402 A1 US. Int. Cl. B22F 9/22. Nickel powder dispersion. method of producing nickel powder dispersion and method of producing conductive paste / T. Ito (JP). H. Takatori (JP). – Appl. No. 09/937.689; filed 28.09.2001; published 19.12.2002. – 12 p.
- [18] Im, D.-H. – Hyun, S.-H. – Park, S.-Y. – Lee, B.-Y. – Kim, Y.-H. (2006): Preparation of Ni paste using binary powder mixture for thick film electrodes. *Mater. Chem. Phys.* Vol. 96. pp. 228-233. <http://dx.doi.org/10.1016/j.matchemphys.2005.07.047>
- [19] Pat. 2011/0141654 A1 US. Int. Cl. H01G 4/30 (2006.01). B22F 1/00 (2006.01). B01B 1/22 (2006.01). C22C 19/03 (2006.01). Nickel powder or alloy powder. comprising nickel as main component. method for producing the same. conductive paste and laminated ceramic capacitor / I. Okada (JP); assignee Sumitomo electric industries. Ltd. (JP). – Appl. No. 13/059.323; filed 26.07.2009; published 16.06.2011. – 12 p.
- [20] Pat. 2007/0108419 A1 US. Int. Cl. H05K 3/00 (2006.01). H01B 1/12 (2006.01). Conductive paste for an electrode layer of a multi-layered ceramic electronic component and a method for manufacturing a multi-layered unit for a multi-layered ceramic electronic component / S. Satou. T. Nomura (JP); assignee TDK Corporation (JP). – Appl. No. 10/580.991; filed 24.11.2004; published 17.06.2007. – 21 p.
- [21] Pat. 2010/0208410 A1 US. Int. Cl. H01G 4/008 (2006.01). C22C 19/03 (2006.01). B22F 9/16 (2006.01). H01B 1/02 (2006.01). Nickel powder or alloy powder. having nickel as main component. method for manufacturing the powder. conductive paste and laminated ceramic capacitor / I. Okada (JP). K. Koyama (JP). – Appl. No. 12/678.684; filed 09.07.2008; published 19.08.2010. – 10 p.
- [22] Pat. 2012/0048452 B2 US. Int. Cl. C04B 35/64 (2006.01). B32B 37/02 (2006.01). C04B 35/622 (2006.01). Method of manufacturing ceramic paste for multilayer ceramic electronic component and method of manufacturing multilayer ceramic electronic component having the same / J.M. Suh (KR). W.S. Choi (KR). J.H. Bae (KR). H. Kim (KR); assignee Samsung Electro-Mechanics Co., LTD (KR). – Appl. No. 13/191.053; filed 26.07.2011; published 01.03.2012. – 6 p.
- [23] Pat. 2012/0147514 A1 US. Int. Cl. H01G 4/30 (2006.01). B32B 37/06 (2006.01). B32B 37/14 (2006.01). C04B 35/00 (2006.01). B32B 37/02 (2006.01). Ceramic paste composition for multilayer ceramic capacitor. multilayer ceramic capacitor comprising the same and methods of manufacturing the same / J.M. Suh (KR). H. Kim (KR). H. Lee (KR); assignee Samsung Electro-Mechanics Co., LTD (KR). – Appl. No. 13/116.526; filed 26.06.2011; published 14.06.2012. – 6 p.
- [24] Pat. 2002/0047109 A1 US. Int. Cl. H01B 1/00. H01C 1/00. Conductive paste/ H. Yoshida (JP). T. Endo (JP). M. Mori (JP). – Appl. No. 9/923.056; filed 06.08.2001; published 25.04.2002. – 6 p.
- [25] Pat. 2007/0012899 A1 US. Int. Cl. H01B 1/12 (2006.01). Phosphate dispersant. paste composition and dispersion method using the same / E.-S. Lee. J.-Y. Choi. S.-M. Yoon. S.-K. Kim. J.-H. Kim. J.-G. Baek. (KR); assignee Samsung Electro-Mechanics Co., Ltd (KR). – Appl. No. 11/319.448; filed 29.12.2005; published 18.01.2007. – 12 p.
- [26] Pat. 2009/0032780 A1 US. Int. Cl. H01B 1/02 (2006.01). Nickel paste / T. Sugiyama (JP); assignee Noritake Co., Limited (JP). – Appl. No. 12/219.828; filed 29.07.2008; published 05.12.2009. – 9 p.
- [27] Pat. 2010/0038604 A1 US. Int. Cl. H01B 1/22 (2006.01). Nickel paste / T. Sugiyama (JP); assignee Noritake Co., Limited (JP). – Appl. No. 12/546.495; filed 24.08.2009; published 18.02.2010. – 9 p.

- [28] Pat. 7.463.477 B2 US. Int. CI. H01G 4/06 (2006.01). Multilayer ceramic electronic part and conductive paste / S.-M. Yoon. E.-S. Lee. J.-Y. Choi. S.-K. Kim. J.-G. Baek. S.-H. Lee (KR); assignee Samsung Electro-Mechanics Co., Ltd (KR). – Appl. No. 11/318.558; filed 28.12.2005; published 09.12.2008. – 16 p.
- [29] Pat. 2007/0014074 A1 US. Int. CI. H01G 4/008 (2006.01). Mixed dispersant. paste composition and dispersion method using the same / S.-M. Yoon. E.-S. Lee. J.-Y. Choi. S.-K. Kim. J.-G. Baek. S.-H. Lee (KR); assignee Samsung Electro-Mechanics Co., Ltd (KR). – Appl. No. 11/318.558; filed 28.12.2005; published 18.01.2007. – 16 p.
- [30] Leppavuori, S. – Uusimäki, A. – Hannula, T. (1981): Electrical properties of thick film capacitors based on barium titanate glass formulations. *Thin Solid Films*. Vol. 86. pp. 287–295. [http://dx.doi.org/10.1016/0040-6090\(81\)90336-9](http://dx.doi.org/10.1016/0040-6090(81)90336-9)
- [31] Pat. 6.366.444 B1 US. Int. CI. H01G 4/06. Multilayer ceramic electronic part and conductive paste / J. Yagi (JP); assignee Taiyo Yuden Co., Ltd. (JP). – Appl. No. 09/537.979; filed 30.03.2000; published 02.04.2002. – 11 p.
- [32] Pat. 6.551.527 B2 US. Int. CI. H01B 1/22. Conductive paste comprising N-acetylamino acid/ H. Yoshida (JP). T. Endo (JP). M. Mori (JP); assignee Shoei Chemical Inc/ (JP). – Appl. No. 9/923.056; filed 06.08.2001; published 22.04.2003. – 5 p.
- [33] Pat. 6.632.524 B1 US. Int. CI. H01B 1/02. Nickel powder. method for preparing the same and paste for use in making electrodes for electronic parts/ Y. Toshima (JP). T. Hayashi (JP). Y. Yamaguchi (JP). H. Shimamura (JP); assignee Mitsui Mining and Smelting Co., Ltd. (JP). – Appl. No. 09/716.238; filed 21.11.2000; published 14.10.2003. – 7 p.
- [34] Pat. 6.454.830 B1 US. Int. CI. B22F 1/00. Nickel powder for multilayer ceramic capacitors / T. Ito (JP). H. Takatori (JP); assignee Toho Titanium Co., Ltd. (JP). – Appl. No. 09/786.032; filed 09.04.2001; published 24.09.2002. – 8 p.
- [35] Pat. 6.632.265 B1 US. Int. CI. C22B 23/00. Nickel powder. method for preparation thereof and conductive paste/ T. Mukuno (JP). T. Araki (JP). Y. Toshima (JP); assignee Mitsui Mining and Smelting Co., Ltd. (JP). – Appl. No. 09/869.970; filed 09.10.2001; published 14.10.2003. – 8 p.
- [36] Pat. 6.494.941 B1 US. Int. CI. B22F 1/00. Nickel powder and conductive paste/ T. Mukuno (JP). T. Araki (JP). Y. Toshima (JP); assignee Mitsui Mining and Smelting Co., Ltd. (JP). – 2001Appl. No. 09/889.149; filed 10.11.2000; published 17.12.2002. – 8 p.
- [37] Pat. 2001/0013263 A1 US. Int. CI. B22F 1/00. Nickel powder and conductive paste/ Y. Yamaguchi (JP). T. Hayashi (JP); assignee Mitsui Mining and Smelting Co., Ltd. (JP). – Appl. No. 09/773.908; filed 02.02.; published 16.08.2001. – 5 p.
- [38] Pat. 2007/0012899 A1 US. Int. CI. H01B 1/12 (2006.01). Phosphate dispersant. paste composition and dispersion method using the same / E.-S. Lee. J.-Y. Choi. S.-M. Yoon. S.-K. Kim. J.-H. Kim. J.-G. Baek. (KR); assignee Samsung Electro-Mechanics Co., Ltd (KR). – Appl. No. 11/319.448; filed 29.12.2005; published 18.01.2007. – 12 p.
- [39] Pat. 6.548.437 B2 US. Int. CI. C04B 35/468. Dielectric ceramics and electronic component / S. Sato (JP). Y. Terada (JP). Y. Fujikawa (JP); assignee TDK Corporation (JP). – Appl. No. 09/835.492; filed 17.04.2001; published 15.04.2003. – 28 p.
- [40] Pat. 2002/0189402 A1 US. Int. CI. B22F 9/22. Nickel powder dispersion. method of producing nickel powder dispersion and method of producing conductive paste / T. Ito (JP). H. Takatori (JP). – Appl. No. 09/937.689; filed 28.09.2001; published 19.12.2002. – 12 p.
- [41] Pat. 6.517.745 B2 US. Int. CI. H01B 1/02. Nickel powder and conductive paste / T. Hayashi (JP). Y. Yamaguchi (JP); assignee Mitsui Mining and Smelting Co., Ltd. (JP). – Appl. No. 09/793.133; filed 27.02.2001; published 11.02.2003. – 7 p.
- [42] Pat. 7.618.474 B2 US. Int. CI. B22F 1/00 (2006.01). Nickel powder. conductive paste. and multilayer electronic component using same / Y. Akimoto. R. Nagashima. H. Ieda (JP); assignee Shoei Chemical Inc. (JP). – Appl. No. 11/602.062; filed 20.11.2006; published 17.11.2009. – 7 p.
- [43] Pat. 2009/0032780 A1 US. Int. CI. H01B 1/02 (2006.01). Nickel paste / T. Sugiyama (JP); assignee Noritake Co., Limited (JP). – Appl. No. 12/219.828; filed 29.07.2008; published 05.12.2009. – 9 p.
- [44] Brodnyan, J.G., Gaskins, F.H. (1958) The rheology of various solutions of cellulose derivatives. *J. of Rheol.* Vol. 2. No 2. pp. 285 – 302. <http://dx.doi.org/10.1122/1.548833>
- [45] Zhurkov, S. N. (1945): Investigation of the mechanism of polymers solidification. *Proceedings of the first and second conferences on high-molecular compounds*. pp. 66 – 73. (in Russian).
- [46] Barshteyn, R. S. – Kirilovich, V. I. – Nosovskiy, Yu. E. (1982): Plasticizers for polymers. *Moscow. Chemistry*. 197 p. (in Russian).
- [47] Tager, A. A. (1978): Physical chemistry of polymers. *Moscow. Chemistry*. 544p. (in Russian).
- [48] Suslov, A. G. – Korsakova, I. M. (2010): Assigning, marking and controlling of parameters of surface roughness of machines. *Moscow. MSIU*. 111 p. (in Russian).
- [49] Tager, A. A. (1990): Some questions about polymers plasticization. *Plasticheskie massy*. No 4. pp. 59–64. (in Russian).
- [50] Prigogine, I. – Defey, R. (1966): Chemical thermodynamics. *Novosibirsk. Science*. 510 p. (in Russian).
- [51] Tinius, K. (1964): Plasticizers. *M.-L., Khimiya*. 916 p. (in Russian).
- [52] Perepechko, I. I. (1978): Introduction in physics of polymers. *Moscow, Khimiya*. 310 p. (in Russian).
- [53] Ikanina, T. V. – Suvorova, A. I. – Tager, A. A. (1986): About polymers antiplasticization in high elastic state. *Visokomol. Soedin*. Vol. A28. No 4. pp. 817. (in Russian).
- [54] Geles, I. S. (2007): Wood raw materials – a strategic framework and civilization reserve. *Petrozavodsk. Karelian Research Centre of Russian Academy of Sciences*. 499 p. (in Russian).
- [55] Shtarkman, B. P. (1975): Plasticization of PVC. *Moscow, Khimiya*. 248 p. (in Russian).
- [56] Baran, A. A. (1986): Polymer dispersions. *Kiev, Naukova dumka*. 204 p. (in Russian).
- [57] Kozlov, P. V. – Papkov, S. P. (1982): Physico-chemical basis of plasticization of polymers. *Moscow, Khimiya*. 224 p. (in Russian).
- [58] Lypatov, Yu. S. – Sergeeva, L. M. (1972): Polymers adsorption. *Kiev, Naukovadumka*. 194 p. (in Russian).
- [59] Lypatov, Yu. S. (1980): Interfacial phenomena in polymers. *Kiev, Naukovadumka*. 255 p. (in Russian).
- [60] Severian, D. (2004): Polysaccharides: structural diversity and functional versatility. Second edition. *CRC Press*. 1224 p.
- [61] O’ Sullivan, A. C. (1997): Cellulose: the structure slowly unravels. *Cellulose*. Vol. 4. No. 2. pp. 173 – 207. <http://dx.doi.org/10.1023/A:1018431705579>
- [62] Kolpak, F. – Blackwell, J. (1976): Determination of the structure of Cellulose. *Macromolecules*. Vol. 9. No. 2. pp. 273 – 278. <http://dx.doi.org/10.1021/ma60050a019>
- [63] Lovleva, M. M. – Papkov, S. V. (1982): Polymer crystallo-solvates. Review. *Polymer science*. Vol. 24. No. 2. pp. 236 – 257. [http://dx.doi.org/10.1016/0032-3950\(82\)90168-X](http://dx.doi.org/10.1016/0032-3950(82)90168-X)
- [64] Frey-Wyssling, A. (1954): The fine structure of cellulose microfibrils. *Science*. Vol. 119. No. 3081. pp. 80 – 81. <http://dx.doi.org/10.1126/science.119.3081.80>
- [65] Sullivan, J. D. – Sachs, I. B. (1966): Research of cellulose morphology. *Forest Product Journal*. Vol. 16. No. 9. pp. 83 – 86.
- [66] Schramm, G. (2003): A practical approach to rheology and rheometry. *Gebrueder HAAKE GmbH. Karlsruhe*. 312 p.
- [67] Matvienko, V. N. – Kirsanov, E. A. (2011): Viscosity and structure of dispersed systems. *Vestn. Mosk. Univ. Ser. 2. Chemistry*. Vol. 52. No 4. pp. 243– 275. (in Russian).
- [68] Efremov, I. Ph. (1982): Dilatancy of colloidal structures and polymer solutions. *Uspekhi khimii*. Vol. 2. No 2. pp. 285 – 304. (in Russian).
- [69] Malkyn, A. Ya. – Isaev, A. I. (2007): Rheology: concepts. methods. and applications. *Moscow, Khimiya*. 560 p. (in Russian).
- [70] Vinogradov, G. V. – Malkyn, A. Ya. (1977): Polymers rheology. *Moscow, Khimiya*. 453 p. (in Russian).
- [71] Barnes, H. A. (2000): Handbook of elementary rheology. *Institute of Non-Newtonian Fluid Mechanics: University of Wales Aberystwyth*. 200 p.
- [72] Pivinskiy, Yu. E. (2001): Rheology of dilatant and thixotropic systems. *Saint Petersburg*. 174 p. (in Russian).
- [73] Losev, I. P. – Trostyanskaya, E. B. (2012): Chemistry of synthetic polymers. *Moscow. Kniga po trebovaniyu*. 610 p. (in Russian).
- [74] Petropavlovskiy, G. A. (1988): Hydrophilic partially substituted cellulose ethers and their modification by chemical crosslinking. *Leningrad, Nauka*. 288 p. (in Russian).
- [75] Im, D.-H. *et al* (2006): Preparation of Ni paste using binary powder mixture for thick film electrodes. *Mater. Chem. Phys.*, Vol. 96. pp. 228–233. <http://dx.doi.org/10.1016/j.matchemphys.2005.07.047>

Ref.:

Umerova, Saide – Dulina, Iryna – Ragulya, Andrey: *Rheology of plasticized polymer solutions*
Építőanyag – Journal of Silicate Based and Composite Materials,
Vol. 67, No. 4 (2015), 119–125. p.
<http://dx.doi.org/10.14382/epitoanyag-jsbcm.2015.19>

The effect of VIATOP[®] plus FEP on the stiffness and low temperature behaviour of hot mix asphalts

CSABA TÓTH MBA, PhD ▪ Assistant Professor, BME Dept. of Highway and Railway Engineering
▪ toth@uvt.bme.hu

ZOLTÁN SOÓS ▪ PhD Student, BME Dept. of Highway and Railway Engineering ▪ soos.zoltan@uvt.bme.hu
Érkezett: 2015. 07. 30. ▪ Received: 30. 07. 2015. ▪ <http://dx.doi.org/10.14382/epitoanyag-jsbcm.2015.20>

Abstract

The trade-off regarding stiffness and low-temperature behaviour of hot mix asphalt (HMA) mixes is well known – the higher the stiffness of an asphalt mix is, the lower its relaxation during fast cooling down in winter, resulting in thermal cracking at higher winter temperatures. The accumulated tensile stress together with the stress deriving from heavy traffic load leads to severe transverse cracking of the pavement. The German company J. Rettenmaier & Söhne has developed several fibre based pellet additives in its research laboratories in Germany. The most commonly used pellet product is used for stone mastic asphalt mixes to prevent the binder drain-down from the surface of the aggregates.

An innovation of the company presented in 2014-2015 was a new type of additive named VIATOP[®] plus FEP (*Functional Elastomer Pellet*), consisting of approx. 20% special cellulose fibre and 80% elastometric additive. This new type of pellet is designed for HMA wearing courses of heavy duty roads, improving pavement performance through superior binder properties. VIATOP[®] plus FEP is probably a competitive of common modified binders regarding performance versus price and simplicity in its application. It is expected to improve stiffness of the mix while somewhat improving low temperature behaviour as well.

As there is little chance of the selected modifications to decrease fatigue life, it is assumed to be at least adequate in all cases and no need to be analysed. Low and high temperature behaviour, however, is a challenge to all modifications. In our research stiffness and low-temperature behaviour of three asphalt mixes were tested and compared: one with polymer modified bitumen and one with the new additive, together with a standard mix used for reference. Plastic deformation at high temperature is tested according to EN 12697-22 using small wheel tracker, low temperature cracking is tested using equipment developed at the laboratory of the BME Department of Highway and Railway Engineering, according to EN 12697-46 *Thermal Stress Restrained Specimen Test* (TSRST) method, and stiffness using test method C of EN 12697-26, *Indirect Tensile strain on Cylindrical Specimen* (IT-CY). Stiffness was measured at different temperatures to obtain a more comprehensive picture of the mixes. To make the research more interesting the chosen mix contains approx. 10% reclaimed asphalt according to endeavours of sustainability in the asphalt industry.

Based on the results, the manufacturer's estimations on mix performance and some prior tests made in Germany an evaluation was made on a mix commonly used in Hungary. The benefits of the selected modifications were compared to each other and the results are presented and evaluated. Keywords: Hot Mix Asphalt, VIATOP[®] Plus FEP, additives, stiffness, low temperature behaviour, asphalt mix modification.

Kulcsszavak: aszfaltkeverék, Viatop[®] Plus FEP, adalékszer, merevség, hidegviselkedés, modifikált aszfaltkeverék

Csaba TÓTH

Member of the Hungarian Chamber of Engineers, the Hungarian Scientific Association for Transport and the Hungarian Road Society. Worked as Head of Division at Csongrád County Road Administration, then ÁKMI Kht. Involved in quality control of Hungarian road developments both national and international researches as part of the Strabag concern. Had a role in several road overlay projects as engineering expert, designer and supervisor. Currently Assistant Professor and Head of Asphalt Unit at the Pavement Laboratory. Research field includes load bearing capacity of road structures and overlay design of flexible pavements.

Zoltán SOÓS

Obtained MSc in Civil Engineering and started PhD research in 2014 at BME Department of Highway and Railway Engineering. Member of the Hungarian Scientific Association for Transportation. Research topics include testing and design of asphalt pavement materials and road structures with emphasis on fatigue behaviour and service life, performance and structural design. Takes part in lecturing at BME and as Deputy Head, in the work of the Pavement Laboratory since 2015.

1. Introduction

Since weather conditions and road traffic, especially road freight became more and more extreme there is a constantly increasing demand for higher performance asphalt mixes.

Worldwide road administrations, being always in the lack of funds, are seeking methods and materials to build pavements with higher quality, durability, lower upkeep needs, in one word - improved life cycle. Performance of pavement structures depends highly on the quality of its components, especially the type and quality of the binder which essentially determines the most important properties of the asphalt mix.

In this respect there are various modification technologies available and there are ongoing researches to develop new methods. The most frequently used technique is to modify the binder itself (modified bitumen) using various polymers, or e.g. using recycled rubber recently. Results lead to improved binder quality at a given, or maybe at even multiple temperature levels.

Additionally to the growing need for structural performance, the need for new techniques and materials is also increased due to the experienced uncertainties in supply and in prices of the most commonly used polymer-modified binders in the past few years. There are ongoing researches to study the effects of various modifiers on the properties of the binders [1, 2], or the ef-

fects of certain fillers on the performance of the asphalt mastic [3, 4]. There are numerous researches which involve methods to improve the performance of the pavement structure itself, using structural improvements [5].

A known issue for Stone Mastic Asphalt (SMA) mixes is the possible drain off of binder from the aggregate due to the gap-graded composition, despite the high (around 20%) fine aggregate content, resulting in inadequate mix quality. This problem is commonly solved by the use of various additives, e.g. the VIATOP® products manufactured by the company J. Rettenmaier & Söhne in Germany, which apply a fibre stabilizing effect. Ongoing research at the company has led to a similar, but novel cellulose-based additive presented in 2014-2015, which is designed to improve asphalt mixes. The new additive is the VIATOP® Plus FEP (Functional Elastomer Pellet). The greatest advantage of this additive is that it may be added directly to the mixing drum during production, thus actually modifying the asphalt mix itself, rather than modifying the binder prior to mixing [6]. This is a useful application as modified binders often require special storage conditions, in some cases even continuous mixing and heating, and often can only be purchased in high volumes from the manufacturer. The possibility of producing smaller volumes, to reach higher independence from binder manufacturers, and competitive prices are all important in the asphalt industry. However, the performance of such mixes must, at a minimum, reach the performance of mixes made with normal or polymer-modified binders.

VIATOP® products were tested in Germany on asphalt mixes to study the performance of the additive, but common mixes used in Hungary were not studied so far.

In the present research, the Indirect Tensile strain on Cylindrical Specimen (IT-CY) stiffness, cold- and warm-temperature behaviour of asphalt mix made with normal bitumen, a mix modified with VIATOP® Plus FEP were tested, with a comparison to a mix made with polymer modified bitumen. The goal of the studies was to find if the properties of asphalt mixes using VIATOP® Plus FEP additive can reach that of conventional mixes made with polymer-modified binder, apart from the several technological advantages, and competitive price attributed to the additive.

2. Materials

The manufacturer recommends the additive primarily for improving wearing courses, thus the tested mix was chosen to be AC11 wear (F), a commonly used wearing course mix in Hungary. During the research it was assumed that a modified mix would probably have better results than a conventional mix made with B50/70 binder. Therefore, three mixes were tested: one made with B50/70 normal binder, one made with VIATOP® Plus FEP additive, and one made with polymer-modified B50/70 binder, PmB 25/55-65. For comparison, one mix containing reclaimed asphalt material was studied as well.

2.1. VIATOP® Plus FEP additive

The additive contains 20% ABROCEL® cellulose fibre and 80% elastomer, and its density is 1.2 g/cm³. The additive is available in grey coloured pelletized, cylindrical form (3-20 × 3-6 mm size) with about 280 kg/m³ density. Breakdown temperature is about 200°C, maximum recommended mixing temperature is 170°C. The

VIATOP® products obtained Hungarian Construction Technical Approval in transportation construction in 2011 (ÉME 16/2011).

2.2. Binders

Properties of the binders were tested as well since the goal of the research was to determine the effects of given modifications. Although VIATOP® additive is designed to modify the asphalt mix itself, eventually it dissolves in the binder. Using wet method, it is possible to modify the binder with the additive under laboratory conditions, and perform conventional rating tests. Results are shown in *Table 1*.

Test	B50/70	B50/70 + VIATOP® Plus FEP	PmB 25/55- 65
Softening point [°C]	50.2	65.4	78
Penetration [0.1mm]	55	32	32

Table 1. Softening point and penetration of base binders and binder modified with VIATOP® Plus FEP

1. táblázat A referencia és a modifikált kötőanyagok lágyuláspontja és penetrációja

It can be seen in *Table 1*, that modification with VIATOP® Plus FEP results lower softening point for the same penetration of the polymer-modified bitumen, which suggests better warm-temperature behaviour.

2.3. Aggregates

Normal aggregates commonly used in Hungarian asphalt mixes were used in the studies. The reclaimed asphalt was of high quality, graded, properly and selectively stored, originating from AC11 wearing course. Its soluble binder content was 5.5 m%, density was 2.793 Mg/m³.

2.4. Mixing ratio

The composition of the mixes, complying with current Hungarian standards, is shown in *Table 2*.

Component	„A” AC11 wear (F) 50/70	„B” AC 11 wear (mF) 50/70 + VIATOP® Plus FEP	„C” AC 11 wear (mF) 25/55-65
Aggregates [aggregate mass%]			
Filler (Dorog)	4.0		
NZ 0/2 limestone, Iszkaszentgyörgy		14.0	
NZ 0/4 basalt, Uzsa	16.0		
NZ 4/8 basalt, Uzsa	29.1		
KZ 8/11 basalt, Uzsa	27.0		
11 RA 0/10 Reclaimed asphalt, Győrújfalu	9.9		
Binders [mix mass%]			
B 50/70, MOL	4.6%	4.6%	-
VIATOP® Plus FEP	-	0.9%	-
PmB 25/55-65, MOL	-	-	4.6%

Table 2. Composition of the studied mixes
2. táblázat A vizsgált keverékek összetétele

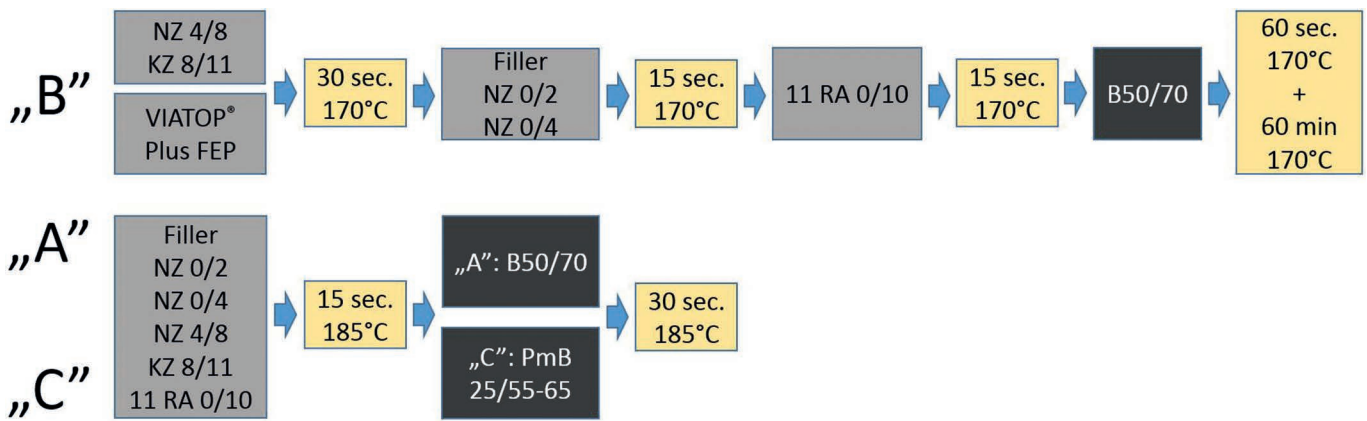


Fig. 1. Mixing sequence of mixes A, B and C
1. ábra Az A, B és C jelű keverékek keverési sorrendje

3. Laboratory mixing

Regarding the mixing procedure, mixes A and C needed attention only for the proper use the reclaimed asphalt. In case of mix B, besides the use of reclaimed asphalt, extra mixing steps were required to mix the additive properly in dry mixing.

3.1. Adding the reclaimed asphalt

Although a study about recycling of asphalt mixes [7] concluded that the technique of adding reclaimed material to the mix may have a great impact on the performance of the mix, the European practice in this topic is considerably diverse [8].

To achieve appropriate bond between the aged bitumen in the reclaimed material and the newly added bitumen, and to ensure the adequate blending of the materials, it is critical to determine the proper mixing sequence and the mixing temperatures. The determination of the dry mass of the reclaimed material was also a challenge, since the material may become gnarly at high temperatures, and the same time water must get evaporated to get a dry mass. It was found that at about 60°C it is possible to dry the reclaimed material and maintain its granulated form.

It was found by numerous literature reviews that the optimal mixing sequence is to first homogenise the coarse aggregate with the reclaimed material, and only add the binder during the last step. According to a questionnaire in [7], 17 out of 23 Western-European asphalt laboratories apply this technique, and in 3 cases they mix the reclaimed asphalt with the binder first, and then add it to the previously homogenised coarse aggregates.

Mixing temperature is also important, since the aged binder may be damaged and easily oxidised during mixing at high temperatures otherwise optimal for normal binders. If the mixing temperature is low then proper bond cannot form between the aged and new binder. If the mixing temperature is optimal then aged binder is not damaged, and forms a good bond with the new bitumen. If the mixing temperature is high then both the aged and even the new bitumen may get burned.

3.2. Adding the VIATOP® Plus FEP additive

The greatest advantage of VIATOP® Plus FEP additive is that it may be added directly to the aggregate at the mixing plant.

Thus it does not require special feeder, storage, pre-heating, and makes mixing more independent of the bitumen provider.

In order to obtain mix quality as close to the mix made at a mixing plant as possible, dry mixing in the laboratory was applied during which the distribution of the pelletized material is done by dry-mixing it only with the aggregate. To minimise the loss of dust of the aggregate during dry mixing, only the coarse aggregate was used for this purpose.

The manufacturer suggests heating the aggregate and the additive to 170 °C while mixing, and continuing mixing for 15 sec while maintaining 170 °C. The hot binder may then be added, and further mixing is required for about 105 sec to gain complete homogenisation. If the mixing time is short then the pellets are not distributed properly, thus the cellulose fibres are not able to bond with the binder, and modification does not take place. If the mixing time is optimal then pellets can crumble, fibres are separated and homogenised with the aggregate, no caking and additive-free parts remain, and the additive makes bond with the bitumen. If the mixing time is long then cellulose fibres may be damaged or broken, such changes will hamper the success of modification.

Optimal mixing process depends on the mixer properties and its performance. To obtain optimal blending, multiple mixing times were tested, sieving after each step, and observing the condition of the additive. It was found that optimal dry mixing time for the additive under laboratory conditions is about 30 sec.

3.3. The mixing sequence

The usual mixing technique is needed to be modified to achieve proper dissipation of the VIATOP® Plus FEP additive, and the proper adding of the reclaimed asphalt. The developed mixing sequence for this case is shown in Fig. 1.

Marshall density of the specimens were determined to make sure the only relevant difference between the mixes is the binder type (see Table 3).

Table 3 shows that a somewhat better compaction can be achieved with the polymer-modified mix, while the density of the mix modified with VIATOP® Plus FEP is about 0.5% lower than that of the reference mix that can be considered irrelevant, since the dose of the additive is 0.9 m%.

Mix	Specimen	Density [Mg/m ³]	Avg. density [Mg/m ³]
„A” AC11 wear (F) 50/70	A1	2.493	2.490
	A2	2.499	
	A3	2.483	
	A4	2.491	
	A5	2.486	
	A6	2.485	
„B” AC11 wear (mF) 50/70 + VIATOP® Plus FEP	B1	2.470	2.476
	B2	2.470	
	B3	2.479	
	B4	2.466	
	B5	2.486	
	B6	2.484	
„C” AC11 wear (mF) 25/55-65	C1	2.487	2.495
	C2	2.492	
	C3	2.503	
	C4	2.503	
	C5	2.487	
	C6	2.500	

Table 3. Density of the prepared specimens
3. táblázat Próbatestek testtűrsége

4. Laboratory tests

The viscoelastic behaviour of asphalt mixes and asphalt pavement structures is rather complex and is strongly dependent on temperature and load history (frequency) [9]. Asphalt mixes are usually tested for typical failure modes, which occur at typical temperature ranges:

- at low temperature the thermal crack resistance,
- at normal temperature the stiffness and fatigue failure,
- at high temperature the plastic deformation resistance.

Fatigue was not tested during this study since Hungarian fatigue criteria is not governing parameter for most of the mixes. Cracking temperature was tested on four specimens for all mixes, stiffness was tested on six specimens for all mixes at different temperatures to obtain more comprehensive results, and plastic deformation was tested on mixes B and C on two specimens for the mixes.

4.1. IT-CY stiffness

Stiffness of the asphalt mixes is one of their most important feature, as it determines the ability of the material to resist loads and deformations. Stiffness depends highly on temperature and varies with depth from the surface in a pavement structure [10]. The effect of stiffness on fatigue performance and thus service life of a layer has also been shown [11]. Stiffness should be interpreted together with the testing temperature and should be tested at different temperatures [12]. The stiffness tests were carried out at 20 °C according to European standard EN 12697-26 and at further three temperature levels (10 °C, 30 °C, 40 °C). Results are shown in Fig. 2.

Stiffness at 20 °C shows higher values than usually found due to the stiffening effect of the aged bitumen added with the reclaimed asphalt. As it was expected, the modified mixes have higher stiffness. At high temperatures, however, the mix made

with VIATOP® Plus FEP had the highest stiffness: stiffness is only 6% higher at 10 °C than that of mix A, but 90% more at 40 °C. It means that this mix loses less of its stiffness with the increase of temperature. Accordingly, a more favourable performance is expected at plastic deformation tests, carried out at 60 °C.

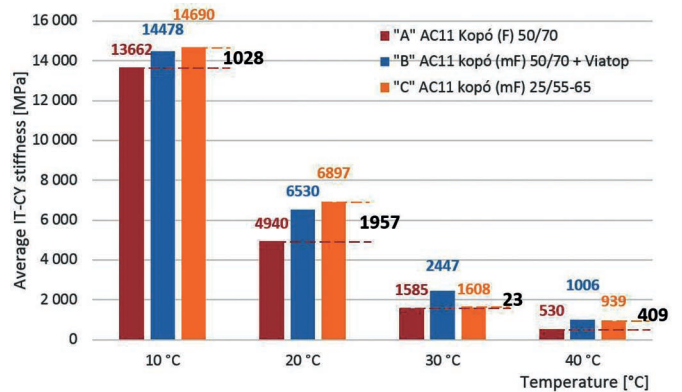


Fig. 2. IT-CY stiffness in function of test temperature for all mixes
2. ábra A vizsgált keverékek IT-CY merevsége a hőmérséklet függvényében

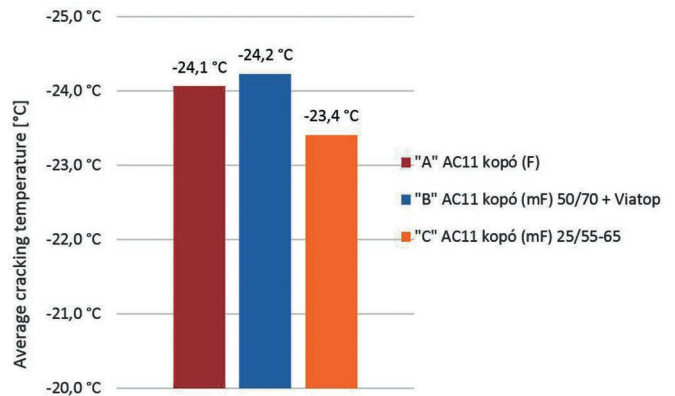


Fig. 3. Average cracking temperature for all mixes
3. ábra A vizsgált keverékek repedési hőmérséklete

4.2. Low temperature behaviour

The laboratory of BME Dept. of Highway and Railway Engineering is the only laboratory in Hungary capable of testing low temperature cracking of asphalts. The equipment – although its development started in the 80s [13] – is fully compatible with the Thermal Stress Restrained Specimen Test (TSRST) method described in European standard EN 12697-46. This test has relevance for fast winter cooling downs during which the relaxation of the asphalt mixes is lower than the increasing thermal stress, due to the higher stiffness of the binder (thus the mix). The slowly accumulated thermal stress is able to form transverse cracks in the pavement structure. The stress deriving from heavy traffic loads results in an even higher tensile stress [14]. The load induced stress and the thermal stress together reach the tensile strength of the material faster that leads to thermal cracking. However, thermal stress alone is also capable of reaching the tensile strength, and the test of EN 12697-46 relates to this phenomenon.

During the test a moderate winter is modelled with a constant -10 °C/h rate of cooling. The thermal stress is accumulated

in the specimen (50×50×250 mm) due to physical restraints which allow no thermal shrinking. As the stress reaches the tensile strength of the specimen, cracks are forming, and the temperature at which this occurs is called cracking temperature. Averages of results for the 4 specimens for each mix are shown in Fig. 3. Lowest cracking temperature is achieved by mix B made with VIATOP® Plus FEP additive.

4.3. Plastic deformation

Both mixes B and C were tested for plastic deformation since high stiffness was found at high temperature for mix B. The temperature of the pavement on hot summer days may exceed even 60 °C and plastic deformation can be critical. At this temperature, the material deforms at a low level of stress, the pavement usually does not crack and there is usually no fatigue damage either. However, due to its viscoelastic properties, only a small part of deformations is elastic, and large part is plastic, which accumulates and results in rutting.

Tests were performed according to EN 12697-22 small wheel tracking, for both B and C mixes. Results are shown in Fig. 4. According to the expectations drawn from the stiffness evaluation, results of mix B made with VIATOP® Plus FEP were somewhat better, tested on two specimens. Mix A was not tested.

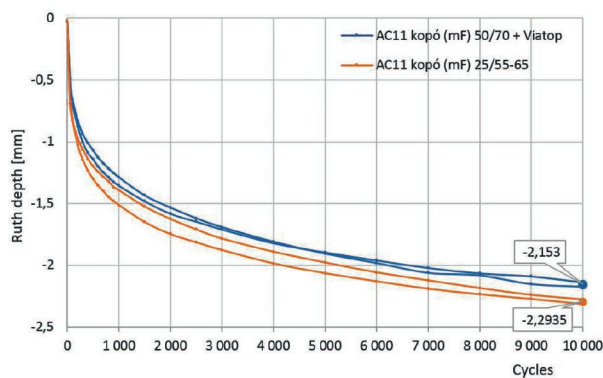


Fig. 4. Plastic deformation in function of load cycles, for mixes B and C
4. ábra Plasztikus deformáció a terhelési ciklusok függvényében (B és C keverék)

4.4. Relationship between stiffness and low-temperature behaviour

The higher is the stiffness, the lower is the relaxation capability of the asphalt mix, which results in faster accumulation of thermal stresses. It is known, that most modifications are designed and capable in improving performance at a given temperature range, only few hybrid-modifications are capable of improving the performance of mixes in a wider range of temperature. This means that the effects are lower at all temperatures. Fig. 5 shows the stiffness and cracking temperatures of all three mixes tested.

Fig. 5 indicates that the stiffness and cracking temperature performance of the mix made with VIATOP® Plus FEP is better than that of mix C (made with polymer-modified bitumen), achieving higher stiffness and resulted in higher cracking temperature.

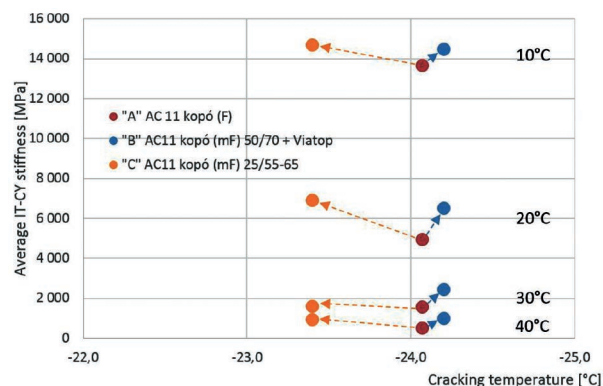


Fig. 5. Stiffness and thermal cracking temperatures for all mixes
5. ábra A vizsgált keverékek merevsége és repedési hőmérséklete

5. Conclusions

Test results of an innovative new asphalt additive have been shown. Accepting that modification would obviously lead to better performance of mixes, the additive was tested on the most commonly used modification in Hungary, a mix made with PmB 25/55-65 bitumen, together with a normal mix. To be able to find the effects of the binders and the modifications, all other components and techniques were the same for all mixes. For comparison, a mix containing 10% of reclaimed asphalt was also tested.

Due to the statistically low number of tests it cannot be stated that adding VIATOP® Plus FEP instead of any other modification would result in a better performance of the mix in all cases, however, it was shown that this additive is probably a true rival to the commonly used modifications. Further laboratory tests are required to reach statistical justification. The presented results indicated high possibility for the additive in improving mix performance, which should be verified on test tracks.

References

- [1] Bíró, S. – Thodesen, C. – Perlaki, R. (2013): Polimerekkel módosított bitumenek reológiai összehasonlítása ismételt kúszás-relaxáció vizsgálatával. *Útiügyi Lapok*, 2013/1.
- [2] Bartha, L. – Geiger, A. – Gergő, P. (2012): A gumibitumen felhasználás áttörést jelenthet a hazai útépitésben. *Műanyag és Gumi*, Vol. 49, No. 8, pp. 297-299.
- [3] Géber, R. – Gömze, L. (2012): Aszfaltkeverékekben felhasznált ásványi töltőanyagok vizsgálata. *Miskolci Egyetem Közleményei*. Vol. 2: Anyagmérnöki Tudományok.
- [4] Géber, R. – Gömze, L. (2010): Characterization of Mineral Materials as Asphalt Fillers. *Materials Science Forum*, Vol. 959, pp. 471-476. <http://dx.doi.org/10.4028/www.scientific.net/MSF.659.471>
- [5] Almássy, K. – Joó, A. (2009): Special materials in the road building - Grids and nets application terms for improving the pavement structures. *Építőanyag*, Vol. 61, No. 2, pp. 55-59. <http://dx.doi.org/10.14382/epitoanyag-jsbcm.2009.10>
- [6] Hauber, F. – Görögh, E. (2015): Aszfaltbeton felületű utak optimalizálása funkcionális elasztomer pelletekkel. *Proceedings XVI. HAPA Aszfaltkonferencia*, Balatonalmádi, 2015.
- [7] De Visscher, J. – Mollenhauser, K. – Raaberg, J. – Khan, R. (2013): Mix design and performance of asphalt mixes with RA. *Re-Road: End of life strategies of asphalt pavements*, Belgium, www.re-road.fehrl.org.
- [8] Mollenhauser, K. – Gáspár, L. (2012): Synthesis of European knowledge on asphalt recycling. Options, best practices and research needs. *Proceedings of 5th Euraspphalt & Eurobitume Congress*, Istanbul, Turkey, European Asphalt Pavement Association, 2012.

- [9] Gömze, L. – Kovács, Á. (2005): Aszfaltkeverékek reológiai tulajdonságainak vizsgálata. *Építőanyag*, Vol. 57, No. 2, pp. 34-38. <http://dx.doi.org/10.14382/epitoanyag-jsbcm.2005.7>
- [10] Pethő, L. – Fi, I. (2008): Calculation of the equivalent temperature of pavement structures. *Periodica Polytechnica Civil Engineering*, Vol. 52, No. 2, pp. 91-96. <http://dx.doi.org/10.3311/pp.ci.2008-2.05>
- [11] Bocz, P. (2009): The effect of stiffness and duration parameters to the service life of the pavement structure. *Periodica Polytechnica Civil Engineering*, Vol. 53, No. 1, pp. 35-41. <http://dx.doi.org/10.3311/pp.ci.2009-1.05>
- [12] Almássy, K. – Tóth, C. (2011): Applying master curve at the grids strengthened asphalt structures. *Építőanyag*, Vol. 63, No. 1-2, pp. 16-17. <http://dx.doi.org/10.14382/epitoanyag-jsbcm.2011.3>
- [13] Török, K. – Pallós, I. (2015): Az aszfaltok téli hidegviselkedését befolyásoló anyagtulajdonságok laboratóriumi vizsgálata. *Útügyi Lapok*, 2015/5.
- [14] Arand, W. (2007): Az aszfalt fáradása alacsony hőmérsékleten. *Közúti és Mélyépítési Szemle*, Vol. 57, No. 7, pp. 4-10.

Ref.:

Tóth, Csaba – Soós, Zoltán: *The effect of VIATOP® plus FEP on the stiffness and low temperature behaviour of hot mix asphalts. Paper of presentation at 2nd International Conference on Rheology and Modeling of Materials*
 Építőanyag – Journal of Silicate Based and Composite Materials, Vol. 67, No. 4 (2015), 126–131. p.
<http://dx.doi.org/10.14382/epitoanyag-jsbcm.2015.20>



DRIVING AHEAD WITH SUSTAINABLE ASPHALT ROADS

European Asphalt Pavement Association

EAPA MISSION STATEMENT

“EAPA’s mission is to be the trusted voice of the Asphalt Paving Industry in Europe and to ensure that the use of asphalt, as the optimum choice for the construction and maintenance of the vital European road infrastructure, is fully appreciated, promoted and implemented.”

AIM

The aim of the Association is to build on its already strong reputation as the voice of the asphalt paving industry, by expanding its membership to be fully representative of the industry in Europe and creating a sound evidence base for promoting the economic, technical and environmental benefits of asphalt paving in road construction and maintenance.

OBJECTIVES

- to promote, within Europe, the legitimate joint interests of all its Members and Associate Members concerned with the production of asphalt or the construction or maintenance of roads, and in particular to promote the effective and sustainable use of asphalt in the construction and maintenance of roads in Europe.
- to collect and facilitate the exchange of information, know-how and best practice between its members and similar international associations.
- to promote knowledge and understanding by all stakeholders of the activities of its members and their important position in the European economy.
- to represent its members with the institutions of the European Union, in particular the Parliament, the Council of Ministers, the Commission, the Economic and Social Committee, the Committee for the Regions, and any other national and international organisations which are concerned with questions of enterprise policy, transport policy and policy related to health, safety and environment.
- to promote the image of the asphalt paving industry in Europe.
- to innovate measures and best practice to improve the health, safety and environmental conditions of all employed in the industry, and to actively cooperate with regulatory bodies in setting appropriate operating standards.
- to participate in European standardisation activity and to be a leading authority on asphalt technology, in particular promoting new developments such as warm mix paving and encouraging higher levels of asphalt recycling.

WWW.EAPA.ORG

Effect of Additives on the Rheological Properties of Fast Curing Epoxy Resins

YOUJIANG WANG ▪ School of Materials Science & Engineering, Georgia Institute of Technology, Atlanta, Georgia, USA ▪ youjiang.wang@mse.gatech.edu

DILDAR ALI LAKHO ▪ QAU Islamabad, Pakistan

DONGGANG YAO ▪ School of Materials Science & Engineering, Georgia Institute of Technology, Atlanta, Georgia, USA

Érkezett: 2015. 07. 30. ▪ Received: 30. 07. 2015. ▪ <http://dx.doi.org/10.14382/epitoanyag-jsbcm.2015.21>

Abstract

Rapid Resin Transfer Molding (RTM) process is suitable for high-throughput manufacturing of complex-shaped composite parts. Ideally the epoxy system should exhibit low viscosity and long gel time at room temperature for quick mold filling, and very fast curing once the resin is inside the heated mold. The present research was performed on different epoxy formulations by varying the concentrations of diluent and catalyst. Rheological studies were carried out to measure the flow viscosity and to determine the gel time at different temperatures. It is noted that the addition of diluent effectively decreases the viscosity of formulation, and the addition of imidazole affects the rate of epoxy cure. Several epoxy resin formulations were studied and compared with the commercially available infusion-grade epoxy system of Araldite LY 8601/Aradur 8602. The results show that epoxy systems such as that containing 5% imidazole and 10% reactive diluent are suitable for the rapid RTM process with balanced flow and cure characteristics.

Keywords: epoxy, composites, processing, curing

Kulcsszavak: epoxi, kompozitok, feldolgozás, utókezelés

1. Introduction

Epoxy resins are widely used as matrix material for advanced composites, which offer superior strength-to-weight and modulus-to-weight ratios, fatigue strength, damage tolerance, tailored coefficient of thermal expansion, chemical resistance, weatherability, temperature resistance, among others. Many products for wind energy, ground transportation, marine, and recreational applications, for instance, are made by the resin infusion process using epoxy and other resins [1]. For some high volume applications such as automotive components, high throughput, fast processing is necessary, and rapid Resin Transfer Molding (RTM) is regarded as one of the most promising technologies for such applications. Epoxy resin used in rapid RTM process should exhibit low viscosity and low cure rate at room temperature for fast infusion into mold cavity and effective impregnation of the reinforcing fabrics. After the resin is injected into the preheated mold the resin must cure rapidly (i.e. rapid increase in viscosity) at the processing temperature. In this study the effect of additives to the epoxy resin such as diluents and reaction accelerators is analyzed which could be used to guide the development of epoxy formulations for rapid resin infusion process of composites.

Epoxy resins show viscoelastic behavior during the curing process. The liquid resin starts to form a network of molecules with molecular weight approaching infinity as the crosslinking reaction proceeds, and this is referred to as the gel point [2, 3]. Eventually the molecular chains become close packed and there is insufficient volume for cooperative chain motion to occur, and this stage is known as vitrification [4]. Rheology is widely used to study gel times, vitrification times and other viscoelastic parameters [5-9].

Youjiang WANG

is a Professor in the School of Materials Science and Engineering, Georgia Institute of Technology, Atlanta, USA. He is a Fellow of the American Society of Mechanical Engineers. His research interests include processing, mechanics, and recycling of fiber, polymer, textile and composites.

Dildar Ali LAKHO

is a Ph.D. student in the Department of Chemistry, Quaid-i-Azam University, Islamabad, Pakistan. He was a visiting scholar at the Georgia Institute of Technology, Atlanta, USA, in 2012-2014 sponsored in part by the Higher Education Commission of Pakistan. His research focuses on polymer chemistry and nano composites.

Donggang YAO

is a Professor in the School of Materials Science and Engineering, Georgia Institute of Technology, Atlanta, USA. He served as project director or principal investigator of many projects sponsored by industry and governmental funding agencies. His group conducts research on novel methods to process polymers, fibers and composites.

2. Experimental

2.1 Materials

Diglycidylether of bisphenol A (DEGBA) based epoxy resin (D.E.R.™ 331™) and Triethylene-tetraamine (TETA) (D.E.H.™ 24, an aliphatic polyamine curing agent) were supplied by the Dow Chemical company. 1-Benzyl-2-methylimidazole (90% purity) was purchased from Sigma-Aldrich®. Diglycidyl ether of 1,4-butanediol (Epodil® 750) used as a reactive diluent in the study was supplied by Air Products and Chemicals. The other epoxy system used was Araldite® LY 8601 (resin) / Aradur® 8602 (hardener), a low-viscosity two-component epoxy system provided by Huntsman Advanced Materials. Araldite® LY 8601 is a blend having major portion of bisphenol A resin.

Different compositions were formulated to study the effect on the rheological properties of the epoxy resin with diluent and imidazole. Detailed formulations are given in *Table 1*.

Sample code	D.E.R.™ 331™ (Epoxy)	D.E.H.™ 24 (Hardener)	Epodil® (diluent)	Imidazole (catalyst)
DD	100.00	13.00	0	0
DD/10E	100.00	15.21	10.00	0
DD/5I	100.00	12.14	0	5.00
DD/5I/10E	100.00	14.51	10.00	5.00
	Araldite®LY 8601 (Epoxy)	Aradur® 8602 (Hardener)		
AA	100.00	25.00		

Table 1. Details of different compositions (mass ratios)
1. táblázat Az egyes összetételek részletei (tömegarányban)

2.2 Rheological measurements

For the rheological measurements, parallel plate AR 2000ex TA instrument was used. All the experiments were carried out with 25 mm steel plates at an air pressure of 200 kPa under isothermal conditions. Preliminary frequency and strain sweeps were carried out to determine the optimum experimental conditions. The test fixture was preheated to the desired isothermal cure temperature and the plate spacing was zeroed. The chamber was then opened, the plates separated and the resin sample was rapidly inserted. The plates were then brought back together to a gap of 1.0 mm. Excessive resin was scraped out carefully before starting the test.

The following two test methods were used: (1) steady state flow tests to measure the viscosity of sample formulations at room temperature at different shear rates from 0.1/s to 100/s, and (2) time sweep experiments to determine gel time based on viscoelastic parameters like shear storage modulus G' , shear loss modulus G'' , and $\tan \delta$ as a function of time at three different temperatures (60, 80, and 100 °C) for 20 minutes at four different frequencies (5, 10, 15 and 20 Hz) at a constant 20% strain.

3. Results and discussions

3.1 Steady state flow tests

To evaluate the effect due to the addition of diluent in the resin matrix, steady state flow tests were performed to determine the viscosity of the formulation at room temperature at different shear rates, and the results are given in Fig. 1. At any shear rate it can be observed that the highest viscosity is shown by the pure epoxy and amine system (DD) and the least viscosity is shown by the commercially available epoxy system (AA). The addition of diluent effectively reduces the viscosity of the resin and hence increases its flow behavior. Imidazole used in the study, such as DD/5I/10E, was a low viscosity liquid, and a decrease in the viscosity is observed. Along with any constant shear rate it was also observed that with increase in shear rate the viscosity of each formulation also increased, due to the cure reaction progress. With the increase in shear rate, molecular mobility increases and hence the cure reaction leads to an increase in viscosity.

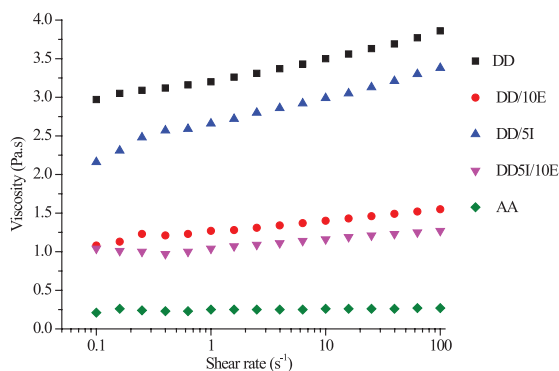


Fig. 1. Graphical representation of viscosity of all the formulations at different shear rates at room temperature obtained from steady state flow tests

1. ábra A vizsgált összetételek viszkozitásának grafikus megjelenítése különböző nyírési sebesség mellett szobahőmérsékleten végzett állandósult folyási vizsgálatból

3.2 Gel time determination (time sweep tests)

The gel time (t_{gel}) of the sample has been evaluated by different methods in the literature [10]. In this paper the crossover of G' and G'' (i.e. $G' = G''$ and $\tan \delta = 1$) was used to evaluate the gel time [11, 12].

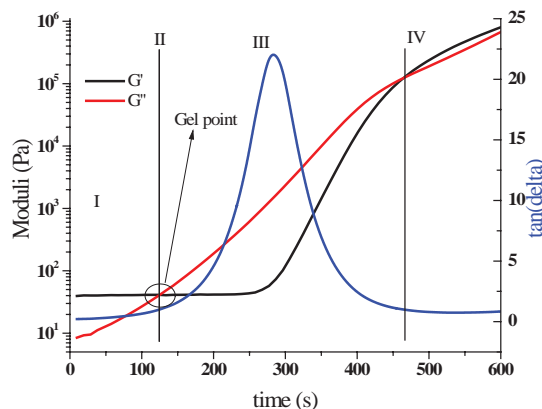


Fig. 2. A representative time sweep test curve for the determination of gel point, G' and G'' values for DD at 80 °C

2. ábra Gélpont meghatározása a G' és G'' keresztezési pontok alapján; DD összetétel, 80 °C hőmérsékleten

Formulation	t_{gel} (s)				
	60 °C	70 °C	80 °C	90 °C	100 °C
DD	375	222	125	84	26
DD/10E	566	398	279	107	37
DD/5I	419	306	218	118	40
DD/5I/10E	500	378	232	123	49
AA	1038	810	530	360	232

Table 2. Gel times calculated from time sweep tests at G' and G'' crossover for all the formulations at different temperatures

2. táblázat Számított gélidők a G' és G'' keresztezési pontok alapján, különböző hőmérsékleteken

Fig. 2 shows a representative response of the time sweep tests for the DD formulation. The plot can be divided into four regions. In the first region, the loss modulus (G'') keeps increasing with time, indicating the increase of viscosity and the structural growth of polymer molecules. By contrast, the storage modulus (G') almost stays constant, indicating that no significant growth of elastic structures due to crosslinking reaction occurs. The second region represents a point where crossover of G' and G'' takes place, and the sample shows similar elastic and viscous behavior. This point is considered as the time where gel formation takes place. In the third region of this plot the shear storage modulus, initially lower than the loss modulus, starts to grow. This indicates that more elastic structure due to crosslinking reaction takes place and the sample becomes semi-solid. The fourth region of the graph represents the sample in solid state where vitrification has occurred. All the samples at different temperatures in this study showed similar type of characteristic curves. Table 2 shows the data of t_{gel} obtained from the time sweep tests for all the formulations at different temperatures. It can be observed that with increase in processing temperature the gel time is reduced for all the formulations. At any particular temperature it can be observed

that the longest time is shown by AA formulation and shortest for DD formulation. Adding 10% diluent increases time to attain gel point because dilution increases molecular mobility and a long time is required for the formulation to become gelled. A similar effect is observed with adding 5% imidazole.

4. Conclusions

In this study, different formulations of DGEBA based epoxy system D.E.R.TM 331TM were developed by varying diluent and catalyst concentration for rapid RTM process. To modify the D.E.R.TM 331TM epoxy system, Epodil[®] was used as epoxy based reactive diluent and 1-Benzyl-2-methylimidazole was employed as catalyst for the formulation. Rheological studies were carried out to determine the resin viscosity at room temperature and the gel time (t_{gel}) at different temperatures for all the formulations. The unmodified D.E.R.TM 331TM epoxy system gels, and thus cures, fast at processing temperature around 100 °C, but it exhibits high viscosity at room temperature. The epoxy system for resin infusion processing (Araldite[®] LY 8601/Aradur[®] 8602) has very low viscosity but it is slow to gel and cure at processing temperature. It was found that the addition of diluent effectively decreases the viscosity of the formulation and improves the resin flow behavior. Although this also increases the gel time, the rate of curing remains fast enough to allow for rapid processing. When better flow characteristics and fiber wetting are desired, compositions with combined addition of imidazole and diluents, such as the DD/5I/10E formulation, could be a good choice, offering good processing characteristics for fast RTM molding.

References

[1] Naffakh, M. – Dumon, M. – Gérard, J. F. (2006): Study of a reactive epoxy-amine resin enabling in situ dissolution of thermoplastic films during resin transfer moulding for toughening composites. *Composites Science and Technology*, Vol. 66, No. 10, pp. 1376-1384. <http://dx.doi.org/10.1016/j.compscitech.2005.09.007>

[2] Pethrick, R. A. – Hayward, D. (2002): Real time dielectric relaxation studies of dynamic polymeric systems. *Progress in Polymer Science*, Vol. 27, No. 9, pp. 1983-2017. [http://dx.doi.org/10.1016/S0079-6700\(02\)00027-8](http://dx.doi.org/10.1016/S0079-6700(02)00027-8)

[3] Ratna, D. (2009): Handbook of Thermoset Resins. *Smithers Rapra Publishing*.

[4] Núñez-Regueira, L. – Gracia-Fernández, C. A. – Gómez-Barreiro, S. (2005): Use of rheology, dielectric analysis and differential scanning calorimetry for gel time determination of a thermoset. *Polymer*, Vol. 46, No. 16, pp. 5979-5985. <http://dx.doi.org/10.1016/j.polymer.2005.05.060>

[5] Dean, D. – Walker, R. – Theodore, M. – Hampton, E. – Nyairo, E. (2005): Chemorheology and properties of epoxy/layered silicate nanocomposites. *Polymer*, Vol. 46, No. 9, pp. 3014-3021. <http://dx.doi.org/10.1016/j.polymer.2005.02.015>

[6] Li, W. – Hou, L. – Zhou, Q. – Yan, L. – Loo, L. S. (2013): Curing behavior and rheology properties of alkyl-imidazolium-treated rectorite/epoxy nanocomposites. *Polymer Engineering & Science*, Vol. 53, No. 11, pp. 2470-2477. <http://dx.doi.org/10.1002/pen.23500>

[7] Ivankovic, M. – Incarnato, L. – Kenny, J. M. – Nicolais, L. (2003): Curing kinetics and chemorheology of epoxy/anhydride system. *Journal of Applied Polymer Science*, Vol. 90, No. 11, pp. 3012-3019. <http://dx.doi.org/10.1002/app.12976>

[8] Liu, Y. – Zhong, X. – Yu, Y. (2010): Gelation behavior of thermoplastic-modified epoxy systems during polymerization-induced phase separation. *Colloid and Polymer Science*, Vol. 288, No. 16-17, pp. 1561-1570. <http://dx.doi.org/10.1007/s00396-010-2288-5>

[9] Mravljak, M. – Sernek, M. (2011): The Influence of Curing Temperature on Rheological Properties of Epoxy Adhesives. *Drvna Industrija*.

[10] Winter, H. H. (1987): Can the gel point of a cross-linking polymer be detected by the $G' - G''$ crossover? *Polymer Engineering & Science*, Vol. 27, No. 22, pp. 1698-1702. <http://dx.doi.org/10.1002/pen.760272209>

[11] Heo, G.-Y. – Park, S.-J. (2012): Rheological and thermal properties of epoxy nanocomposites reinforced with alkylated multi-walled carbon nanotubes. *Polymer International*, Vol. 61, No. 9, pp. 1371-1375. <http://dx.doi.org/10.1002/pi.4215>

[12] Chow, W. S. – Grishchuk, S. – Burkhart, T. – Karger-Kocsis, J. (2012): Gelling and curing behaviors of benzoxazine/epoxy formulations containing 4,4'-thiodiphenol accelerator. *Thermochimica Acta*, Vol. 543, pp. 172-177. <http://dx.doi.org/10.1002/pi.4215>

Ref:

Wang, Youjiang – Lakho, Dildar Ali – Yao, Donggang: *Effect of Additives on the Rheological Properties of Fast Curing Epoxy Resins* Építőanyag – Journal of Silicate Based and Composite Materials, Vol. 67, No. 4 (2015), 132–134. p. <http://dx.doi.org/10.14382/epitoanyag-jsbcm.2015.21>

**International Workshop
Dispersion Analysis
& Materials Testing 2016**

Berlin, Germany, September 26-27, 2016
<http://workshop2016.lum-gmbh.com>
 Find out more at www.dispersion-letters.com

Towards the development of self-compacting no-slump concrete mixtures

HOOMAN HOORNAHAD ▪ Microlab, Faculty of Civil Engineering and Geosciences, Delft University of Technology ▪ h.hoornahad@gmail.com

EDUARDUS A. B. KOENDERS ▪ Institute for Construction and Building Materials, Technische Universität Darmstadt ▪ koenders@wib.tu-darmstadt.de

KLAAS VAN BREUGEL ▪ Microlab, Faculty of Civil Engineering and Geosciences, Delft University of Technology ▪ k.vanbreugel@tudelft.nl

Érkezett: 2015. 07. 31. ▪ Received: 31. 07. 2015. ▪ <http://dx.doi.org/10.14382/epitoanyag-jsbcm.2015.22>

Abstract

No-slump concrete (NSLC) and self-compacting concrete (SCC) are two types of concretes, which became increasingly adapted by the concrete industry because of their specific rheological characteristics. For NSLC mixtures the high shape holding ability allows formworks to be removed shortly after concrete placing. However, NSLC needs a large amount of energy to be properly compacted. For SCC mixtures it is the high flowability and self-compactability that makes them unique. However, as SCC is not able to preserve its shape right after placing, formwork cannot be removed directly after casting. By comparing these two extreme cases, an ideal mixture would have been obtained, i.e. a self-compacting no-slump concrete (SCNSLC), which can compact under its own weight and maintains its shape right after casting. In this paper the possibility of a self-compacting no-slump concrete (SCNSLC) is discussed. The rheological behaviour of these mixtures in the dormant period is in focus, when the degree of hydration is still very limited. The shape holding ability of both mixtures is characterized by a shape preservation factor $0 < \text{SPF} \leq 1$. SPF shows the ability of a mixture to preserve its shape after lifting the cone during a slump test. SPF is the ratio of the vertical cross sectional area of a sample after and before lifting the cone. By increasing flowability of a mixture, the SPF decreases. Results show how to design such mixtures having optimized rheological properties between those of NSLC and SCC.

Keywords: Rheological behaviour, self-compacting no-slump concrete, two-phase aggregate-paste model, shape preservation factor

Kulcsszavak: Reológiai viselkedés, roskadásmentes öntömörödő beton, kétfázisú adalékanyag-pép modell, alaktenyező

1. Introduction

Fresh concrete is a material with continuously changing properties [1]. Concrete gradually changes from a workable mixture into an artificial stone as a result of the hydration process. With respect to the degree of hydration, the period after mixing can be divided into three main periods [2]:

The dormant stage, representing the time interval when the degree of hydration is still very limited and does not significantly affect the rheological behaviour of concretes.

The setting period, representing the time interval in which the development of the degree of hydration leads to a gradual transition of fresh concrete to a solid.

The hardening period, representing the time interval in which concrete gradually gains strength.

Concrete mixtures vary between two extremes with respect to the early age rheological behaviour: no-slump concrete (NSLC) and self-compacting concrete (SCC) [3].

A NSLC mixture has almost zero flowability [4]. A NSLC mixture is able to preserve its shape right after placing. Slip forming method can be used for construction [5]. However, a no-slump concrete is basically a low cement paste mixture that needs a large amount of energy for a proper compaction [4, 5].

A SCC mixture has high flowability. The high flowability is usually achieved by reducing the aggregate content and increasing the paste content with excellent deformability [6].

The deformability can be adjusted by incorporating fillers and admixtures. A SCC mixture is able to compact under its own weight, without applying any external compaction energy [3, 6]. However, as it is not able to preserve its shape right after placing, formwork cannot be removed shortly after placing [5].

By comparing NSLC and SCC, it can be concluded that a very efficient mixture from rheological perspective would be the one which behaves like SCC during casting and behaves like NSLC right after placing. The objective of this paper is to study the possibility of developing such a self-compacting no-slump concrete (SCNSLC), i.e. a self-compacting mixture which can preserve its shape completely right after casting.

2. Rheological model

Fresh concrete is considered as a discontinuous system in this study and it is represented by a two-phase model [7]. These phases are aggregate and paste (see Fig. 1.a). The paste consists of powder particles dispersed in water. 0.125 mm is considered for the boundary size between the aggregate and powder particles [8].

The granular phase is characterized by a factor ζ , i.e. the packing density of the aggregate. ζ is expressed as follows:

$$\zeta = \frac{V_a}{V_b} \leq 1 \quad (1)$$

Hooman HOORNAHAD

received his PhD from Faculty of Civil Engineering and Geosciences, Delft University of Technology. His field of interest is rheology of paste, mortar, concrete and granular material. He is RILEM member and (co-)author of about 20 conference and journal papers. He was a lecturer and research associate in American Concrete Institute (ACI), Iran Chapter.

Eduardus A. B. KOENDERS

is Full Professor and Head of the Institute for Construction and Building Materials, Faculty of Civil and Environmental Engineering, Technical University of Darmstadt. His research interests include multi-scale modeling of hydration and moisture transport, sustainable and durable materials, recycled aggregates and energy saving material concepts for construction. He is RILEM member and chairman of the RILEM EAC MMC course on multi-scale modeling of concrete.

Klaas van BREUGEL

is Full Professor and Head of the Section Materials and Environment, Faculty of Civil Engineering and Geosciences, Delft University of Technology. His fields of expertise concerns design of concrete containment structures, extreme load conditions, early age concrete and modelling and simulation for materials and structures. He is member of several international organisations ACI, RILEM, IABSE and fib. He has chaired several national and international research committees. In 2013 the Ageing Centre for Materials, Structures and Systems was launched under his supervision.

V_a is the specific (solid) volume of aggregate and V_b is the bulk volume of aggregate which represents an aggregate skeleton in a compacted state (see Fig. 1.b). The packing density of aggregate depends on the particle size distribution, shape characteristics of the aggregate particles and packing method [9]. Hu and de Larrard [10] proposed the following expression for the maximum packing density of aggregate with a broad particle size distribution:

$$\zeta_{\max} = 1 - 0.45 \left(\frac{D_{\min}}{D_{\max}} \right)^{0.19} \quad (2)$$

where D_{\min} and D_{\max} are the diameters of the smallest and the largest aggregate particles in the granular skeleton, respectively. In a system of multiple sizes of aggregate, smaller aggregate particles fill up the gaps between the larger aggregate particles and lead to a smaller void volume of the granular skeleton and thus higher packing density [9].

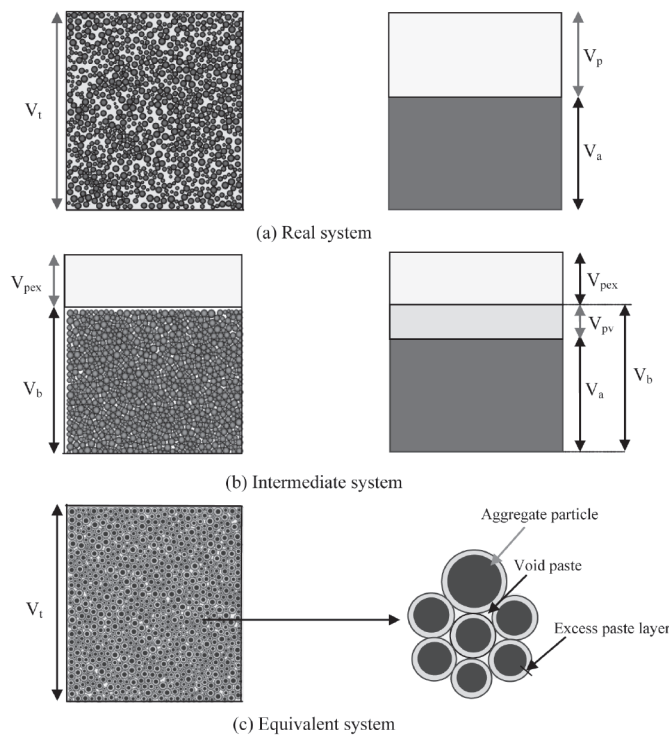


Figure 1. Two-phase aggregate-paste model for concrete. V_t , V_a , V_b , V_p , V_{pv} , and V_{pex} are volume of the sample, specific volume of the aggregate, bulk volume of the aggregate in compacted state, total paste volume, void paste volume and excess paste volume, respectively.

1. ábra Beton kétfázisú adalékanyag-pép modellje. V_t , V_a , V_b , V_p , V_{pv} és V_{pex} a minta térfogata, az adalékanyag térfogata, az adalékanyag tömör térfogata, a teljes péptérfogat, a hézag péptérfogat és a többlet péptérfogat.

The paste phase is divided into two parts, i.e. the void paste and the excess paste (see Fig. 1.b). Void paste is used to fill the void space between the aggregate particles when they are in the compacted state. Void paste behaves like glue and tries to keep the aggregate particles in their positions. The volume of the void paste (V_{pv}) is calculated with Eq. (3) [7]:

$$V_{pv} = \left(\frac{1}{\zeta} - 1 \right) V_a \quad (3)$$

Excess paste is used to form a paste layer with a constant thickness around every single aggregate particle (see Fig. 1.c). Excess paste layers try to facilitate the mobility of the aggregate particles. The volume of the excess paste (V_{pex}) can be calculated with Eq. (4).

$$V_{pex} = V_p - V_{pv} \quad (4)$$

where V_p is the total volume of the paste in the system. The workability of a mixture is strongly correlated with two parameters, i.e. the consistency of the paste and the volume of the excess paste [7]. With increasing paste consistency and excess paste volume, an increase in workability would be expected for a given mixture [7].

3. Workability assessment

As there is no direct test method for the evaluation of workability, this property is indicated indirectly by measuring other performance parameters that are considered to be correlated somehow to the behaviour that must be controlled [11]. Focus is on the shape holding ability of fresh mixtures in this study. In order to evaluate the shape holding ability of mixtures, a slump test is performed [7]. The cone used in this study is selected according to EN 12350-5 [12]. Shape holding ability of mixtures is characterized by the shape preservation factor, $0 < SPF \leq 1$. SPF shows the ability of a mixture to preserve its shape after demolding. SPF is defined as the ratio of the vertical cross sectional area of a three dimensional (3D) sample after and before demolding, i.e. A_f/A_o (see Fig. 2). SPF is equal to 1 for a mixture with zero flowability, i.e. no-slump concrete (NSLC). With increasing flowability of mixtures SPF gradually decreases [7].

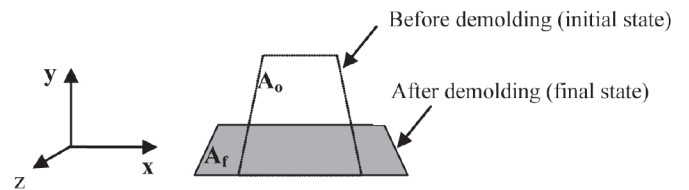


Figure 2. The vertical cross section of a three dimensional (3D) sample before and after demolding. A_o and A_f are the vertical cross sectional area of a 3D sample before and after demolding, respectively. For a 3D sample $A_f \leq A_o$.

2. ábra A 3 dimenziós minta függőleges metszete kiszalasztás megelőzően. A_o és A_f a 3 dimenziós minta függőleges metszetének területe kiszalasztás előtt és után. Egy 3 dimenziós minta esetén $A_f \leq A_o$.

4. Materials and mix composition

Aggregates used in this study consist of natural aggregate particles. The characteristics of the aggregates are given in Table 1. The packing density of aggregates is determined according to ASTM C29-1997 [13]. The paste phase consists of Portland cement CEM I 52.5 with specific density of 3.15 g/cm³, limestone powder with specific density of 2.64 g/cm³, water and superplasticizer. Three different combinations of water-cement ratio, W/C and water-powder ratio, W/P are considered for the pastes (see Fig. 3).

Characteristics

Well graded aggregates with specific density of 2.56 g/cm³, maximum size of 8 mm, minimum size of 0.125 mm and packing density of about 0.80±0.2.

Aggregate particles with a shape deviation of about 3% from the spherical shape. Shape deviation determines the minimum inter-particle distance at which particles become in direct contact [7].

Fineness modulus of granular material is kept between 3.5 and 5.0 to avoid 1) the effect of the gravitational forces acting on aggregate particles [7, 14] and 2) the effect of the very fine aggregate particles, i.e. the aggregate particles which are in the size range of the large powder particles [7, 14], on deformability of the mixtures.

Table 1. Characteristics of the aggregates.
1. táblázat Az adalékanyag jellemzői.

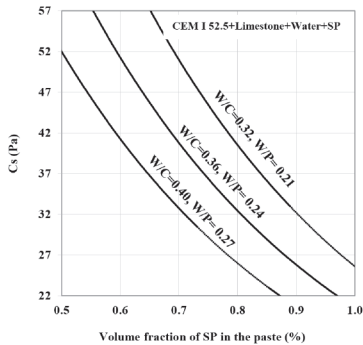


Fig. 3. Critical (yield) stress of the paste vs. volume fraction of superplasticizer SP in the paste for different combinations of water-cement ratio W/C and water-powder ratio W/P. Higher critical stress implies lower consistency (lower ability to flow).

3. ábra Kritikus (folyási) feszültség a pép – folyósítószer (SP) térfogatarányára vonatkoztatva, különböző víz-cement tényező, W/C és víz-kötőanyag tényező, W/P kombinációk esetén. Nagyobb kritikus feszültséghez kisebb konzisztencia (kisebb folyási képesség) tartozik.

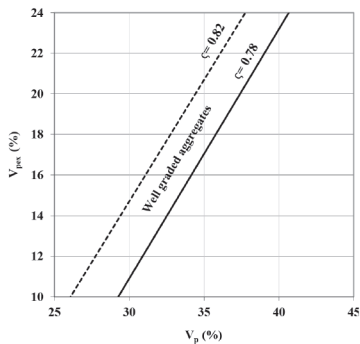


Fig. 4. Correlation between the volume fraction of excess paste V_{pex} and the volume fraction of total paste V_p in the mixtures made with a well graded aggregate. In this figure χ represents the packing density of the aggregates.

4. ábra Korreláció a többlet péptérfogat, V_{pex} és a teljes péptérfogat, V_p között, folytonos szemeloszlású adalékanyag esetén. Az ábrán χ az adalékanyag halmaztömörtségét jelenti.

The consistency of the paste, which is controlled by the amount of superplasticizer (see Fig. 3), is characterized by the critical (yield) stress of the paste Cs [7]. A higher critical stress implies lower consistency (lower ability to flow). The excess paste volume fraction V_{pex} varies from 10 % to 24 % (the maximum volume fraction of the excess paste, which is usually recommended for a concrete mixture, is about 24 % [6]). The correlation between the volume fraction of excess paste V_{pex} and the volume fraction of total paste V_p in the mixtures is represented in Fig. 4.

5. Results and discussion

Correlation between the mix composition, which is characterized by the volume fraction of the excess paste V_{pex} and critical (yield) stress of the paste Cs, and shape holding ability of mixtures is presented in Fig. 5. With increasing volume fraction of the excess paste and decreasing critical stress of the paste, the relative slump H_s/H₀ increases and the shape preservation factor SPF decreases. The slump value H_s is the height reduction of the sample after lifting the cone [7]. The slump value H_s and shape preservation factor SPF are equal to zero and one, respectively, for the mixtures which show no deformation after demolding, i.e. no-slump concrete mixture (NSLC).

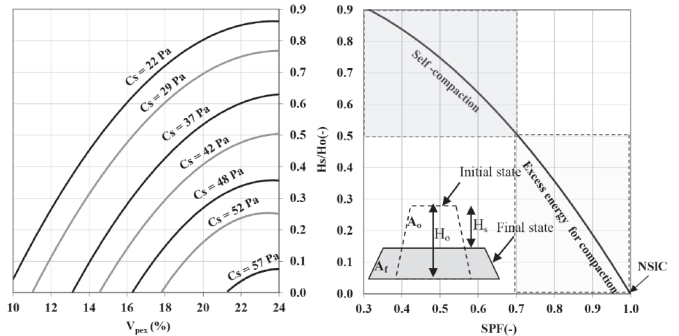


Figure 5. Correlation between the mix composition, which is characterized by the volume fraction of the excess paste V_{pex} and critical (yield) stress of the paste Cs, and shape preservation factor SPF. SPF is equal to the ratio of the vertical cross sectional area of a sample after and before demolding, i.e. A_f/A₀.

5. ábra Korreláció az összetételi jellemzők között; ennek paraméterei a többlet péptérfogat, V_{pex} a pép kritikus (folyási) feszültsége, Cs, és az alaklétényező, SPF. Az alaklétényező, SPF a minta függőleges metszete területének arányát mutatja kiszaladás előtt és után, = A_f/A₀.

The maximum SPF for a self-compacting mixture is about 0.7 (see Fig. 5). For SPF>0.7, extra energy is required for proper compaction. A mixture with SPF≈0.7 shows a relative slump H_s/H₀≈0.5 (see Fig. 5). For a mixture with SPF≈0.7, the spread diameter at final state D_f is equal to 290 mm ± 10 mm and thus the relative spread diameter D_f/D₀≈1.4-1.5 [7]. H_s/H₀≈0.5 and D_f/D₀≈1.4-1.5 are in the range of those proposed by Wang et al [5] for self-compacting mixtures used in pavement construction. They stated that those mixtures can preserve their shape without any additional support after the slip form paving process. For a conventional self-compacting concrete mixture (SCC) with a relative spread diameter D_f/D₀≥3, the SPF is less than about 0.4 [7].

A self-compacting no-slump concrete (SCNSLC) could be achieved if we were able to increase the critical stress of the paste Cs shortly after placing and before demolding. A self-compacting mixture with SPF≈0.7 would behave like a no-slump concrete with SPF≈1 after demolding if we were able to increase Cs after placing of the mixture as presented in Fig. 6. The required increase of Cs is about 17 Pa. With decreasing the shape preservation factor SPF of the reference mixture the larger increase of Cs is required [7].

At early age, i.e. when the hydration effect is still negligible, the rheological behaviour of a paste strongly depends on the attractive van der Waals forces and the repulsive electrostatic forces between the powder particles [15, 16]. With decreasing repulsive forces between the particles the flowability (consistency) of the paste decreases. The repulsive electrostatic

forces between the powder particles strongly depend on the ion concentration in the liquid in which particles are dispersed [17]. Therefore, if we could change the ion concentration in the mixture after placing, we would be able to control the paste consistency, and thus the shape holding ability of the mixture. A consistency change of the paste shortly after placing can theoretically be obtained by adding *smart particles* to a mixture before placing. Smart particles are made of materials with properties engineered to undergo changes in a controlled manner [18, 19]. A smart particle usually consists of a core (fill) coated with a layer called membrane. The core contains a material that is released by breaking or dissolving the membrane under particular conditions. The inside content can be a latex material, i.e. a dispersion of charged particles [20]. The membrane can be made of a material which is engineered to dissolve in water in a controlled manner. This topic is beyond the scope of this paper. Further research is recommended.

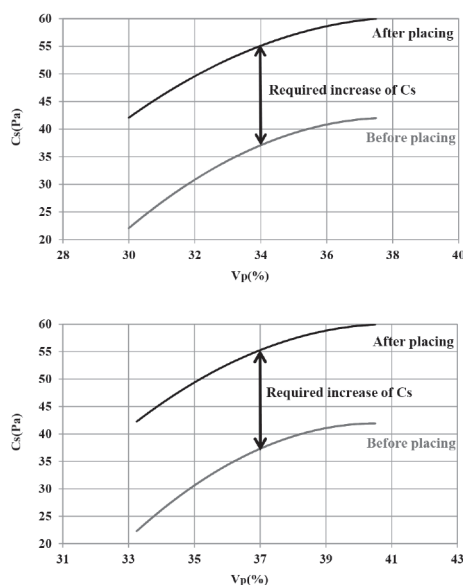


Figure 6. Required change of critical stress C_s of the paste for mixtures with shape preservation factor $SPF=0.7$ to behave like a no-slump concrete after demolding. V_p is the volume fraction of the total paste.

6. ábra A kritikus feszültség, C_s szükséges értéke a roskadásmentes beton eléréséhez az alaktényező $SPF=0.7$ értéke esetén; V_p a teljes péptérfogat.

6. Conclusions

The objective of this paper was to study the possibility of developing a self-compacting no-slump concrete mixture (SCNSLC), i.e. a concrete mixture which can compact under its own weight while preserving its shape almost completely right after placing. In order to evaluate the shape holding ability of mixtures, slump test was performed. The shape holding ability of a mixture is indicated with the shape preservation factor ($0 < SPF \leq 1$). SPF is defined as the ratio of the vertical cross sectional area of a three dimensional (3D) sample after and before demolding. For a no-slump concrete mixture (NSLC), i.e. a mixture with zero deformation after demolding, it holds $SPF=1$. It was found that the maximum SPF for a self-compacting mixture is about 0.7. For a self-compacting mixture with a higher shape preservation factor, i.e. $SPF > 0.7$, especially SCNSLC, it is required to increase critical stress of the paste

Cs shortly after placing and before demolding. A consistency change of the paste shortly after placing can theoretically be obtained by, for example, adding smart particles to the mixture before placing. Further research on this topic is recommended.

References

- [1] Neville, A. M. (1995): Properties of Concrete 4th Ed. *Pearson Education Limited*, England.
- [2] Schindler, A. K. (2004): Prediction of concrete setting. *Proc. Int. RILEM Symp. on Concrete Science and Engineering: A Tribute to Arnon Bentur*. RILEM Publications SARL.
- [3] Koehler, E. P. – Fowler, D. W. (2003): Summary of Concrete Workability Test Methods. *International Center for Aggregates Research, The University of Texas, USA*.
- [4] ACI Committee 211.3R (2002): Guide for Selecting Proportions for No-Slump Concrete.
- [5] Wang, K. et al (2011): Self-Consolidating Concrete—Applications for Slip-Form Paving: Phase II. *National Concrete Pavement Technology Center, Institute for Transportation, Iowa State University, USA*.
- [6] RILEM TC 174 SCC (2000): Self-Compacting Concrete. *RILEM Publications SARL*.
- [7] Hoornahad, H. (2014): Toward Development of Self-Compacting No-slump Concrete Mixtures - PhD Thesis. *Ipskamp Drukkers BV, Delft*.
- [8] EFNARC (2002): Specification and Guidelines for Self-Compacting Concrete.
- [9] Kwan, A. K. H. – Mora, C. F. (2001): Effects of various shape parameters on packing of aggregate particles. *Magazine of Concrete Research*, Vol. 53, No. 2, pp. 91-100. <http://dx.doi.org/10.1680/mac.53.2.91.39505>
- [10] Hu, C. – De Larrard, F. (1996): The rheology of fresh high performance concrete. *Cement and Concrete Research*. Vol. 26, No. 2, pp. 283-294. [http://dx.doi.org/10.1016/0008-8846\(95\)00213-8](http://dx.doi.org/10.1016/0008-8846(95)00213-8)
- [11] Wong, G. S. et al (2001): Portland-Cement Concrete Rheology and Workability: Final Report. *USAE Research and Development Center*.
- [12] EN 12350-5 Testing Fresh Concrete - Part 5: Flow Table Test.
- [13] ASTM C29/C29M (1997): Standard Test Method for Bulk Density (“Unit Weight”) and Voids in Aggregate.
- [14] Hoornahad, H. – Koenders, E. A. B. (2011): Consistency assessment method for granular-cement paste systems. *Advanced Materials Research*, Vols. 295-297, pp. 2178-2184. <http://dx.doi.org/10.4028/www.scientific.net/AMR.295-297.2178>
- [15] Chappuis, J. (1982): Concrete Rheology. *Materials Research Society*, p. 38.
- [16] Chappuis, J. (1986): *Proceedings of the 8th International Congress on Chemistry of Cement*. Vol. 6, p. 544.
- [17] Coussot, P. (2005): Rheometry of Pastes, Suspensions, and Granular Materials. *John Wiley & Sons, New Jersey*.
- [18] Nayak, S. – Lyon, L. A. (2004): Photoinduced phase transitions in poly (n-isopropylacrylamide) microgels. *Chemistry of Materials*. Vol. 16, pp. 2623-2627. <http://dx.doi.org/10.1021/cm049650i>
- [19] Ballauff, M. – Lu, Y. (2007): Smart nanoparticles: preparation, characterization, and applications. *Polymer*. Vol. 48, No. 7, pp. 1815-1823. <http://dx.doi.org/10.1016/j.polymer.2007.02.004>
- [20] Rixom, R. – Mailvaganam, N. (1999): Chemical Admixtures for Concrete. *E & FN Spon, London*.

Ref:

Hoornahad, Hooman – Koenders, Eduardus A. B. – van Breugel,
 Klaas: *Towards the development of self-compacting no-slump concrete mixtures*
 Építőanyag – Journal of Silicate Based and Composite Materials,
 Vol. 67, No. 4 (2015), 135–138. p.
<http://dx.doi.org/10.14382/epitoanyag-jsbcm.2015.22>

Wettability of particles and its effect on liquid bridges in wet granular materials

HOOMAN HOORNAHAD ▪ Microlab, Faculty of Civil Engineering and Geosciences, Delft University of Technology ▪ h.hoornahad@gmail.com

EDUARDUS A. B. KOENDERS ▪ Institute for Construction and Building Materials, Technische Universität Darmstadt ▪ koenders@wib.tu-darmstadt.de

KLAAS VAN BREUGEL ▪ Microlab, Faculty of Civil Engineering and Geosciences, Delft University of Technology ▪ k.vanbreugel@tudelft.nl

Érkezett: 2015. 07. 31. ▪ Received: 31. 07. 2015. ▪ <http://dx.doi.org/10.14382/epitoanyag-jsbcm.2015.23>

Abstract

This paper provides results of an experimental study on the force-distance relationship between two particles connected by a liquid bridge. This experimental research is based on water bridges and extended to cement paste bridges with the aim to explain and model the rheological behaviour of fresh concrete mixtures, and to create a fundamental basis for developing mixtures with a predefined deformation performance. The research approach is based on a conceptual idea where the mixture is considered as an assembly of mutually interacting “particle-paste-particle” systems and the rheological behaviour of the mixture is related to the inter-particle interactions. The concept of capillary cohesion in wet granular materials, which describes the interaction between two particles connected by a liquid bridge, is considered the first step in the investigations. The effect of the wettability of the particles on the force-distance relation of two particles connected by a liquid bridge is studied. Static and/or quasi-static situations are in focus, i.e. where the cohesion dominates over other effects generated by the liquid, such as viscosity and lubrication. Tests were carried out using spherical stainless steel and glass particles and water was used as the liquid with a surface tension of $\sigma_{in}=0.072$ mN/mm. The contact angle between water and glass is about 15° while between water and stainless steel it is about 60° . It is found that the wettability of particles has a great influence on the force-distance relation of the interacting particles. Conclusion is drawn regarding the possibility to use the generated data as a basis for modelling the rheological behaviour of cement-based mixtures.

Keywords: Fresh concrete, rheological model, wet granular material, liquid bridge, wettability, contact angle, interaction force

Kulcsszavak: frissbeton, reológiai modell, nedves szemcsehalmoz, folyadék-híd, nedvesíthetőség, nedvesítési szög, kölcsönhatási erő

Hooman HOORNAHAD received his PhD from Faculty of Civil Engineering and Geosciences, Delft University of Technology. His field of interest is rheology of paste, mortar, concrete and granular material. He is RILEM member and (co-)author of about 20 conference and journal papers. He was a lecturer and research associate in American Concrete Institute (ACI), Iran Chapter.

Eduardus A. B. KOENDERS is Full Professor and Head of the Institute for Construction and Building Materials, Faculty of Civil and Environmental Engineering, Technical University of Darmstadt. His research interests include multi-scale modeling of hydration and moisture transport, sustainable and durable materials, recycled aggregates and energy saving material concepts for construction. He is RILEM member and chairman of the RILEM EAC MMC course on multi-scale modeling of concrete.

Klaas van BREUGEL is Full Professor and Head of the Section Materials and Environment, Faculty of Civil Engineering and Geosciences, Delft University of Technology. His fields of expertise concerns design of concrete containment structures, extreme load conditions, early age concrete and modelling and simulation for materials and structures. He is member of several international organisations ACI, RILEM, IABSE and fib. He has chaired several national and international research committees. In 2013 the Ageing Centre for Materials, Structures and Systems was launched under his supervision.

1. Introduction

Fresh concrete is considered as an intermediate class between cement pastes and granular materials from a rheological perspective [1, 2, 3]. Fresh concrete exhibits a complex behaviour which can be close to either a cement paste or a granular system, depending on the properties and proportion of constituents in the mixture. The aim of this research is to explain and model the rheological behaviour of fresh concrete mixtures and to create a fundamental basis for developing mixtures with a predefined deformational performance [2].

In this study, a mixture is considered as an assembly of mutually interacting “particle-paste-particle” systems (see Fig. 1.a), in which the rheological behaviour of the mixture is related to the inter-particle interactions [4, 5]. A system consists of a pair of two-phase elements connected by a paste bridge (see Fig. 1.b). Each element consists of an aggregate particle covered with a paste layer. A paste bridge represents the cohesion between the elements and resists increasing distance between two elements [2].

In order to characterize the interaction in a “particle-paste-particle” system the concept of capillary cohesion in wet granular material [6], which describes the interaction between two particles connected by a liquid bridge (see Fig. 1.c), is considered the first step in the investigation. First, the interactions in

“particle-liquid-particle” systems are studied experimentally. These tests are then extended for “particle-paste-particle” systems. In this paper preliminary results of the experimental work on “particle-liquid-particle” systems are provided.

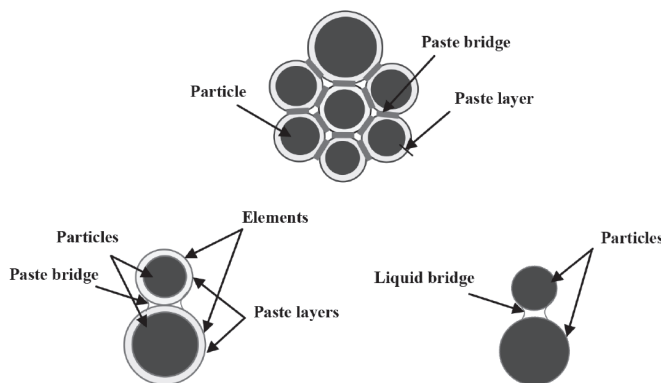


Fig. 1. Features of two-phase modeling approach [2, 4].
 (a) Scheme of an assembly of mutually interacting “particle-paste-particle” systems
 (b) “Particle-Paste-Particle” system
 (c) “Particle-Liquid-Particle” system
 1. ábra A két fázisú model alapelvei [2, 4].
 (a) Kölcsönhatásban lévő szemcse-pép-szemcse rendszer sémája
 (b) Szemcse-pép-szemcse rendszer
 (c) Szemcse-folyadék-szemcse rendszer

2. Interaction between two particles connected by a liquid bridge

In a static or quasi-static situation, where the cohesion dominates over other effects generated by the liquid, such as viscosity and lubrication, the magnitude of the liquid bridge force is related to the geometry of a liquid bridge [6, 7, 8]. The geometry of a liquid bridge depends on 1) the characteristics of the particles (shape, size and wettability), 2) the surface tension of the liquid, 3) the volume of the liquid and 4) the inter-particle distance [2, 6, 9]. In this paper the wettability of solid particles and its effect on the force-distance relation of two particles connected by a liquid bridge is in the main focus.

Wettability is the ability of a solid surface to be wetted when it is in contact with a liquid. Wettability can be characterized by the contact angle θ_0 , i.e. the angle at which the liquid-gas interface meets the solid-liquid interface (see Fig. 2). When the solid is extremely easy to wet, the contact angle has a low value. In this case a thin film of liquid is formed on the surface (see Fig. 2.a). It means that the liquid is strongly attached to the solid surface. With decreasing wettability of solid surface and thus increasing contact angle θ_0 the solid-liquid interface decreases (see Fig. 2.b). When the solid is extremely difficult to wet, the contact angle θ_0 approaches 180°, corresponding to the spherical drop having only one point of contact with the solid [10].

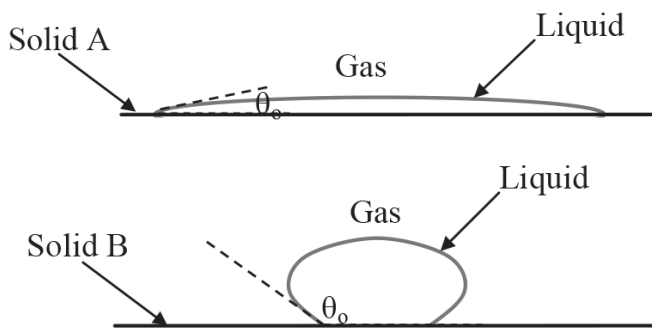


Fig. 2. Scheme of configuration of a liquid on a solid surface.
 (a) Solid surface with high wettability (low contact angle θ_0)
 (b) Solid surface with low wettability (high contact angle θ_0)
 2. ábra Folyadéksepp elhelyezkedésének vázlata szilárd felületen.
 (a) Jól nedvesíthető szilárd felület (kis nedvesítési szög θ_0)
 (b) Rosszul nedvesíthető szilárd felület (nagy nedvesítési szög θ_0)

3. Experimental test

In order to study the force-distance relationship between two particles connected by a liquid bridge a displacement controlled tensile test was performed by a specially designed experimental apparatus (see Fig. 3) [2]. In the set-up, one of the particles (lower one) is fixed to a support mounted at a highly sensitive balance (10^{-4} g) and the other particle (upper one) is fixed on a cantilever and can move vertically. The movement of this cantilever is controlled by a velocity controlled micrometer screw and its displacement is recorded by a LVDT sensor connected to a computer.

After putting the liquid drop of a given volume on the stationary particle, the two particles are brought into contact.

At this stage, the test starts and the distance between the two particles is gradually increased until the point is reached at which rupture of the liquid bridge occurs [2]. At selected inter-particle distances, the magnitude of the interaction force is measured. During the test, a picture of the liquid bridge is recorded for the profile analysis. Temperature and relative humidity in the chamber around the specimen is kept between 22-23° C and between 97-100 %, respectively.

Tests were carried out using spherical stainless steel and glass particles and water was used as the liquid with a surface tension of $\sigma_{in}=0.072$ mN/mm. The contact angle θ_0 between water and stainless steel is about 60° and between water and glass about 15° (see Fig. 4).

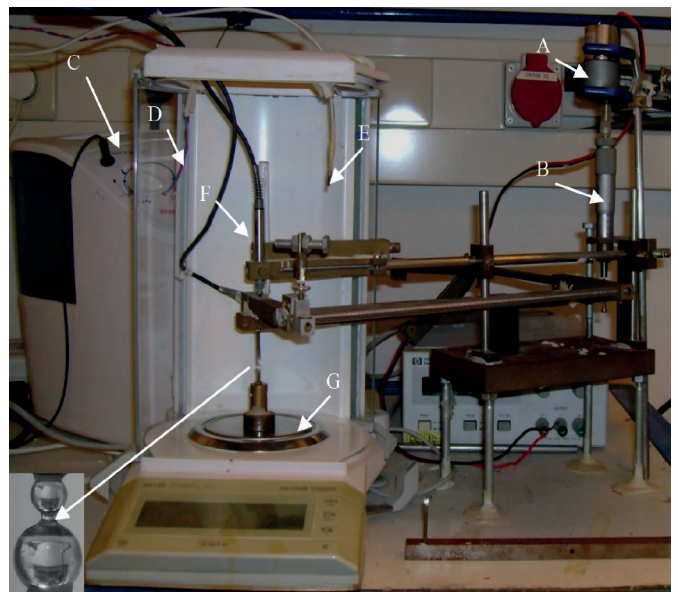


Fig. 3. Test device used for studying the interaction between two particles connected by a liquid bridge or two elements connected by a paste bridge. A: Velocity control armature, B: Micrometer screw, C: Humidifier, D: Temperature sensor, E: Humidity sensor, F: LVDT sensor, G: Scale.
 3. ábra Vizsgálóeszköz két szemcse folyadékbróval vagy két szemcse péphiddal történő érintkezésének vizsgálatához. A: Sebesség szabályzó állványzat, B: Mikrométercsavar, C: Párásító készülék, D: Hőmérő szenzor, E: Páratartalom szenzor, F: Útadó szenzor, G: Mérleg.

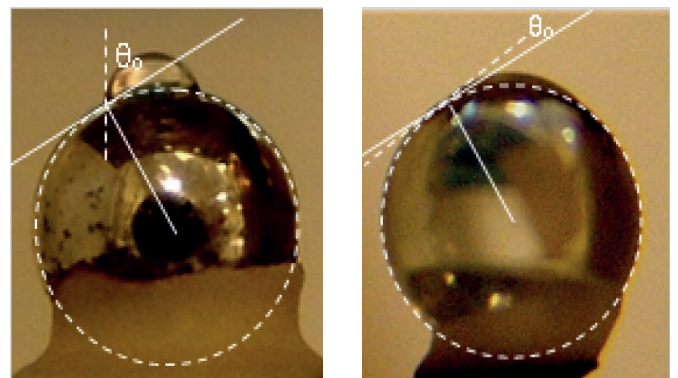


Fig. 4. Contact angle between a water drop and the surface of a particle.
 (a) Stainless steel particle ($\theta_0=60^\circ$)
 (b) Glass particle ($\theta_0=15^\circ$)
 4. ábra Nedvesítési szög vízsepp és szemcsfelület között.
 (a) Rozsdamentes acél szemcse ($\theta_0=60^\circ$)
 (b) Üveg anyagú szemcse ($\theta_0=15^\circ$)

4. Results and discussion

The results for 4 mm stainless steel and glass particles for two different volumes of the water bridge (0.1 mm³ and 0.5 mm³) are shown in Fig. 5. Results show that with increasing inter-particle distance, S the interaction force first increases and then gradually decreases. This behaviour is more noticeable for the stainless steel-water-stainless steel system than for the glass-water-glass system. This behaviour can be explained as follows.

Any force that tries to change the actual shape of the drop in the equilibrium condition causes some instability inside the drop [2]. During the experimental test, it turned out that instability happens in the system when the inter-particle distance becomes less than the height of the drop due to the compressive stress applied to the drop. The applied force tries to increase the solid-liquid interface while the liquid naturally resists against this deformation. This leads to an increase in the contact angle between the profile of the bridge and the solid surface at the intersection of the three-phase interfaces (see Fig. 6) [2, 6].

The instability in the system increases by gradually decreasing the inter-particle distance. As the contact angle between water and glass is small ($\theta_0=15^\circ$), water can spread more easily over the surface of the glass particle in comparison with a spread of water on the surface of stainless steel particles, where the contact angle is considerably larger ($\theta_0=60^\circ$) (see Fig. 4). Therefore, in the case of glass and water, the drop experiences less instability during the test than in the case of stainless steel and water.

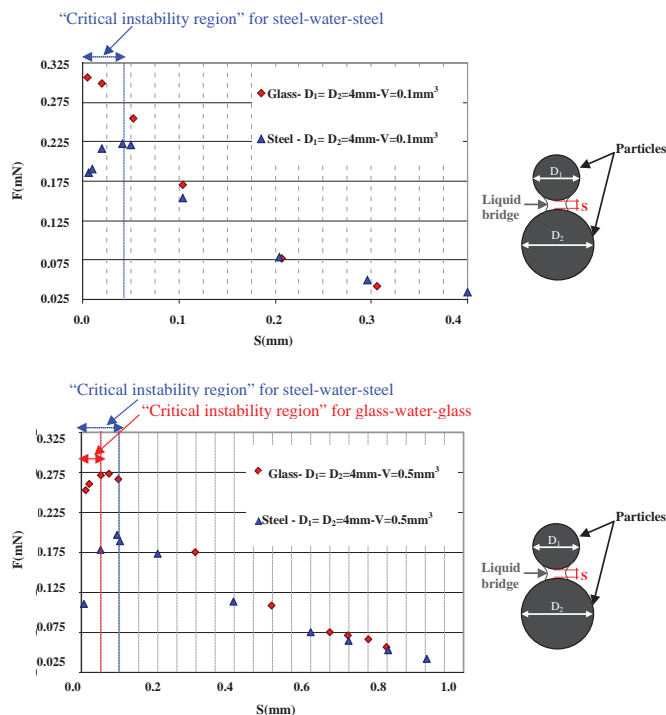


Fig. 5. Force-distance plot for 4 mm stainless steel and glass particle-pairs.

- (a) Volume of the water bridge $V=0.1 \text{ mm}^3$
- (b) Volume of the water bridge $V=0.5 \text{ mm}^3$

5. ábra Erő-elmozdulás ábrák 4 mm átmérőjű rozsdamentes acél és üveg anyagú szemcsékre.

- (a) Vízhid térfogata $V=0.1 \text{ mm}^3$
- (b) Vízhid térfogata $V=0.5 \text{ mm}^3$

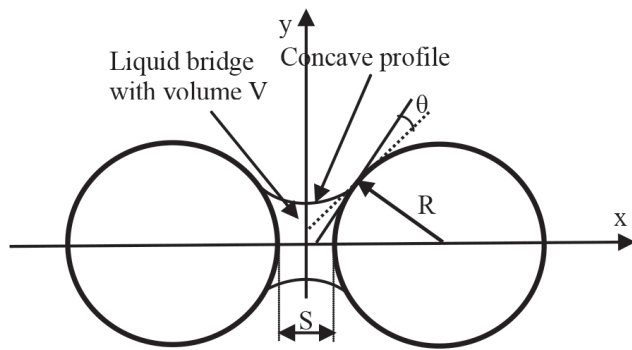


Fig. 6. Characteristic geometrical scheme of a symmetrical liquid bridge between two particles. θ , contact angle between the liquid bridge and particle surface, is the angle between a line tangent to the gas-liquid interface and a line tangent to the liquid-solid interface at the intersection of three-phase interfaces.

6. ábra Két szemcse között kialakuló folyadék-híd jellegzetes geometriai sémája. A nedvesítési szög θ , a gáz-folyadék határfelülethez húzott érintő és a folyadék-szilárd fázis határfelülethez húzott érintő által bezárt szög, a három fázis érintkezési pontjában.

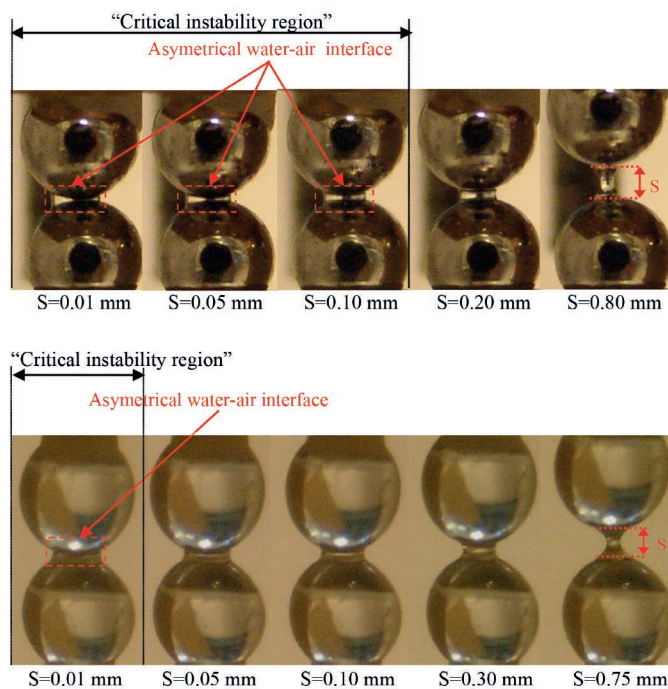


Fig. 7. Evolution of the shape of the water bridge with the inter-particle distance corresponding to the results indicated in Fig. 5.b. S_c is critical inter-particle distance.

- (a) 4 mm stainless steel particles ($\theta_0=60^\circ$, $S_c \sim 0.10 \text{ mm}$)
- (b) 4 mm glass particles ($\theta_0=15^\circ$, $S_c \sim 0.05 \text{ mm}$)

7. ábra A vízhid alakjának változása a szemcsék közötti távolság változtatásának hatására, az 5.b ábrán bemutatott eredményekhez kapcsolódóan. Az ábrán S a szemcsék közötti kritikus távolság.

- (a) 4 mm átmérőjű rozsdamentes acél szemcsék ($\theta_0=60^\circ$, $S_c \sim 0.10 \text{ mm}$)
- (b) 4 mm átmérőjű üveg anyagú szemcsék ($\theta_0=15^\circ$, $S_c \sim 0.05 \text{ mm}$)

The evolution of the shape of the liquid bridges, corresponding to the results of Fig. 5.b, is shown in Fig. 7. It is observed that the instability effect becomes significant in the “critical instability region”, i.e. the region where the water-air interface becomes asymmetrical concave-convex (see Fig. 7). In this region the contact angle, θ between the liquid bridge and the particle surface becomes larger than the contact angle between the drop and the particle surface, θ_0 [2]. This effect becomes clearer by gradually decreasing the distance between the two

particles. The “critical instability region” can be distinguished by the critical inter-particle distance, S_c representing the inter-particle distance below that liquid bridge profile becomes asymmetrical. As it is shown in Fig. 7 the critical inter-particle distance, S_c depends on the wettability of the particles. Critical inter-particle distance, S_c increases with decreasing wettability of particles.

For the stainless steel-water case, with contact angle of $\theta_o=60^\circ$ between the water drop and surface of the particle and with drop volume of $V=0.5 \text{ mm}^3$, the instability effect became significant when the distance between the two particles becomes less than about 0.10 mm (see Fig. 5.b). In this case the maximum contact angle between the profile of the bridge and the solid surface becomes more than 90° with decreasing inter-particle distance (see Fig. 7.a). For the glass-water case, with a contact angle of $\theta_o=15^\circ$ between the water drop and surface of the particle and with drop volume of $V=0.5 \text{ mm}^3$, the instability effect became significant at a shorter inter-particle distance, S than that for the stainless steel-water case. In this case the critical inter-particle distance, S_c is less than about 0.05 mm (see Fig. 5.b). With decreasing inter-particle distance the maximum contact angle between the profile of the bridge and the solid surface approaches to about 40° . Outside the “critical instability region” a quite symmetrical concave profile is observed for the liquid bridge between the particles (see Fig. 7). In this region the interaction force decreases with gradually increasing inter-particle distance (see Fig. 5). For the stainless steel-water case with drop volume of $V=0.1 \text{ mm}^3$, the instability effect became significant for an inter-particle distance less than about 0.05 mm (see Fig. 5.a). For the glass-water case with drop volume of $V=0.1 \text{ mm}^3$, instability effect was not observed (see Fig. 5.a). It is also observed that rupturing of the liquid bridge happens at a larger inter-particle distance with increasing contact angle, θ_o . For the stainless steel-water case the rupture distance is about 20% larger than that of the glass-water case (see Fig. 5).

5. Conclusions

Results of an experimental study of the force-distance relation between two particles connected by a liquid bridge have been addressed in this paper. The experimental research on water bridges was the part of the experimental study which has been performed with the aim to create a fundamental basis for developing concrete mixtures with a predefined deformational performance. The effect of the wettability of the particles on the force-distance relation of two particles connected by a liquid bridge in static and/or quasi-static situations was in focus in this paper, where the magnitude of interaction force is related to the geometry of the liquid bridge. Wettability, which is defined as the ability of a solid surface to be wetted when in contact with a liquid, can be characterized by the contact angle θ_o , i.e. the angle at which the liquid-gas interface meets the solid particle-liquid interface. The displacement controlled tensile tests were carried out using spherical stainless steel with low wettability ($\theta_o=60^\circ$) and glass particles with high wettability ($\theta_o=15^\circ$) and water was used as the liquid with a surface tension of

$\sigma_{in}=0.072 \text{ mN/mm}$. With respect to the inter-particle distance (S), two regions have been distinguished:

- Region A (critical instability region), with an inter-particle distance $0 < S < S_c$, where the profile of the liquid bridge is asymmetrical concave-convex. In this region the interaction force increases with increasing inter-particle distance.
- Region B, with an inter-particle distance $S \geq S_c$, where the profile of the liquid bridge is symmetrical concave. In this region interaction force decreases with increasing inter-particle distance.

It was found that the critical inter-particle distance S_c depends on the wettability of the particles. With decreasing wettability of particles, increasing θ_o , the critical inter-particle distance S_c increases. It is also observed that with decreasing wettability of particles, increasing θ_o , rupturing of the liquid bridge happens at a larger inter-particle distance.

References

- [1] Coussot, P. (2005): Rheometry of Pastes, Suspensions, and Granular Materials. *John Wiley & Sons*, New Jersey.
- [2] Hoornahad, H. (2014): Toward Development of Self-Compacting No-slump Concrete Mixtures- PhD Thesis. *Ipskamp Drukkers BV*, Delft.
- [3] Hoornahad, H. – Koenders, E. A. B. (2013): Effect of the mix composition on rheological behavior of a fresh granular-cement paste material. *Proc. 1st RILEM Int. Conf. on Rheology and Processing of Construction Materials*, Paris.
- [4] Hoornahad, H. – Koenders, E. A. B. (2014): Modelling rheological behavior of fresh cement-sand mixtures. *Proc. 33rd Int. Conf. on Ocean, Offshore and Arctic Engineering*, San Francisco.
- [5] Hoornahad, H. – Koenders, E. A. B. (2012): Simulation of the slump test based on the discrete element method (DEM). *Advanced Materials Research*, Vols. 446-449, pp. 3766-3773. <http://dx.doi.org/10.4028/www.scientific.net/AMR.446-449.3766>
- [6] Soulié, F. – Cherblanc, F. – El Youssoufi, M. S. – Saix, C. (2006): Influence of liquid bridges on the mechanical behavior of polydisperse granular materials. *Int.J. for Numerical and Analytical Methods in Geomechanics*. Vol. 30, pp. 213-228. <http://dx.doi.org/10.1002/nag.476>
- [7] Mitarai, N. – Noriz, F. (2006): Wet granular materials. *Advances in Phys.* Vol. 55, No. 1-2, pp. 1-45. <http://dx.doi.org/10.1080/00018730600626065>
- [8] Lambert, P. (2007): Capillary Forces in Microassembly - Modeling, Simulation, Experiments and Case Study. *Springer*. <http://dx.doi.org/10.1007/978-0-387-71089-1>
- [9] Hoornahad, H. – Koenders, E. A. B. – van Breugel, K. (2010): Capillary cohesion between two spherical glass particles. *Key Engineering Materials*, Vols. 417-418, pp. 449-452. <http://dx.doi.org/10.4028/www.scientific.net/KEM.417-418.449>
- [10] Miller, C. A. – Neogi, P. (1985): Interfacial Phenomena Equilibrium and Dynamic Effects Surfactant Science Series 17, *Taylor & Francis Group*.

Ref:

Hoornahad, Hooman – Koenders, Eduardus A. B. – van Breugel, Klaas: *Wettability of particles and its effect on liquid bridges in wet granular materials*
Építőanyag – Journal of Silicate Based and Composite Materials, Vol. 67, No. 4 (2015), 139–142. p.
<http://dx.doi.org/10.14382/epitoanyag-jsbcm.2015.23>

Methods and equipment for the investigation of rheological properties of complex materials like convectional brick clays and ceramic reinforced composites

L. A. GÖMZE ▪ University of Miskolc Institute of Ceramics and Polymer Engineering
▪ femgomze@uni-miskolc.hu

L. N. GÖMZE ▪ Igrax Engineering Service Ltd. Igrici, Hungary ▪ igrex2009@yandex.ru

N. S. KULKOV ▪ Tomsk State University, Russia

L. I. SHABALIN ▪ University of Salford, United Kingdom

I. GOTMAN ▪ University of Technion, Israel

F. PEDRAZA ▪ University of La Rochelle, France

G. L. LECOMTE ▪ Université de Limoge - ENSCI, France

T. MAYOROVA ▪ Syktyvkar State University, Russia

E. KUROVICS ▪ University of Miskolc Institute of Ceramics and Polymer Engineering

A. HAMZA ▪ University of Miskolc Institute of Ceramics and Polymer Engineering

Érkezett: 2015. 08. 01. ▪ Received: 01. 08. 2015. ▪ <http://dx.doi.org/10.14382/epitoanyag-jsbcm.2015.24>

Abstract

In the present work two special instruments are described and introduced which were developed for the rheological tests of materials like minerals, raw materials and semi-finished products of ceramic industry or complex materials like ceramic particles and fibre reinforced metal alloys and hetero-module, hetero-viscous and hetero-plastic materials with increased dynamic strength. The working principles of introduced 'rheotesters' are relatively simple and easy for use to determine rheological parameters like instantaneous elastic modulus, delayed elastic modulus or viscosity of damaged and undamaged material structures. The instruments give the opportunity to easily and quickly prepare the rheological model of tested materials.

Keywords: ceramics, composites, instrument, modulus of elasticity, rheology, viscosity

Kulcsszavak: kerámiák, kompozitok, vizsgáló berendezés, rugalmassági modulus, reológia, viszkozitás

1. Introduction

There are many scientific works can be found recently for the investigation of rheological properties of materials in nanoscale [1-4]. Nevertheless, it is quite difficult to determine in macro-scale the most important rheological parameters of complex materials like

- mined convectional brick clays,
- concrete mixtures reinforced with fibres,
- asphalt pavements and asphalt concretes,
- ceramic particles and ceramic fibre reinforced metallic matrix composites,
- hetero-module, hetero-viscous and hetero-plastic complex materials.

During the production of ceramics and ceramic reinforced composites it is obvious that the chemical and structural transformations in the materials are taking place as reactions in solid phase [5-10]. At a certain temperature and chemical or mineralogical composition the rate of these solid phase reactions are very high depending on the concentration of components and the volumes of their contact surfaces. Due to these, one of the most important technological goals during the production of convectional bricks, ceramic roof tiles, technical ceramics and ceramic reinforced composite materials

is to give specific surface area as large as possible for the used raw materials during their crushing and comminuting. The achieved specific surface area of the components has very strong influence not only on forming processes and quality but on the required energy consumption of heat treatment or firing as well [11-15]. To get the necessary magnitude of specific surfaces of the raw materials the required energy consumption depends not only on their chemical and mineralogical

László A. GÖMZE

is establisher and former head of Department of Ceramics and Silicate Engineering in the University of Miskolc (Hungary). Author or co-author of 2 patents, 5 books and more than 250 scientific papers.

Ludmila N. GÖMZE

is MSc (civil engineer), managing director of the IGREX Engineering Ltd. Author or co-author more than 30 scientific papers.

Sergey N. KULKOV

is head of Department of Ceramics in the Institute of Strength Physics and Materials Science of the Russian Academy of Science Author of 5 books, more than 150 articles and 18 patents.

Igor SHABALIN

is member of the Materials and Physics Research Centre at University of Salford (United Kingdom). He has a wide range experience in research of various high-temperature/hard ceramic and composite materials.

Irena GOTMAN

is a senior research and teaching Fellow at Department of Materials Science & Engineering at Technion as a Levi Eshkol Post-doctoral Fellow. She is a member of European Society for Biomaterials (ESB).

Fernando PEDRAZA

is a professor at Laboratoire des Sciences de l'Ingénieur pour l'Environnement in the Université de La Rochelle (France). Vice-president of Université de La Rochelle and responsible for the international relations.

Gisèle LECOMTE-NANA

is a member of the Groupe d'Etude des Matériaux Hétérogènes (GEMH), Ecole Nationale Supérieure de Céramique Industrielle, Centre Européen de la Céramique (France). Author or co-author of 36 scientific papers.

Tatiana MAYOROVA

is working at Institute of Geology, Komi Science Centre, Ural Division, Russian Academy of Sciences, Syktyvkar (Russian Federation). She has considerable success in research of gallium and gold deposits.

Emese KUROVICS

is a student of the Faculty of Materials Science and Engineering at University of Miskolc and preparing her diploma thesis under the supervision of Prof. Gömze.

Alexandra HAMZA

is a student of the Faculty of Materials Science and Engineering at University of Miskolc and carrying out her research under the supervision of Prof. Gömze.

composition and the working principle of crusher and mixture machines and equipment, but also on physical, mechanical and rheological parameters of the used materials.

The importance of rheological properties of raw materials during production of convectional bricks and ceramic roof tiles was first declared by Hallmann [16]. By his determination, most of the raw materials used in the building material industry can be described with the rheological equation of Eq. (1) as:

$$(\tau - \tau_0)^m = \eta(\dot{\epsilon})^n \text{ [Pa]} \quad (1)$$

where:

τ – the shear stress developed in the materials during processing (Pa);

τ_0 – the yield stress or static yield point of used materials (Pa);

η – the dynamic viscosity of materials during processing (Pas);

$\dot{\epsilon}$ – the shear rate developed in the material (s^{-1});

m, n – power law exponents.

Later, many authors have confirmed the above declaration of Hallmann during their investigations of rheological parameters of raw materials used for the production of different kinds of building materials. For example melted glasses, cement pastes with high water content, mortars, porcelain and china slurries for slip casting can be determined as:

$$\tau = \eta \dot{\epsilon} \text{ [Pa]} \quad (2)$$

It is obvious that Eq. (2) is generated from Eq. (1) under the following conditions:

$$m = 1, n = 1 \text{ and } \tau_0 = 0 \quad (3)$$

According to [17] the well prepared conventional brick clay during its extrusion can be characterized with the rheological equation of Eq. (4):

$$\tau - \tau_0 = \eta \dot{\epsilon} \text{ [Pa]} \quad (4)$$

The above equation is also generated from Eq. (1) at boundary conditions of:

$$m = 1 \text{ and } n = 1 \quad (5)$$

In the 1970s Russian scientists [18-21] have achieved remarkable results in the investigation of mined convectional brick clays with relative water content of $w_r \geq 15$ m%. From the beginning of the 1970s the researchers have more and more intensively investigated the physical, mechanical and rheological properties of clay minerals. For example [22] has shown that the convectional brick clays with water content of >12-15 m% have lost their mechanical strength and elastic behaviour and they have turned into plastic materials. On this basis [23] has supposed that the conventional clays with mined moisture condition (water content) are viscous-plastic materials which can be characterized with the rheological equation of Eq. (6) as:

$$\tau = \tau_0 + \eta \frac{dv}{dx} \text{ [Pa]} \quad (6)$$

where η is the dynamic viscosity and dv/dx is the deformation rate gradient i.e. the shear rate during crushing the materials on high speed smooth rollers. This conception was later confirmed experimentally (Fig. 1) by [24].

Taking into consideration the rheological properties of mined convectional brick clays as non-Newtonian materials

gave new opportunities to authors [25-31] to determine and optimize technological parameters of processing machines like crushers, extruders, etc. The basis of non-Newtonian rheological properties of ceramic raw materials and achieved results in theory of continuum mechanics gave also opportunities to develop mathematical methods for design smooth high speed rollers [32-35] and vacuum extruders for forming ceramic building materials and asbestos cement wall panels [36]. To examine the rheo-mechanical properties of elastic fibre reinforced viscous-plastic complex materials, new universal 'rotovisco' equipment was also developed [37].

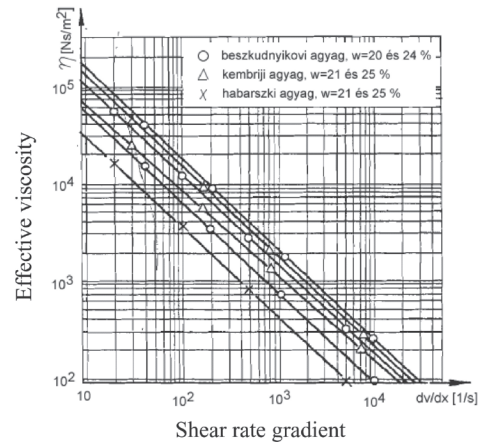


Fig. 1. The dynamic (effective) viscosity of mined clay minerals as function of shear rates (taken from [29])

1. ábra Téglaipari agyagásványok effektív viszkozitása a deformációs gradiens függvényében (átvéve: [29])

The knowledge of rheological properties and parameters of convectional brick clays is required to understand the physical and mechanical processes taking place during crushing, comminuting and forming of ceramic materials as well as to increase the efficiency of the machines used in ceramic technologies and industries [38-46]. For example [47] recommends the use of the rheological model of Eq. (7) to investigate and determine the physical and mechanical processes taking place in the materials in the working 'gaps' of pan mills:

$$\eta_g = a^n \eta_m \text{ [Pas]} \quad (7)$$

where:

η_g – the dynamic viscosity of materials in the working gap of pan mill (Pas),

η_m – the measured dynamic viscosity of materials by the laboratory equipment (Pas),

a – coefficient; of which the value for 'Malyi-clay' is: 0.5-0.6,

n – power law exponent.

The value of the power law exponent can be determined as:

$$n = \frac{\lg \frac{\dot{\epsilon}_g}{\dot{\epsilon}_m}}{\lg 2} \quad (8)$$

where:

$\dot{\epsilon}_g$ – the shear rate developed in the material during processing by industrial equipment (Pas),

$\dot{\epsilon}_m$ – the shear rate developed in the material during rheological tests by laboratory equipment (Pas).

2. Traditional methods and equipment

There are many relatively simple methods and equipment available to determine and measure certain physical and mechanical properties of materials but it is quite difficult to measure and determine the physical, mechanical and rheological properties of complex materials like ceramic raw materials and ceramic particles or fibre reinforced composites [48-52]. The reason is that the instruments which are successfully working for rheological tests of materials in chemical, plastic, pharmaceutical, dairy and food industry cannot be used for tests of ceramic raw and semi-finished green materials because of their abrasivity, hardness, strength, etc. The advantages of these traditional rheometers and instruments are their shortage in development the required shear stresses, mechanical pressures and/or temperatures or shear rates. Because of these for the rheological test of raw materials of ceramic and building materials industry are generally used so-called capillary viscometers (Fig. 2) with high value of mechanical pressure [39, 41, 53].

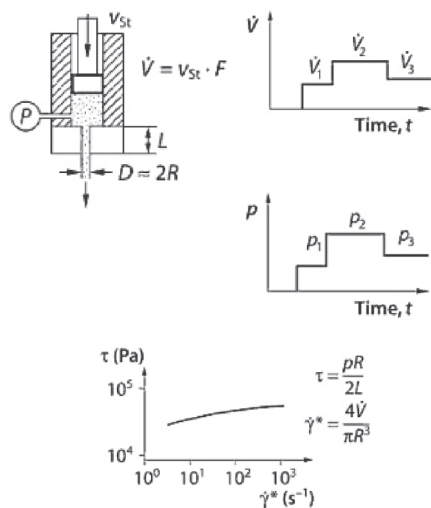


Fig. 2. The principle of capillary rheometers and the generated curves of volume flow ($V(t)$), pressure stress ($p(t)$) and shear stress

2. ábra A kapilláris reométer működési elve és az általa mért tömegáram ($V(t)$), nyomófeszültség ($p(t)$) és nyírófeszültség az idő függvényében

Using the capillary viscometer first necessary to determine the volume flow ($V(t)$) and saw pressure ($p(t)$) as function of time and further from these data can be determined the shear stress and shear rate in the materials passing through the capillary with D . So, from determined by experiment the values of shear stress as function of shear rate is:

$$\tau = f(\dot{\gamma}) \quad [\text{Pa}] \quad (9)$$

The effective viscosity of materials can be determined as:

$$\eta_e = \frac{\frac{PR}{2L}}{\frac{4\dot{V}}{\pi R^3}} = \frac{\pi PR^4}{8LV} \quad [\text{Pas}] \quad (10)$$

where:

L – the working length of capillary viscometer (m),

P – the mechanical pressure stress at the working length of capillary (Pa),

R – the radius of capillary (m),

\dot{V} – the volume speed of tested material in the capillary (m^3/s).

The advantages of the capillary viscometer are the simplicity of construction, the optional value of pressure strength due to the hydraulic movement of the stamp in the cylinder, and the working ability at wide range of moisture or plasticizer. The main disadvantage of these kinds of rheometers that the pressure stress p_{ny} at the capillary is not permanent as its value during the measurement is changing as:

$$p_{ny} = p_b \cdot e^{-4\mu \frac{H}{D_0}} \quad [\text{Pa}] \quad (11)$$

where:

μ – coefficient of external friction of tested materials at the walls of instrument,

D_0 – diameter of the saw stamp (m),

H – height of tested material in the cup of the viscometer (m),

p_b – pressure stress at the surface of the saw stamp (Pa).

During the rheological tests, the heights of the tested materials in the cup of viscometer are changing as shown in Eq. (12):

$$0 \leq H \leq H_0 \quad [\text{m}] \quad (12)$$

The heights of the tested materials at a certain moment can be determined as:

$$H = H_0 - v_0 t \quad [\text{m}] \quad (13)$$

where:

H_0 – the starting height of the tested material in the cup (m),

t – the time of measurement from the starting (s),

v_0 – the speed of the saw stamp in the cup (m/s).

3. The developed instruments and applied methods

The rheotester is reliable during the rheological investigation of ceramic raw materials, semi-finished products and ceramic particles or fibre reinforced metal matrix composites, it is relatively cheap and must satisfy the following requirements:

- the instrument must be capable to measure and determine the rheological parameters of the frequently used raw materials and/or semi-finished products in wide range of technical and technological conditions in different sectors of silicate industry,
- the instrument must be capable to develop the mechanical stresses and shear rates in the materials at the same level that happen during their passing through machines and mechanical equipment of technology lines,
- the instrument must be capable to develop temperature used to be in technological process in the silicate industry and must be controllable inside of the materials during the whole testing process,
- the instrument must be capable to measure also the compaction ratio, external friction coefficient and effective viscosity of tested materials under variation of mechanical stresses, temperature and shear rates,
- the developed new construction must be simple, easy to produce and use,
- the new instrument must be capable for quick testing of rheological parameters and the measured data must be reproducible.

So, the above requirements must also satisfy the following mathematical functional relationship for the compaction ratio:

$$\Delta H/H = f(\sigma, H_0, P, Q, T, w) \quad [m] \quad (14)$$

and for the external friction coefficient:

$$\mu = F(\sigma, n, P, Q, T, w) \quad (15)$$

as well as for effective viscosity:

$$\eta_e = \Phi(\phi, \sigma, P, Q, T, w) \quad [Pas] \quad (16)$$

where:

σ – the normal mechanical pressure acting on the working surface of the tested material (Pa),

H_0 – the filling heights of material in the instrument (m),

P – the volume of used plasticizer (%),

Q – the chemical or oxide composition of the tested material,

T – the temperature of material during the measurement (°C),

w – the moisture content of tested material (%),

n – axis rotation rate (rpm),

γ – shear rate (s⁻¹).

To satisfy the above requirements a universal ‘rotovisco’ (Fig. 3) and a combined rheo-tribometer (Fig. 4) were developed partly in Russia and at Igrex Engineering Service Ltd. in Hungary.

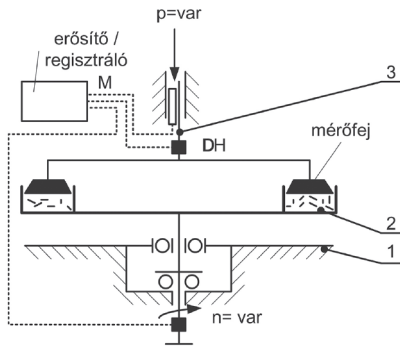


Fig. 3. Sketch of the developed universal ‘rotovisco’ laboratory instrument
1-rigid metallic frame, 2-rotatable ring-shaped measuring pot with tested materials, 3-unrotatable ring-shaped disk pressed down by a special hydraulic cylinder with variable pressure

3. ábra A kifejlesztett univerzális rotoviszko elvi vázlat
1-rigid metallic frame, 2-rotatable ring-shaped measuring pot with tested materials, 3-unrotatable ring-shaped disk pressed down by a special hydraulic cylinder with variable pressure

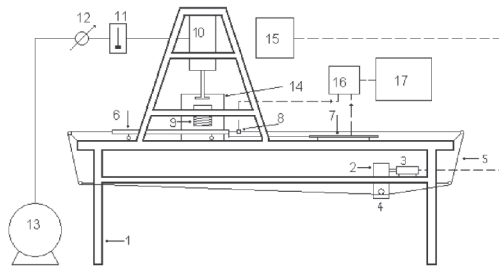


Fig. 4. Scheme of combined rheo-tribometer
1-instrument table, 2-small drive, 3-electric motor, 4-cable drum, 5-cableway, 6-batching car (with the shearing plate), 7-inductive displacement detector, 8-force-meter (spider), 9-heatable specimen holder, 10-pneumatic power cylinder, 11-magnetic valve, 12-pressure gauge, 13-compressor, 14-thermostat, 15-control unit, 16-data recorder (spider 8), 17-computer (capturing and processing data)

4. ábra A kifejlesztett kombinált reotribométer elvi vázlat
1-instrument table, 2-small drive, 3-electric motor, 4-cable drum, 5-cableway, 6-batching car (with the shearing plate), 7-inductive displacement detector, 8-force-meter (spider), 9-heatable specimen holder, 10-pneumatic power cylinder, 11-magnetic valve, 12-pressure gauge, 13-compressor, 14-thermostat, 15-control unit, 16-data recorder (spider 8), 17-computer (capturing and processing data)

The universal ‘rotovisco’ can be successfully used to the rheological tests of plasticized cement pastes and concretes reinforced with mineral fibres [51-54] as function of setting time and temperature [55]. The combined rheotribometer can be successfully used for rheological tests not only asphalt mixtures and pavements [56] but for different silicon-carbide composites [57-58] and for aluminum-titan alloys [59-60]. The complex rheological and mechanical test of complex materials like mined conventional brick clays also possible on this instrument [61]. The instrument measures the shear rates ($\dot{\gamma}$), shear stress (τ) and effective viscosity (η_e), during the rheological test and computes their values by Eqs. (17)-(18)-(19) as follows:

$$\dot{\gamma}_0 = \frac{\omega R_0}{H} \quad [s^{-1}] \quad (17)$$

$$\tau = \frac{M}{A \cdot R_0} = \frac{M}{\pi(R^2 - r^2)R_0} \quad [Pa] \quad (18)$$

$$\eta_e = \frac{H \cdot M}{\pi \omega (R^2 - r^2) R_0^2} \quad [Pas] \quad (19)$$

where:

$\dot{\gamma}_0$ – the shear rate developed in the materials in the ring-shaped pot,

η_e – the effective viscosity of the material,

ω – the angular speed of ring-shaped container (s⁻¹),

A – the magnitude of sheared surface (m²),

H – the height of the tested materials in the ring-shaped pot,

M – the value of the measured torque (Nm),

r – internal radius of ring-shaped pot (m),

R – external radius of ring-shaped pot (m),

R_0 – the radius belongs to the average volume speed of materials in the pot (m).

The working principle of the combined rheotribometer – patented in Hungary – is even simpler. The rheological parameters of tested materials also can be measured as function of chemical and mineralogical composition (Q), temperature (T), developed mechanical stress (σ), moisture content (w) and volume ratio of used plasticizer (P), etc. During the rheological tests the instrument measures and computes the values of shear rate ($\dot{\gamma}$), shear stress (τ) and the effective viscosity (η_e) as:

$$\dot{\gamma}_0 = \frac{v}{H} \quad [s^{-1}] \quad (20)$$

$$\tau = \frac{F}{A} \quad [Pa] \quad (21)$$

$$\eta_0 = \frac{\tau}{\dot{\gamma}_0} = \frac{F \cdot H}{A \cdot v} \quad [Pas] \quad (22)$$

where:

A – the magnitude of sheared surface (m²),

F – the pulling force (N),

H – the working height of the tested materials (m),

v – the speed of batching car with the shearing plate (m/s).

Converting the batching car with shear plate into Tolstói’s instrument (Fig. 5), it is possible to get the deformation-times curves (Fig. 6) of the tested materials as function of their compositions, temperatures, and loading forces.

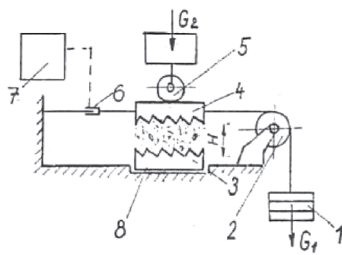
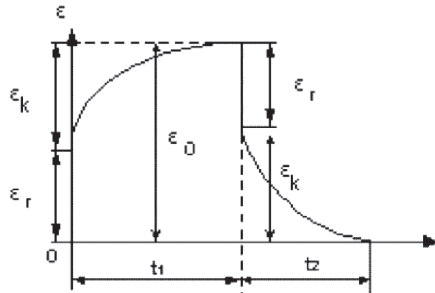
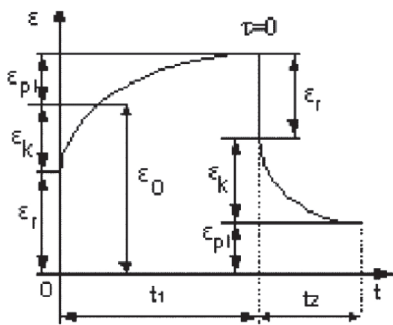


Fig. 5. Scheme of Tolstoi's instrument
1-loading force, 2-rope pulley, 3-lower tool, 4-upper tool, 5-hold-down roller, 6-displacement beacon, 7-printer, 8-material
5. ábra A Tolstoj-féle készülék elvi vázlatja
1-loading force, 2-rope pulley, 3-lower tool, 4-upper tool, 5-hold-down roller, 6-displacement beacon, 7-printer, 8-material



Below yield stress / Below yield stress



Over yield stress / Over yield stress

Fig. 6. Typical deformation of plasticized asbestos cement pastes as function of time
6. ábra A képlékeny nyers asbesztcement massza jellegzetes deformációja az idő függvényében

On the basis of the deformation-time curves created by combined rheotribo-meter it is possible to determine the instantaneous elastic modulus (E_1), the delayed elastic modulus (E_2) and viscosity of damaged (η_1) and undamaged material structures (η_2) as well as their static yield points (τ_0) for complex hetero-modulus, hetero-viscous-plastic materials like ceramic reinforced metal alloys and shield materials with extreme dynamic strength [62] in functional relationship as:

$$E_1 = f(\tau, p, Q, T, w), \quad [\text{Pa}] \quad (23)$$

$$E_2 = f(\tau, p, Q, T, w), \quad [\text{Pa}] \quad (24)$$

$$\eta_1 = f(\tau, p, Q, T, w), \quad [\text{Pas}] \quad (25)$$

$$\eta_2 = f(\tau, p, Q, T, w), \quad [\text{Pas}] \quad (26)$$

$$\tau_0 = f(\tau, p, Q, T, w), \quad [\text{Pa}] \quad (27)$$

where:

τ – the shear stress developed in the tested material by loading force F_1 (Pa),

p – the pressure stress developed in the tested material by loading force F_2 (Pa),

Q – the mineralogical, chemical and grain structure of the tested material,

T – the temperature of the tested material during the measurement ($^{\circ}\text{C}$),

w – ratio of the moisture or quantity of used plasticizer in the tested material (m%).

On the basis of the deformation-time curves it is quite easy to determine and find the rheological parameters of tested materials and create their rheological models [63]; see for example Figs. 7 and 8.

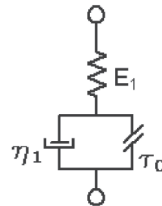


Fig.7. The typical rheological model of mined convectonal brick clays used for production of ceramic roof tiles

7. ábra A téglá és a kerámia tetőcserép gyártásához használt bányanedves agyagásvány reomechanikai anyagmodellje

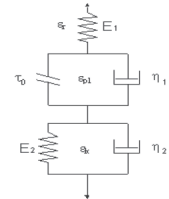


Fig. 8. The typical rheological model of asphalt pavements, asphalt concretes and elastic fibre reinforced cement pastes

8. ábra A lehült, megszilárdult útburkolati aszfaltkeverékek, valamint az ásványi szállal erősített friss beton reomechanikai anyagmodellje

4. Conclusions

The developed universal 'rotovisco' and combined rheotribo-meter fully satisfied the requirements explained in section 3. The instruments are not complicated and easy to use them to measure the most important rheological parameters of complex materials like convectonal brick clays, asphalt pavements or other raw materials and semi-finished products of the building industry. By the requirements the instruments can be armed with special heating furnace of high temperature and they can be used for rheological test for complex materials like ceramic particles and ceramic fibre reinforced metal alloys and other hetero-modulus, hetero-viscous and hetero-plastic materials for safety and protection of transport equipment and flying objects.

5. Acknowledgement

The authors would like to acknowledge to *Igrex Ltd.* for financial support and for manufacturing the combined rheotribo-meter and allowing the use it for rheological tests of different materials free of charge.

References

- [1] Mukhopadhyay, A. – Granick, S. (2008): Micro and nanorheology, 2001. *Current Opinion in Colloid & Interface Science*, Vol. 6, No. 5-6, pp. 423-429. [http://dx.doi.org/10.1016/S1359-0294\(01\)00119-4](http://dx.doi.org/10.1016/S1359-0294(01)00119-4)
- [2] Maali, A. – Buschan, B. (2008): Nanorheology and boundary slip in confined liquids using atomic force microscopy, *Journal of Physics: Condensed Matter*, Vol. 20, No. 31, p. 315201 <http://dx.doi.org/10.1088/0953-8984/20/31/315201>
- [3] Hung, J. – Yan, B. – Faghihnejad, A. – Xu, H. – Zeng, H. (2014): Understanding nanorheology and surface forces of confined thin films. *Springer, Korea-Australia Rheology Journal*, Vol. 28, pp. 3-14. <http://dx.doi.org/10.1007/s13367-014-0002-8>
- [4] Li, T. D. – Chin, H. C. – Young, D. O. – Riedo, E. (2014): Nanorheology by atomic force microscopy. *AIP Review of Scientific Instruments*, Vol. 85, p. 123707. <http://dx.doi.org/10.1063/1.4903353>

- [5] Kingery, W. D. – Bowen, H. K. – Uhlman, D. R. (1970): Introduction to Ceramics; 2nd Edition; *John Wiley&Sons Inc.*, New York
- [6] Bukanov, V. S. – Lukin, E. S. (2008): Special features of high density technical ceramic technology. Crystal growth upon sintering; *Steklo i Keramika*, No. 8, pp. 15-21.
- [7] Csányi, J. – Gömze, A. L. (2008): Impact of nitrogen atmosphere on sintering of alumina ceramics. *Építőanyag*, Vol. 60, No. 1, pp. 15-18. <http://dx.doi.org/10.14382/epitoanyag-jsbcm.2008.4>
- [8] Hampshire, S. (2009): Silicon Nitride Ceramics, *Materials Science Forum*, Vol. 606, pp. 27-42. <http://dx.doi.org/10.4028/www.scientific.net/MSF.606.27>
- [9] Gömze, A. L. – Gömze, L. N. (2009): Alumina-based hetero-modulus ceramic composites with extreme dynamic strength – phase transformation of Si_3N_4 during high speed collisions with metallic bodies; *Építőanyag*, Vol. 61, No. 2, pp. 38-42. <http://dx.doi.org/10.14382/epitoanyag-jsbcm.2009.7>
- [10] Freyburg, S. – Schwarz, A. – Finger, F. A. (2007): Effects of sintering aids on the material evolution process of structural ceramic body microstructures. *ZI-Annual 2007*; Bauverlag BV GmbH, Gütersloh, pp. 59-73.
- [11] Kocserha, I. – Gyórfy, B. – Menyhért, G. – Szúnyog, D. (2012): Adalékanyagok hatása égetett kerámia építőelemek tulajdonságaira. *microCAD proceeding CD*.
- [12] Géber, R. – Kocserha, I. – Orosz, V. – Simon, A. – Paróczai, Cs. (2010): Optimization of the mixing ratio of two different clays used for ceramic roof tiles. *Materials Science Forum*, Vol. 659, pp. 477-482. <http://dx.doi.org/10.4028/www.scientific.net/MSF.659.477>
- [13] Krause, E. – Berger, I. – Paul, T. – Schulle, W. (1982): Technologie der Keramik, Band 2, *Mechanische Prozesse*; Verlag für Bauwesen, Berlin
- [14] Geigle, A. – Hauswurtz, K. – Mager, S. (1998): A porlasztva szárított granulátumok optimalizálása kerámiaedények izostatikus sajtóláshoz. *Építőanyag*, Vol. 50, No. 2, pp. 65-70.
- [15] Kocserha, I. – Kristály, F. (2010): Effects of Extruder Head's Geometry on the Properties of Extruded Ceramic Products. *Materials Science Forum*, Vol. 659, pp. 499-504. <http://dx.doi.org/10.4028/www.scientific.net/MSF.659.499>
- [16] Gömze, A. L. (1980): Agyagásványok aprítására használt simahengerek méretezésének néhány specifikus problémája. *Építőanyag*, Vol. 32, No. 11, pp. 428-432.
- [17] Wachtman, B. J. (1996): Mechanical Properties of Ceramics. *John Wiley & Sons Inc.*; New York, Chichester, Brisbane, Toronto, Singapore
- [18] Déri, M. – Lőcsei, B. et al (1966): Szilikátkémia technológia. Egyetemi jegyzet (kézirat), Veszprém, pp. 29-31.
- [19] Zverhovskiy, Yu. E. (1974): Issledovanie reologicheskikh svoystv glinistyh elektroprovodnyh suspenzii; Reologicheskoe issledovanie. *Sbornik nauchnih trudov* pod. Red. DSc Sulman, Minsk, pp. 100-107.
- [20] Zolotarskij, A. Z. (1974) Obrabotka glinyanoi massy v val'tzah; *Stroitelni materialy*, Vol. 15, No 10, pp. 30-31.
- [21] Turenko, A. V. (1978): Issledovanie rezhimnyh parametrov raboty glinoobratyvatyushhego oborudovaniya; *Stroitelni materialy*, Vol. 19, No.1., pp. 30-32.
- [22] Turenko, A. V. – Silenok, S. G. (1978): Opredelenie optimal'nyh rezhimov glinopererabatyvatyushhego oborudovaniya na osnove svoystv plastichnyh glin; *Izdatel'stvo MISI; Stroitel'nye mashiny i oborudovanie*, pp. 156-172.
- [23] Gömze, A. L. – Turenko, A. V. – Nazarov, V. (1974): A képlékeny agyag aprításának matematikai elemzése. *Építőanyag*, Vol. 26, No. 9, pp. 348-354.
- [24] Hajnal, L. (1972): Betonadalékok agyagrögsszenyeződesének hidromechanikus aprítása, *Építőanyag*, Vol. 24, No. 2.
- [25] Baumann, V. A. – Kushantzev, B. V. – Martinov, V. D. (1981): Mehanicheskoe oborudovanie predpriyatii stroitelnyh materialov, izdelii i konstruktzii; *Mashinostroenie*, Moscow
- [26] Chirskoy, A. S. (1982): Obosnovanie i vybor ratzionalnyh parametrov valtzov dlya pererabotki plastichnyh glin; *Avtoreferat dissertatsii; Tipografiya MISI im V. V. Kuybisheva*; Moscow
- [27] Gömze A. L. (2003): Az aprítási elmélet néhány aktuális kérdése – képlékeny viszkoelasztikus anyagok aprítása görgőjáraton; *Építőanyag*, Vol. 55, No. 4, pp. 133-140 <http://dx.doi.org/10.14382/epitoanyag-jsbcm.2003.23>
- [28] Turenko, A. V. (2003): Lektzii po mehanicheskomu oborudovaniyu pererabatyvaniya glinyannyh mass. Rukopis, *Trudi Moskovskoy Inzhenerno Stroitel'noy Akademii*; Moscow
- [29] Turenko, A. V. (1977): Sovremenniy otechestvennye i zarubezhnye mashiny dlya proizvodstva stroitel'noy keramiki; *obzornaya informtziya CNIITESTroymash*, Moscow
- [30] Kocserha, I. (2012): Agyag-adalékanyag keverékek reológiai vizsgálata. *Anyagmérnöki Tudományok*, Miskolc, Vol. 37. ISSN 2063-6784, pp. 199-210.
- [31] Orosz, V. – Kocserha, I. – Géber, R. – Paróczai, Cs. (2010): Examination of tile industrial usability of high-quartz content clay. *Materials Science Forum*, Vol. 659, pp. 67-72. <http://dx.doi.org/10.4028/www.scientific.net/MSF.659.67>
- [32] Kocserha, I. – Gömze, A. L. (2000): KEMA PVP5/S kerámiaipari vákuumextruder diagnosztikai vizsgálatának néhány eredménye. *Építőanyag*, Vol. 52, No. 1, pp. 20-22.
- [33] Nagy, A. – Haussler, K. – Gömze, A. L. (2000): Reologische Untersuchungen an Calciumsilikat Suspensionen; microCAD 2000., *Proceedings of Section B: Materials Technology, Metallic and Non-metallic Materials*; Miskolc, pp. 71-76.
- [34] Papp, I. – Gömze, A. L. – Nagy, A. (2000): How does the Preparedness influence on Rheological Behaviour of Aluminium-Silicon Materials, microCAD 2000., *Proceedings of Section B: Materials Technology, Metallic and Non-metallic Materials*; Miskolc, pp. 77-82.
- [35] Papp, I. – Gömze, A. L. – Olasz-Kovács, K. – Nagy, A. (2000): Änderung der rheologischen Eigenschaften des Kaolins A1; *Keramische Zeitschrift*, Vol. 52., pp. 788-795.
- [36] Csányi J. – Gömze A. L. (2001): A technológiai paraméterek hatása az Al_2O_3 oxidkerámiák makrostruktúrájára, valamint kopásállóságára. *Építőanyag*, Vol. 53, No. 3, pp. 66-72.
- [37] Ewais, E. M. M. – Ahmed, Y. M. Z. – El-Amir, A. A. M. – El-Didamony, H. (2014): Cement kiln dust/rice husk ash as a low temperature route for wollastonite processing, *Építőanyag-Journal of Silicate Based and Composite Materials*, Vol. 66, No. 3, pp. 69-80. <http://dx.doi.org/10.14382/epitoanyag-jsbcm.2014.14>
- [38] Gömze, A. L. (1980): Kerámiaipari simahengerművek hatékonyságnövelésének matematikai alapjai I. *Építőanyag*, Vol. 32, No. 4, pp. 134-140.
- [39] Gömze, A. L. (1986): Choice of Technical Parameters for Screw Presses; *Interbrick*, Vol. 2., No. 2., pp. 30-34.
- [40] Gömze, A. L. – Eller, E. A. (1983): Univerzális rotoviszkozó szilikátipari anyagok reológiai vizsgálatához. *Szilikátechnika*, No. 1., pp. 19-22.
- [41] Ilevich, A. P. (1979): Mashini i oborudovanie dlya zavodov po proizvodstvu keramiki i ogneporov. *Vishhaya Shkola*, Moscow
- [42] Sommerfeld, A. (1978): Mechanik der deformierbaren Medien – Vorlesung über theoretische Physik. *Verlag Harri Deutsch Thun*, Frankfurt am Main
- [43] Laenger, F. (1992): Designing an extruder with allowance for the properties extrusion compounds – part 50. *Ceramic Forum International*, Vol. 69, pp. 397-401.
- [44] Benbow, J. J. – Lawson, T. A. – Oxley, E. W. (1989): Prediction of Paste Extrusion Pressure. *Ceramic Bulletin*, Vol. 68, pp. 1821-1824.
- [45] Graczyk, J. – Gleissle, W. (1992): The rheometric characterization of ceramic pastes for catalysts. *Proceedings of XIth Int. Congress on Rheology*; Brussels, pp. 601-603.
- [46] Kocserha, I. – Gömze, A. L. – Fülöp, T. (2003): Agyagásványok külső súrlódási együtthatójának alakadás-technológiai jelentősége és mérése; *A Miskolci Egyetem Közleményei, Anyag- és Kohómérnöki Tudományok II. sorozat*, 31. kötet, Miskolci Egyetemi Kiadó, Miskolc, pp. 5-14.
- [47] Gömze, A. L. (2004): Kollerjáratok energiaigénye I. Bányanedves agyagásványok aprításakor ébredő csúszatófeszültség előállításához szükséges energia- és teljesítményfelvétel meghatározása. *Építőanyag*, Vol. 56, No. 2, pp. 46-53. <http://dx.doi.org/10.14382/epitoanyag-jsbcm.2004.5>
- [48] Klein, G. (2001): Rheologische Bewertung und Beurteilung keramischer Suspensionen, Teil I.; *Keramische Zeitschrift*, Vol. 53, pp. 578-584.
- [49] Klein, G. (2001): Rheologische Bewertung und Beurteilung keramischer Suspensionen, Teil II.; *Keramische Zeitschrift*, Vol. 53, pp. 688-694.

- [50] Papp, I. – Gömze, A. L. – Olasz-Kovács, K. – Nagy, A. (2000): Änderung der rheologischen Eigenschaften des Kaolins A1. *Keramische Zeitschrift*, Vol. 52, pp. 788-795.
- [51] Gömze, A. L. (2004): Kollerjáratok energiaigénye II.; Bányanedves agyagásványokban aprításkor ébredő nyomófeszültségek előállításához szükséges energia- és teljesítményfelvétel meghatározása. *Építőanyag*, Vol. 56, No 3, pp. 93-100.
<http://dx.doi.org/10.14382/epitoanyag-jsbcm.2004.12>
- [52] Gömze, A. L. – Kovács, Á. (2005): Aszfaltkeverékek reológiai tulajdonságainak vizsgálata. *Építőanyag*, Vol. 57, No 2, pp. 34-38.
<http://dx.doi.org/10.14382/epitoanyag-jsbcm.2005.7>
- [53] Händle, Fr. (2007): Extrusion in Ceramics. *Springer-Verlag*, Berlin, Heidelberg, New York
- [54] Gömze, A. L. – Géber, R. – Tamásné, J. Cs. (2008): The effect of temperature and composition to the rheological properties of asphalt pavements. *Materials Science Forum*, Vol. 589, pp. 85-91.
<http://dx.doi.org/10.4028/www.scientific.net/MSF.589.85>
- [55] Gömze, A. L. – Gömze, L. N. (2009): Alumina-based hetero-modulus ceramic composites with extreme dynamic strength – phase transformation of Si_3N_4 during high speed collisions with metallic bodies. *Építőanyag*, Vol. 61, No. 2, pp. 38-42. <http://dx.doi.org/10.14382/epitoanyag-jsbcm.2009.7>
- [56] Gömze, A. L. – Kovács, Á. (2005): Investigation of Rheological Properties of Asphalt Mixtures, MicroCAD 2005, *Proceedings of Section Applied Mechanics*, Miskolc, pp. 55-61.
- [57] Gömze, A. L. (1986): Choice of Technical Parameters for Screw Presses. *Interbrick*, Vol. 2, No. 2, pp. 30-34.
- [58] Gömze, A. L. (1997): Szilikátipari csigaprések méretezésének néhány kérdése. *Proceedings of microCAD '97*, Section Q, Silicate Industry and powder Metallurgy; Miskolc, pp. 63-70.
- [59] Dellisanti, F. – Valdre, G. – Mondanico, M. (2009): Changes of the main physical and technological properties of talc due to mechanical strain. *Applied Clay Science*, Vol. 42, No. 3-4, p. 398-404.
<http://dx.doi.org/10.1016/j.clay.2008.04.002>
- [60] Gömze A. L. – Csirszkoj, A. Sz. – Szilenko, Sz. G. – Turenko, A. V. (1981): Agyagok reológiája és áramlási viszonyai simahengerekkel végzett aprításkor. *Építőanyag*, Vol. 33, No. 12, pp. 441-446.
- [61] Magyar, Á. – Gömze, L. A. (2009): Mechanochemical Transformation of Muscovite-2M1 Part of Clay Mineral during Fine Comminution. *Proceedings of the 11th ECERS Conference*, Krakow, pp.:937-939.
- [62] Gömze, A. L. – Gömze, L. N. (2013): Ceramic based lightweight composites with extreme dynamic strength, *IOP Conference series: Materials Science and Engineering*, Vol. 47.
<http://dx.doi.org/10.1088/1757-899X/47/1/012033>
- [63] Gömze, A. L. (1983): Csigasajtóval előállított azbesztcement-termékek préselés utáni feszültség-állapotának matematikai elemzése. *Építőanyag*, Vol. 35, No. 5, pp. 173-177.

Ref.:

Gömze, A. L. – Gömze, L. N. – Kulkov, N. S. – Shabalin, L. I. – Gotman, I. – Pedraza, F. – Lecomte, G. L. – Mayorova, T. – Kurovics, E. – Hamza, A.: *Methods and equipment for the investigation of rheological properties of complex materials like convectional brick clays and ceramic reinforced composites* *Építőanyag – Journal of Silicate Based and Composite Materials*, Vol. 67, No. 4 (2015), 143–149. p.
<http://dx.doi.org/10.14382/epitoanyag-jsbcm.2015.24>



**32nd, International Conference of the
POLYMER PROCESSING SOCIETY
July 25-29, 2016
LYON, France.**

GENERAL CONSPECTUS

The Polymer Processing Society was founded in March 1985 at the University of Akron, Akron, Ohio, USA. The intent was to provide a mechanism and format for interaction and presentation of research results in the international polymer processing community. The Polymer Processing Society (PPS) was founded with the intention to foster advancement and innovation in science, technology and engineering of polymer processing. www.tpps.org

Goals

The goals of the Polymer Processing Society (PPS) as embodied in its constitution are to foster scientific understanding and technical innovation in polymer processing by providing a discussion forum for the worldwide community of engineers and scientists in the field. The thematic range of the PPS encompasses all formulation, conversion and shaping operations applied to polymeric systems in the transformation from their monomeric forms to commercial products. The Annual PPS Meeting is held to establish a discussion forum for the worldwide community of engineers and scientists in the field.

PPS 32 in Lyon, France – July 25-29.

The 32nd International Conference of the Polymer Processing Society (PPS-32) will be held in Lyon, France. It provides cutting edge research results and latest developments in the field of polymer engineering and science. The thematic range comprises conventional processing technologies as well as materials based macromolecular research.

General Symposia and a series of Special Symposia will offer a forum for more than 600 oral and 200 poster presentations. Further highlights are the Plenary Lectures given by speakers from academia and companies focusing on topics from the academic science and global challenges for industrial polymer engineering. On top of that the 2016 Awardees of two notable prizes of the Polymer Processing Society will present their contributions. **A technical exhibition and a splendid social program will accompany the conference. Besides, there will be opportunity to join several industry plant tours to regional plastic processing companies and institutions.**

<http://pps-32.sciencesconf.org/>

Microrheology of Mucin: Tracking Particles and Helicobacter Pylori Bacteria

RAMA BANSIL • Physics Dept., Boston University ▪ rb@bu.edu

JOSEPH HARDCASTLE • Physics Dept., Boston University ▪ hardacjm@bu.edu

MAIRA CONSTANTINO • Physics Dept., Boston University ▪ maira@bu.edu

Érkezett: 2015. 08. 10. ▪ Received: 10. 08. 2015. ▪ <http://dx.doi.org/10.14382/epitoanyag-jsbcm.2015.25>

Abstract

The gastric ulcer and cancer causing bacteria, *Helicobacter Pylori* have uniquely adapted to swim across the viscoelastic mucus gel that lines the stomach epithelial surface and colonize in the harsh acidic environment of the stomach. In this paper we first briefly review results of bacteria tracking and oscillatory shear rheology studies to suggest how the bacteria get across the viscoelastic mucus gel by using a chemical mechanism to raise the pH from acidic to neutral which also triggers a gel to sol transition of mucin. We then present new microrheology studies to show that the bacterium influences the Brownian motion of spherical tracer particles in culture broth solution and in solutions of gastric mucin. The elastic and viscous moduli obtained by tracking particles in the mucin solutions are found to decrease in the presence of bacteria. We also examined the Brownian motion of the bacteria themselves and find that motile bacteria display super-diffusive anomalous Brownian motion while the immotile bacteria exhibit regular diffusive Brownian motion.

Keywords: Microrheology, particle tracking, bacteria tracking, mucin, *H. pylori*

Kulcsszavak: Mikroreológia, részecskemozgás, bacterium mozgás, mucin, *H. pylori*

1. Introduction

Mucus, the material that lines the epithelial surfaces of all organs exposed to the outside, such as the respiratory tract, gastrointestinal tract, oral, ocular, and cervical surfaces etc. provides a fascinating example of the importance of viscoelasticity to lubricate, hydrate and protect the underlying organs from contamination with undesirable materials. In this paper we focus on how the rheological properties of gastric mucus are influenced by the presence of the bacterium *Helicobacter Pylori* (*H. pylori*). Mucus is about 95% water and owes its viscoelastic, lubricant and water-retention properties to a highly negatively charged poly-electrolytic glycoprotein called mucin (about 3% in concentration, the remaining 2% being fats, lipids and other small proteins). For a review of the structure and properties of mucin and mucus see *Bansil et al.* 2013 [1] and *Bansil and Turner* 2006 [2]. Understanding the rheology of mucin is especially relevant to its protective and lubricating function, and many rheology studies have been reported on both commercially available gastric mucin [3] and purified porcine gastric mucin, PGM [4, 5] which is analogous to human mucin, MUC5AC. Previous work from our group and others has established that purified gastric mucin and mucus forms a viscoelastic gel under acidic conditions at pH below 4 [4, 5, 6, 7, 8]. Using oscillatory shear rheology *Celli et al.* [5] showed that PGM undergoes a sol-gel transition at pH 4 forming a viscoelastic gel below pH 4 with frequency dependent elastic and viscous moduli, G' and G'' respectively. *Celli et al.* [5] also showed that mucin is a shear thinning fluid with a yield stress of such a magnitude that a layer of mucus 1 mm or thicker would yield under its own weight.

The acidic pH induced gelation coupled with the finding that acid secreted by the glands in the stomach is transported via the mechanism of viscous fingering [9] as opposed to diffusion

provides a plausible explanation for why the acidic gastric juice does not digest the stomach itself. The jet-like finger of secreted acid punctures through the mucus layer and causes the mucus surrounding the finger to gel forming a viscoelastic tube that confines the acid [10]. Furthermore, mucin is a negatively charged polyelectrolyte and thus swells tremendously in the hydrated state due to electrostatic repulsion. The elasticity of the gel network opposes this stretching, and thus the gel-network exerts an electro-osmotic pressure on the positively charged H^+ preventing them from diffusing out. This interplay of a hydrodynamic instability (viscous fingering) with gelation and electrostatics is exquisitely tuned to prevent the stomach from being digested by its own secretion.

The gelation of mucus prevents large macromolecules and toxic particles such as bacteria from penetrating the mucus barrier of the stomach. However, the bacterium *H. pylori* has evolved to survive in the harsh acidic environment of the stomach and somehow manages to swim across the viscoelastic mucus gel and colonize on the epithelial surface [11]. Infection of the stomach by *H. pylori* is directly associated with gastritis and gastric ulcers, and can lead to gastric cancer [12, 13]. How the bacterium swims across the gel-like mucus is not well understood. The original hypothesis that the helical shape of the bacterium enables it to corkscrew its way through the mucus gel [11] was questioned in another study from our group [14]. *Celli et al.* [14] showed that *H. pylori* bacteria were immobile in mucin gels buffered at pH 2 or 4, but swam freely in mucin solutions at pH above 4. From bulk rheology measurements they showed that the gels at low pH infected with *H. pylori* transformed to

Rama BANSIL

Rama Bansil is a Professor of Physics and Professor of Materials Science and Engineering at Boston University. She works in the area of soft condensed matter physics and biophysics. Her current research project investigating the motility of the ulcer causing bacterium and its impact on the gelation of mucin is funded by a grant from NSF. Professor Bansil held a Junior Faculty Fellowship of the American Cancer Society and was also a Bunting Fellow at Radcliffe College, Harvard University. She is a Fellow of the American Physical Society.

Joseph HARDCASTLE

Joseph Hardcastle is a physics Ph. D student at Boston University working under the supervision of Professor Rama Bansil. His research focuses on *Helicobacter Pylori*'s swimming behavior and motility. Currently he is exploring how cell morphology influences bacterial motility and their ability to penetrate a mucus layer. In addition to his academic research Joseph is active in STEM education and outreach. Joseph earned his M. S. from Boston University and B. S. from James Madison University, USA.

Maira Constantino

Maira Constantino is a Physics graduate student at Boston University. She works in experimental biophysics under the supervision of Professor Rama Bansil. She is currently investigating the helical trajectory of *Helicobacter Pylori* and its relationship with the bacterium's body parameters. Maira earned a B.Sc. and M.Sc. in Physics at Universidade Estadual de Campinas, Brazil.

solutions with a higher pH (about 6), provided urea was present in the bacterial broth. From these observations we suggested that *H. pylori* uses the elevation of pH by urease receptor mediated hydrolysis of urea to produce ammonia and neutralize acid *both* for survival in the harsh acidic environment of the stomach as well as trigger a pH dependent gel to sol transition of the mucin gel allowing the bacteria to move across the mucus layer.

Due to the heterogeneous structure of mucin hydrogels and the fact that *H. pylori* may affect the gel in their immediate vicinity either biochemically or by a local gel-sol transition it is important to examine the length scale dependence of the elastic and viscous moduli. These local microrheological properties can be probed by tracking the Brownian motion of micron sized polystyrene latex particles in the medium of interest. From the particles trajectories the mean square displacement, $\langle \Delta r^2 \rangle$, can be calculated from which the complex elastic modulus $G(\omega)$ can be obtained using a Fourier-Laplace transform [15, 16]. Using this method, *Celli* [17] found that in a mucin solution at pH 6 the elastic or storage and viscous or loss moduli, $G'(\omega)$ and $G''(\omega)$ respectively, have similar magnitudes to those obtained in bulk rheology, as expected for particles moving in a viscous solution. However in the mucin gel at pH 2 the moduli obtained by microrheology were significantly lower than those obtained by bulk rheology; see Fig. 4 of ref. [1]. The decrease of local moduli in the gel implies that the particles in the gel moved in an inhomogeneous micro-environment consisting of water filled pores in the gel, i.e. in a less viscous environment than the bulk gel. Heterogeneities have also been observed in particle tracking experiments in mucin gels by *Lieleg et al.* [18].

The differences reported between bulk and micro-rheology of mucin gels, and the strong influence of bacteria on bulk rheology raises intriguing questions regarding the Brownian motion of particles in the presence of *H. pylori* bacteria in the medium. The first question is whether the rheological parameters determined by tracking the Brownian motion of particles is influenced by the presence of motile bacteria. Moreover, the bacteria can themselves be used as probe particles. In this case, is the Brownian motion different for the motile bacteria which exhibit active swimming as compared to dead or otherwise immobile bacteria which only exhibit passive Brownian motion? In this paper we address both these questions by tracking particles in the presence of *H. pylori* in porcine gastric mucin solutions, and by tracking the Brownian motion of active and passive bacteria in PGM.

2. Materials and Methods

2.1 Bacterial strains and culture conditions

We used the wild-type *H. pylori* strain: LSH100, a derivative of the sequenced human clinical isolate G27 [19, 20]. Bacteria were streaked and grown on horse blood plates after which they were moved to liquid media containing 90% (v/v) Brucella broth (BD Biosciences) and 10% fetal bovine serum (GIBCO) (BB10) in the absence of antimicrobials as previously described [21]. Cells were maintained at 37 °C under microaerobic conditions in a tri-gas incubator equilibrated to 10% CO₂ and 10% O₂. Plates were incubated 24-72 hours and liquid cultures were incubated for 12-16 hours under constant agitation at 200 rpm.

2.2 Preparation of purified PGM

PGM was isolated from mucosal scrapings of pig stomach epithelium and purified by Sepharose CL-2B column chromatography followed by density gradient ultracentrifugation as described in [14]. Lyophilized PGM powder was allowed to reach room temperature before opening tubes to avoid condensation. The powder was weighed and appropriate amount of PGM was dissolved in sterile H₂O to prepare a 15 mg/mL or 30 mg/mL solution. PGM solution was allowed to hydrate and equilibrate for 48 hours at 4°C before use.

2.3 Preparation of bacteria and latex particle solutions

Bacteria were grown in liquid culture broth to an O.D.₆₀₀ of 0.5 and 10 µL of culture was added to 80 µL of PGM solution. For samples including only bacteria 10 µL of pH 6 buffer (0.1 M phosphate-succinate) was added to produce a 10% bacteria mixture by volume with a final PGM concentration of 15 mg mL⁻¹ or 30 mg mL⁻¹. For samples including bacteria and fluorescent beads, 10 µL of fluorescent polystyrene latex beads (1.001 +/- 0.01 µm diameter) (Polysciences Inc.) diluted in pH 6 buffer (0.1 M phosphate-succinate) were added to produce a 10% bacteria mixture by volume with a final bead concentration of 0.05% beads by volume and final PGM concentration of 15 mg/mL or 30 mg/mL. Bacteria were incubated for 45 min in their respective PGM or PGM+bead solutions at 37 °C under microaerobic conditions prior to imaging. After the incubation period, each cell suspension was mixed by gentle pipetting and 10 µL was applied to standard glass microscope slides with secure imaging spacers (9 mm in diameter × 0.12 mm depth, Secure-Seal, Sigma-Aldrich), and secured with a coverslip.

2.4 Phase contrast and fluorescent microscopy

Samples were immediately imaged using an Olympus IX70 inverted microscope (40X Plan N, 0.65 NA Phase lens). Fluorescent beads were excited using an Olympus BH2 Mercury arc source while samples of only bacteria were imaged using phase contrast with light from a halogen bulb. Focus was set to the center and middle Z-positions of the sample in order to minimize edge effects. Videos of beads were captured using a QImagingRolera CMOS camera (10 millisecond exposure at 30 frames per sec, 0.09 µm/pixel). Videos of samples containing only bacteria without particles were taken using an Andor Zylas CMOS (1 msec exposure at 200 frames per sec). Videos were digitally recorded onto a lab workstation using micromanager software (MDS Analytical Technologies).

2.5 Particle-tracking microrheology

Videos were analyzed in MATLAB v7.12.0 using a particle-tracking routine that finds the center of intensity of each bead or bacterium using a polynomial Gaussian fit [22]. Videos and trajectories were inspected to remove any superfluous tracked objects. If drift was present trajectories were de-drifted using a custom MATLAB routine. Using the trajectories data the mean square displacement $\langle \Delta r^2 \rangle$ (MSD), storage (G'), and loss moduli (G'') were calculated using previously described microrheology routines [15, 16, 23].

3. Results and Discussion

3.1 Particle tracking in the presence and absence of bacteria

We first discuss the tracking of polystyrene latex particles in bacterial culture broth (BB10). Particle tracking data for latex beads in broth and in PGM *without added bacteria* has been reported in ref. [21]. In this work we report the results of two sets of experiments in BB10 with 1 μm particles in the presence of *H. pylori* at optical densities of 0.05, 0.25, and 0.45. Fig. 1.A shows that at the lowest concentration of bacteria, OD = 0.05, we observe Brownian diffusion with the MSD being linear in time for particles with and without bacteria present.

However the diffusion constant is slightly larger for particles diffusing in the presence of bacteria, indicating that the broth viscosity is slightly reduced in the presence of bacteria (motile and non-motile). Fig. 1.B shows that as bacterial concentration is increased to OD of 0.25 and 0.45 there is a slight decrease in MSD for long lag times. In the literature it has been observed that particles show super-diffusive behavior at small lag times ($t < 0.1$ sec) in the presence of bacteria [24]. This is followed by diffusive behavior for long lag times ($t > 1$ sec). Our experiments agree with the long lag time observations but cannot provide any information on the small lag time behavior because of the large frame rate used (30 frames per second).

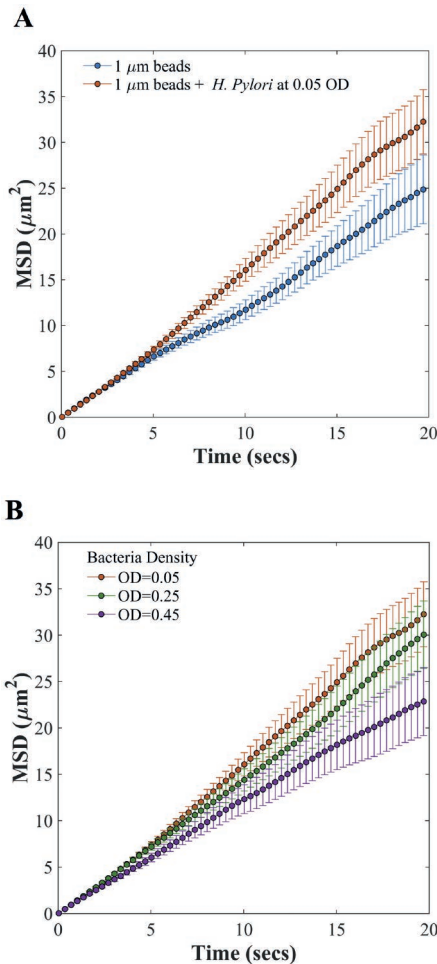


Fig. 1. Average mean square displacement of 1 μm beads in bb10 solution without *H. Pylori* and with *H. Pylori* at various concentrations

1. ábra 1 μm méretű részecskék átlagos négyzetes elmozdulása bb10 oldatban, *H. Pylori* nélkül és különböző *H. Pylori* koncentrációk mellett

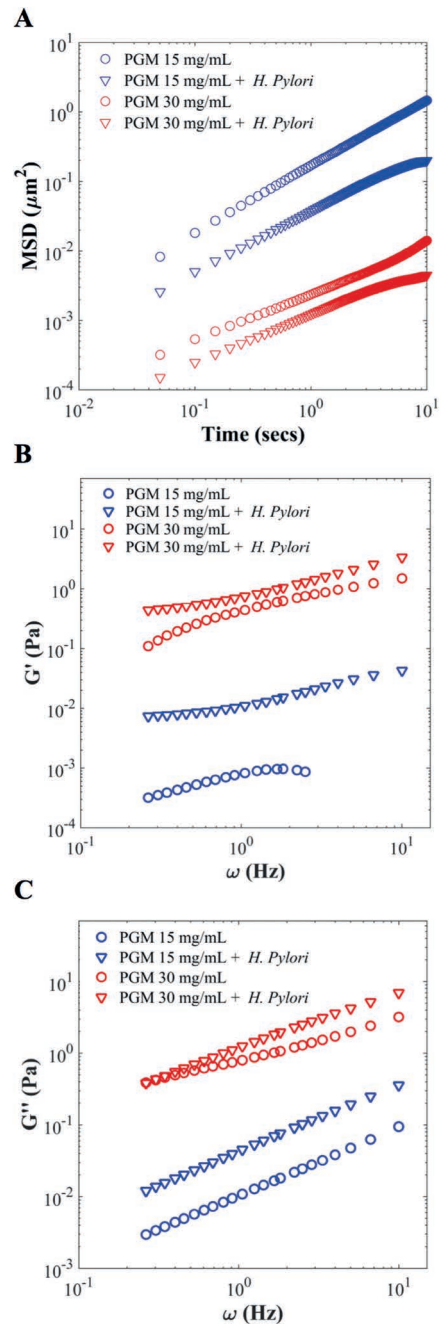


Fig. 2. Average mean squared displacement, G' , and G'' for 1 μm beads in PGM 15 mg/mL and 30 mg/mL with and without *H. Pylori* present
2. ábra 1 μm méretű részecskék átlagos négyzetes elmozdulása, G' , és G'' értéke PGM 15 mg/mL és 30 mg/mL oldatban *H. Pylori* nélkül és *H. Pylori* jelenlétében

To examine the influence of bacteria on micro-rheological properties of mucin particle tracking experiments with latex particles were done with and without the bacteria LSH100 added at an OD of 0.05 in PGM 15 mg/mL and PGM 30 mg/mL. Fig. 2.A shows log-log plots of the ensemble averaged MSD of the latex particles versus time in PGM at 15 mg/mL and 30 mg/mL both with and without *H. pylori* present. The data without bacteria are averaged from the tracks presented in ref. [21]. As expected the MSD is decreased in the more viscous PGM at 30 mg/mL. At both concentrations we observe that the MSD is decreased due to the presence of bacteria, and moreover the MSD plot shows sub-diffusive behavior at large times (MSD

$\sim t^\alpha$, $\alpha < 1$). The MSD was analyzed to get the complex modulus $G(\omega)$. Fig. 2.B shows the frequency dependence of the storage modulus $G'(\omega)$ in PGM 15 mg/mL and 30 mg/mL solutions while Fig. 2.C shows the loss modulus, $G''(\omega)$. Comparing PGM at the two concentrations without bacteria, we note that at both concentrations $G' < G''$ indicating that the mucin at pH 6 is solution at both concentrations, in agreement with the results of Celli et al. [5] and Georgiades et al. [25]. As expected both moduli are larger in the more concentrated solution. From the ratio $\tan(\delta) = G''/G'$ we note that PGM at 30 mg/mL is more viscoelastic than at 15 mg/mL; in fact the storage modulus for PGM 15 mg/mL drops to zero beyond $\omega \approx 3$ Hz, implying that beyond this frequency PGM at 15 mg/mL is a purely viscous solution. In the presence of bacteria at both concentrations the moduli G' and G'' increase, and the ratio also increases, i.e. the particles encounter greater resistance in the presence of bacteria consistent with sub-diffusive behavior. PGM at 15 mg/mL now displays a non-zero G' beyond $\omega \approx 3$ Hz, i.e. the bacteria are enhancing the viscoelastic response to higher frequencies.

3.2 Brownian motion of active versus passive bacteria

The final results we present explore the use of bacteria as tracer particles to probe microrheology. For these experiments we tracked *H. pylori* in a solution of culture broth (BB10) at a bacterial density of 0.05 OD. These experiments were done using a fast camera at 200 fps and magnification of 40 \times . Within the bacteria population some bacteria were swimming (referred to as motile) while other are non-motile. Fig. 3.A shows the MSD of each bacterium tracked and Fig. 3.B shows a histogram obtained by fitting the each MSD to a power law in time with exponent α , $MSD \sim t^\alpha$. Motile bacteria in the population exhibit super-diffusive motion with $\alpha > 1$ while non-motile bacteria exhibited simple Brownian motion $\alpha = 1$. To segment motile and non-motile populations we defined any bacteria with $\alpha > 1.2$ to be actively swimming while bacteria with $\alpha < 1.2$ were taken to exhibit only passive Brownian motion. Most of the population (83%) was found to be non-motile, i.e. exhibiting regular Brownian diffusion and can be treated as passive tracer particles.

Fig. 4 shows the mean MSD of all the non-motile, diffusive bacteria compared with that of 1 μm fluorescent latex particles in the initial time domain (from Fig. 1). While both particles and non-motile bacteria exhibit Brownian motion the diffusion constant of bacteria was found to be approximately half that of a 1 μm spherical particle. This suggest an effective hydrodynamic radius of ~ 2 μm on average, likely due to their different size and shape (bacterium is an ellipsoid with cell length ≈ 3 μm , cell width ≈ 0.5 μm).

From the values of G'' at 1 Hz we can obtain the effective viscosity of the medium. We find from the data for 1 μm latex particles in BB10 ($G' = 0$, $G'' = 0.012$ Pa) which gives an estimated viscosity of 1.2 cP at 1 Hz, close to that of water. From 1 μm particles in PGM 15 mg/mL ($G' = 0.025$ Pa, $G'' = 0.063$ Pa) we get the viscosity of PGM at 15 mg/mL as 6.3 cP, in agreement with previous estimates, and using particles in PGM at 30 mg/mL ($G' = 0.44$ Pa, $G'' = 0.80$ Pa) we get the viscosity of PGM at 30 mg/mL as 80 cP. Comparing the data for 1 μm beads in the presence and absence of motile bacteria we conclude that the effective viscosity of PGM 15 mg/mL decreases from 6.3 cP to 4.5 cP in the presence of bacteria.

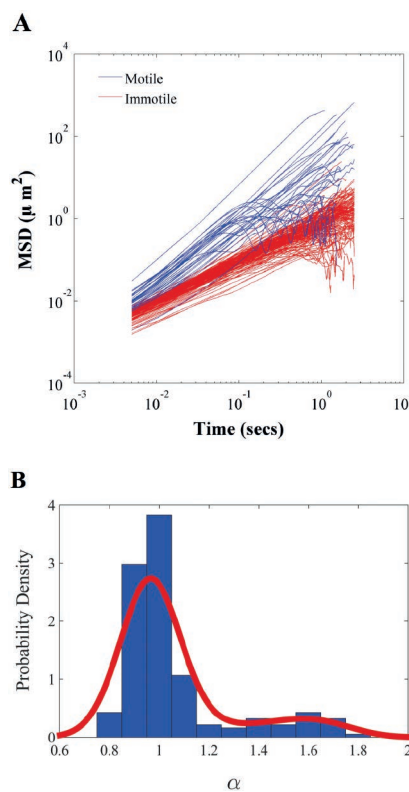


Fig. 3 Mean squared displacement and histogram of power law exponent of bacteria tracked in bb10 solution

3. ábra Átlagos négyzetes elmozdulás és hatványtörvény kitevőjének histogramja egy baktérium mozgásából bb10 oldatban

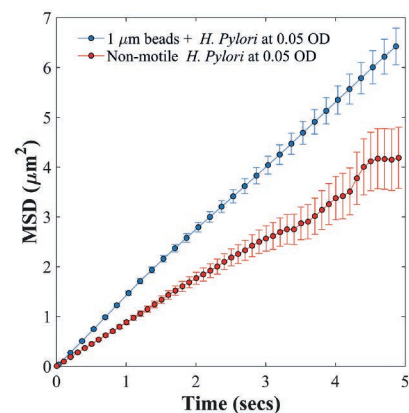


Fig. 4 Comparison of the mean squared displacement when tracking 1 μm beads vs. tracking non-motile *H. Pylori* cells

4. ábra 1 μm méretű részecskék és nem mozgékony *H. Pylori* baktériumok átlagos négyzetes elmozdulásának összehasonlítása

4. Conclusions

In summary, our studies show that the presence of the *H. pylori* bacterium alters the microrheology probed by latex tracer particles. In bacterial culture broth solution the latex particles diffuse somewhat faster in the presence of bacteria at the lowest concentration of bacteria tested (OD 0.05) while at higher concentrations the diffusion constant decreases. In PGM solutions that also contain bacteria the latex particles exhibit sub-diffusive behavior with a marked decrease in the MSD and resulting elastic and viscous moduli of mucin. The effect is more pronounced in PGM at 15 mg/mL as compared to 30 mg/mL.

Surprisingly PGM at 15 mg/mL exhibits viscoelastic response up to higher frequencies in the presence of bacteria. We also were able to examine the Brownian motion of bacteria by themselves in culture broth solution. The trajectories could be classified into two groups, those corresponding to motile active swimmers exhibiting super-diffusive motion, while those bacteria which were immotile exhibited regular diffusive Brownian motion. The non-motile population of bacteria were found to have an effective hydrodynamic radius of $\sim 2 \mu\text{m}$. In future work we seek to use this same method in PGM solutions to test whether PGM alters the Brownian motion of *H. pylori*. Comparing the MSD of immotile bacteria in PGM to that of immotile bacteria in broth solution should allow for immotile bacteria to be used to examine the viscoelastic environment a bacteria experiences.

5. Acknowledgements

This work was supported by the National Science Foundation PHY 1410798 (PI: R. Bansil). The funders have no role in study design, data collection and interpretation, or the decision to submit the work for publication. The contents are solely the responsibilities of the authors and do not necessarily represent the official views of these funding agencies. We thank Prof. Nina Salama and Ms. Laura Martinez for providing the parent bacterial strain LSH 100 for initiating cultures and for extensive discussions regarding *H. pylori* motility in PGM. We also thank Dr. Bradley Turner for very helpful discussions regarding mucin and providing purified porcine gastric mucin.

References

- [1] Bansil, R. – Celli, J. P. – Hardcastle, J. M. – Turner, B. S. (2013): The influence of mucus microstructure and rheology in *Helicobacter pylori* infection. *Frontiers in immunology*, Vol. 4, <http://dx.doi.org/10.3389/fimmu.2013.00310>
- [2] Bansil, R. – Turner, B. S. (2006): Mucin structure, aggregation, physiological functions and biomedical applications. *Current Opinion in Colloid & Interface Science*, Vol. 11, No. 2, pp. 164-170. <http://dx.doi.org/10.1016/j.cocis.2005.11.001>
- [3] Waigh, T. – Papagiannopoulos, A. – Voice, A. – Bansil, R. – Unwin, A. – Dewhurst, C. – Turner, B. – Afdhal, N. (2002): Entanglement coupling in porcine stomach mucin. *Langmuir*, Vol. 18, No. 19, pp. 7188-7195. <http://dx.doi.org/10.1021/la025515d>
- [4] Maleki, A. – Lafitte, G. – Kjøniksen, A. L. – Thuresson, K. – Nyström, B. (2008): Effect of pH on the association behavior in aqueous solutions of pig gastric mucin. *Carbohydrate Research*, Vol. 343, No. 2, pp. 328-40. <http://dx.doi.org/10.1016/j.carres.2007.10.005>
- [5] Celli, J. P. – Turner, B. S. – Afdhal, N. H. – Ewoldt, R. H. – McKinley, G. H. – Bansil, R. – Erramilli, S. (2007): Rheology of gastric mucin exhibits a pH-dependent sol-gel transition. *Biomacromolecules*, Vol. 8, No. 5, pp. 1580-1586. <http://dx.doi.org/10.1021/bm0609691>
- [6] Cao, X. – Bansil, R. – Bhaskar, K. R. – Turner, B. S. – LaMont, J. T. – Niu, N. – Afdhal, N. H. (1999): pH-dependent conformational change of gastric mucin leads to sol-gel transition. *Biophysical Journal*, Vol. 76, pp. 1250-1258. [http://dx.doi.org/10.1016/S0006-3495\(99\)77288-7](http://dx.doi.org/10.1016/S0006-3495(99)77288-7)
- [7] Hong, Z. – Chasan, B. – Bansil, R. – Turner, B. – Bhaskar, K. – Afdhal, N. (2005): Atomic force microscopy reveals aggregation of gastric mucin at low pH. *Biomacromolecules*, Vol. 6, No. 6, pp. 3458-3466. <http://dx.doi.org/10.1021/bm0505843>
- [8] Celli, J. – Gregor, B. – Turner, B. – Afdhal, N. – Bansil, R. – Erramilli, S. (2005): Viscoelastic properties and dynamics of porcine gastric mucin. *Biomacromolecules*, Vol. 6, No. 3, pp. 1329-1333. <http://dx.doi.org/10.1021/bm0493990>
- [9] Bhaskar, K. – Garik, P. – Turner, B. – Bradley, J. – Bansil, R. – Stanley, H. – LaMont, J. (1992): Viscous fingering of HCl through gastric mucin. *Nature*, Vol. 360, No. 6403, pp. 458-461. <http://dx.doi.org/10.1038/360458a0>
- [10] Bansil, R. – Celli, J. – Chasan, B. – Erramilli, S. – Hong, Z. – Afdhal, N. H. – Bhaskar, K. R. – Turner, B. S. (2005): pH-Dependent Gelation of Gastric Mucin. *MRS Proceedings*, Vol. 897, pp. 0897-J02. Cambridge University Press. <http://dx.doi.org/10.1557/PROC-0897-J02-04>
- [11] Montecucco, C. – Rappuoli, R. (2001): Living dangerously: how *Helicobacter pylori* survives in the human stomach. *Nature Reviews Molecular Cell Biology*, Vol. 2, No. 6, pp. 457-466. <http://dx.doi.org/10.1038/35073084>
- [12] Mobley, H. L. – Mendz, G. L. – Hazell, S. L. (2001): *Helicobacter pylori*: Physiology and Genetics. *ASM press*.
- [13] Marshall, B. J. (2002): *Helicobacter* pioneers: firsthand accounts from the scientists who discovered *Helicobacters*, 1892-1982. *Wiley-Blackwell*, New York.
- [14] Celli, J. P. – Turner, B. S. – Afdhal, N. H. – Keates, S. – Ghiran, I. – Kelly, C. P. – Ewoldt, R. H. – McKinley, G. H. – So, P. – Erramilli, S. – Bansil, R. (2009): *Helicobacter pylori* moves through mucus by reducing mucin viscoelasticity. *Proceedings of the National Academy of Sciences*, Vol. 106, No. 34, pp. 14321-14326. <http://dx.doi.org/10.1073/pnas.0903438106>
- [15] Mason, T. G. – Weitz, D. A. (1995): Optical measurements of frequency-dependent linear viscoelastic moduli of complex fluids. *Physical review letters*, Vol. 74, No.7, pp. 1250-1253. <http://dx.doi.org/10.1103/PhysRevLett.74.1250>
- [16] Mason, T. G. (2000): Estimating the viscoelastic moduli of complex fluids using the generalized Stokes-Einstein equation. *Rheologica Acta*, Vol. 39, No.4, pp. 371-378. <http://dx.doi.org/10.1007/s003970000094>
- [17] Celli, J. P. (2007): Gastric mucin and *Helicobacter pylori*: Rheology, Microrheology and Microscopy studies. *Ph.D Dissertation*. Boston University.
- [18] Lieleg, O. – Vladescu, I. – Ribbeck, K. (2010): Characterization of particle translocation through mucin hydrogels. *Biophysical Journal*, Vol. 98, No. 9, pp. 1782-1789. <http://dx.doi.org/10.1016/j.bpj.2010.01.012>
- [19] Baltrus, D. A. – Amieva, M. R. – Covacci, A. – Lowe, T. M. – Merrell, D. S. – Ottemann, K. M. – Stein, M. – Salama, N. R. – Guillemin, K. (2009): The complete genome sequence of *Helicobacter pylori* strain G27. *Journal of bacteriology*, Vol. 191, No. 1, pp. 447-448. <http://dx.doi.org/10.1128/JB.01416-08>
- [20] Lowenthal, A. C. – Hill, M. – Sycuro, L. K. – Mehmood, K. – Salama, N. R. – Ottemann, K. M. (2009): Functional analysis of the *Helicobacter pylori* flagellar switch proteins. *Journal of bacteriology*, Vol. 191, No. 23, pp. 7147-7156. <http://dx.doi.org/10.1128/JB.00749-09>
- [21] Martinez, L. E. – Hardcastle, J. M. – Wang, J. – Pincus, Z. – Tsang, J. – Hoover, T. R. – Bansil, R. – Salama, N. R. (2015): *Helicobacter pylori* strains vary cell shape and flagellum number to maintain robust motility in viscous environments. *Molecular Microbiology*. Submitted.
- [22] Rogers, S. S. – Waigh, T. A. – Zhao, X. – Lu, J. R. (2007): Precise particle tracking against a complicated background: polynomial fitting with Gaussian weight. *Physical Biology*, Vol. 4, No. 3, pp. 220-227. <http://dx.doi.org/10.1088/1478-3975/4/3/008>
- [23] Crocker, J. C. – Hoffman, B. D. (2007): Multiple-Particle Tracking and Two-Point Microrheology in Cells. *Methods in cell biology*, Vol. 83, pp.141-178. [http://dx.doi.org/10.1016/S0091-679X\(07\)83007-X](http://dx.doi.org/10.1016/S0091-679X(07)83007-X)
- [24] Wu, X. L. – Libchaber, A. (2000): Particle diffusion in a quasi-two-dimensional bacterial bath. *Physical Review Letters*, Vol. 84, No. 13, pp. 3017-3020. <http://dx.doi.org/10.1103/PhysRevLett.84.3017>
- [25] Georgiades, P. – Pudney, P. D. – Thornton, D. J. – Waigh, T. A. (2014): Particle tracking microrheology of purified gastrointestinal mucins. *Biopolymers*, Vol. 101, No. 4, pp. 366-377. <http://dx.doi.org/10.1002/bip.22372>

Ref:

Bansil, Rama – Hardcastle, Joseph – Constantino, Maira:
Microrheology of Mucin: Tracking Particles and Helicobacter Pylori Bacteria
 Építőanyag – Journal of Silicate Based and Composite Materials,
 Vol. 67, No. 4 (2015), 150–154. p.
<http://dx.doi.org/10.14382/epitoanyag-jsbcm.2015.25>

Rheology and porosity effect on mechanical properties of zirconia ceramics

Sergey N. KULKOV

Head of Department of Ceramics in the Institute of Strength Physics and Materials Science of the Russian Academy of Science. Author of 5 books, more than 150 articles and 18 patents. Member of The American Ceramic Society of The APMI - International and the DYM AT Society (France).

SERGEY N. KULKOV ▪ Institute of Strength Physics and Materials Science of the Siberian Branch of the Russian Academy of Sciences ▪ kulkov@ispms.tsc.ru

SVETLANA P. BUYAKOVA ▪ Institute of Strength Physics and Materials Science of the Siberian Branch of the Russian Academy of Sciences ▪ sbuyakova@ispms.tsc.ru

MARIA CHATZINIKOLAIDOU ▪ Crete University, Greece ▪ mchatzin@materials.uoc.gr

ISTVÁN KOCSERHA ▪ Miskolc University, Hungary ▪ fempityu@uni-miskolc.hu

Érkezett: 2015. 08. 12. ▪ Received: 12. 08. 2015. ▪ <http://dx.doi.org/10.14382/epitoanyag-jsbcm.2015.26>

Abstract

Porous ceramics obtained from ultra-fine powders have been studied. The porosity of ceramic samples was found between 15 to 80 %. The structure of the ceramic materials was a cellular structure. A distinctive feature of all the deformation diagrams obtained in the experiment was their nonlinearity at low deformations which was described by parabolic law. It was shown that the observed nonlinear elasticity for low deformations on deformation diagrams is due to mechanical instability of the cellular elements in the ceramic carcass.

Keywords: zirconia, porosity, sintering, activation energy, mechanical properties

Kulcsszavak: cirkónium-oxid, porozitás, szinterelés, aktiválási energia, mechanikai jellemzők

Svetlana P. BUYAKOVA

Doctor of Sciences, full Professor, chief scientist in IS PMS RAS and professor in Tomsk State University and Tomsk Polytechnic University. Author and co-author of more than 100 papers.

Maria CHATZINIKOLAIDOU

Assistant professor at the Department of Materials Science and Technology, University of Crete. Post-doctoral associate at the University Medical School of Essen (2004-2006). Post-doctoral fellow at the Institute of Molecular Biology and Biotechnology (2006-2008). Visiting assistant professor at the Department of Materials Science and Technology of the University of Crete (2007-2010).

István KOCSERHA

Associate professor and Head of the Department at the Department of Ceramic and Silicate Engineering (DCSE) in University of Miskolc (Hungary). Since 1999 he was involved into 68 research projects in the DCSE which were financed by different multinational companies or government. Author or co-author of 32 articles and 1 Hungarian patent.

1. Introduction

Porous ceramic materials have been successfully used in various fields, including thermal insulating building materials, because they are durable, corrosion resistant and they possess stable thermal features [1-3]. Porous ceramics are also promising materials for medical use as osteoplastic material or as 3D scaffold for tissue engineered bone equivalent modeling [4].

Ceramics based on partially stabilized zirconium are the most interesting among the variety of ceramic materials due to their inherent high fracture toughness because of their inherent transformational conversion. It is known that the characteristics are determined by the quality of source ceramic powder (particle shape, particle size distribution), the conditions of compacting and sintering modes and any features that are presented in each phase, and how these phases, including pores, are arranged in relation to each other. The most important factor in the successful application of materials is to understand the features of a structure emerging in them on their behavior under mechanical impact.

Plasma spray synthesis and chemical co-precipitation methods are the main efficient routes for ultra-fine powder production as it activates a sintering process [5]. The sintering process for these powders with identical chemical composition may be very different and final structure of a sintered body depends on particle size, surface energy strain conserved in the whole system etc. [6]. For example, one can obtain hollow-ball particles, which forms will stipulate a special morphology structure of materials [7].

The aim of the work is the investigation of densification, structure and mechanical properties of materials based on zirconia-based powders produced by plasma spray synthesis and sintered at different temperatures.

2. Materials and methods

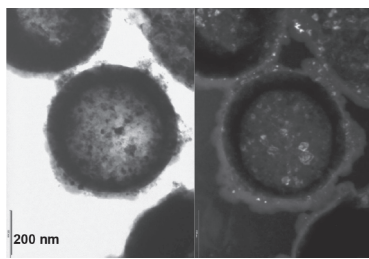
The materials for the study were ceramics obtained from powders of $ZrO_2(MgO)$, $ZrO_2(Y_2O_3)$, liquid-phase

decomposition of precursors synthesized in high-frequency discharge plasma (the plasma chemistry method). Porous ceramic $ZrO_2(MgO)$, $ZrO_2(Y_2O_3)$ powder was prepared by pressing and subsequent sintering of compacts homologous temperatures ranging from 0.63 to 0.56 during the isothermal holding duration of 1 to 5 hours. The porosity of ceramics $ZrO_2(MgO)$, $ZrO_2(Y_2O_3)$ ranged from 15 to $\approx 45\%$ and ≈ 30 to 80%, respectively. X-ray studies were carried out on a diffractometer with filtered $CuK\alpha$ radiation. The studies on the ceramic structure were carried out on the scanning electron microscope (SEM) Philips SEM 515.

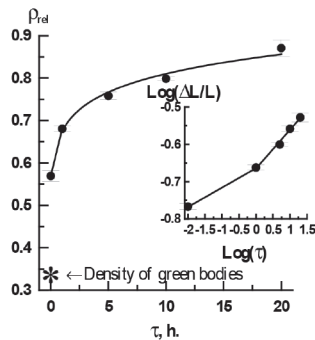
3. Results and discussion

Zirconia powder was characterized by spherical particles and their agglomerates, Fig. 1.a. An average particle size was 0.5 μm . It was measured that specific surface of chemically precipitated powder was equal to 7 m^2/g . According to the X-ray data the tetragonal phases of ZrO_2 was predominant in the amount of 95 % with an average CDD size 20 nm. An average CDD size of monoclinic phase was equal to 20 nm.

Density dependences during sintering process are represented in Fig. 1.b and one can conclude that most intensive densification occurred at heating stage. The analyzing of this dependence using equation of the form $DL/L = K \cdot t^n$, DL/L – relative shrinkage, K – kinetic coefficient; n – constant of densification rate, in log-log coordinates, were revealed that n for the samples made from plasma-sprayed powder is twice as much as for samples based on chemically precipitated powder; 0.1 and 0.04 accordingly [7].



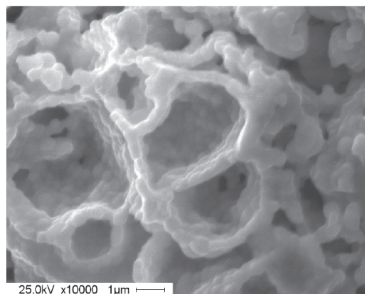
(a)



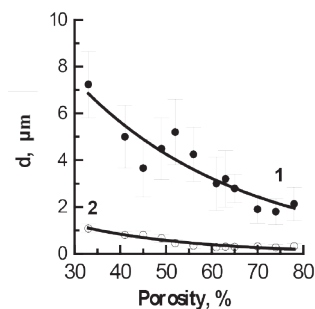
(b)

Fig. 1. ZrO_2 powder, synthesized by plasma-sprayed method: a) TEM image, bright and dark filed; b) dependences of relative density on the duration of isothermal holding for ZrO_2 powder and kinetic dependences of samples shrinkage during isothermal holding

1. ábra Plazma eljárással szintetizált ZrO_2 por jellemzői: a) TEM felvétel, világos és sötét kiemelés; b) izotermális kezelés hatása a sűrűsége és a zsugorodásra



(a)



(b)

Fig. 2. a) Fracture surface of sintered ceramic samples. Cellular structure of porous ceramics (Porosity 30 %);
 2. b) The dependence of average size of the interior of the cells (1) and of average size of grain (2) from porosity.
 2. a) ábra Szinterelt kerámia minták törési felülete. Porozus kerámiák (30% porozitás) cellás szerkezete;
 2. b) ábra Porozitás hatása a belső cellák méretére (1) és az átlagos szemcseméretre (2)

X-ray analysis had shown, that the tetragonal phase content in sintered ceramics was decreasing with increasing of the holding time up to 5 hours for materials based on plasma-sprayed powder from 95 up to 60 %, further increasing of holding time did not influence the phase composition.

The structure of the ceramic materials produced from plasma-sprayed ZrO_2 powder was represented as a system of cell and rod structure elements, Fig. 2.a. Cellular structure formed by stacking hollow powder particles can be easily seen at the images of fracture surfaces of obtained ceramics. There were three types of pores in ceramics: large cellular hollow spaces, small interparticle pores which are not filled with powder particles and the smallest pores in the shells of cells. The cells generally did not have regular shapes. The size of the interior of the cells many times exceeded the thickness of the walls which was a single-layer packing of ZrO_2 grains.

The increase of the pore space in the ceramics was accompanied by the decrease of the average size of voids inside the cells and the average grain size. Quantity and the size of pores and the grain size in the materials produced by powder technology are highly depended on thermokinetic sintering conditions, Fig. 2.b.

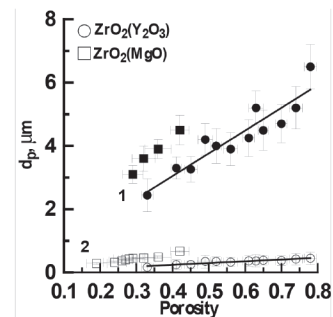


Fig. 3. The dependence of the average pore size vs. porosity of ZrO_2 ceramics: 1) - the average size of large pores spherical-like shape; 2) - the average size of interparticle pores.

3. ábra Az átlagos pórusméret függése a porozitástól: 1) nagyméretű, gömb alakú pórusok átlagos mérete; 2) szemecskézői pórusok átlagos mérete

The average pore size vs. porosity of ZrO_2 ceramics are shown in Fig. 3. As one can see the average size of interparticle pores does not depend on porosity, but sizes of cellular-like pores increases significantly - it is seen that the increase in the volume of pores in the material from ≈ 30 to 80 % which was achieved by reducing the sintering temperature of the samples and it was accompanied by an increase in the average size of large pores from 2 to 6 microns.

So, changing the porosity of the material had practically no influence on the average size of interparticles pores, the average size of which was 0.5 microns. It can be assumed that the presence of large pores close to a spherical shape in the ceramics is due to the presence of hollow spherical particles in source powders, since their average size is commensurate with an average size of presented large pores in the sintered material.

By using these data we have determined the activation energy of the crystallites growth for $ZrO_2(Y_2O_3)$ and $ZrO_2(MgO)$ ceramics, see Fig. 3. It was obtained according to re-plotting of crystallite sizes with increasing sintering temperature (Fig. 6). Activation energy for growth of crystallites of $ZrO_2(Y_2O_3)$ was 160 kJ/mol, for system $ZrO_2(MgO)$ – 75 kJ/mol (Fig. 6), these values are well agree with literature data [8], suggest that the predominant mechanism in the sintering $ZrO_2(MgO)$ is the surface diffusion and for the system $ZrO_2(Y_2O_3)$ is a bulk diffusion.

Stress-strain diagram of porous ceramics which were gained from plasma-sprayed method are presented in Fig. 5.a. The

obtained stress-strain diagrams had descending branch with a monotonic decrease of stress. It is an evidence of damage accumulation in the samples in contrast to the stress-strain diagrams of brittle materials with a homogeneous structure. Micro-damages appearing in the material had local nature and the sample under load retained the ability to resist increasing load. A distinctive feature of all the $s - \epsilon$ diagrams obtained in the experiment was their nonlinearity at low deformations which was described by parabolic law. Cyclic loading of samples on parabolic section of diagrams did not reveal residual strain. Therefore, the nonlinearity in the stress-strain diagrams was due to the elastic deformation of ceramics with cellular structure.

Replotting deformation diagrams in log-log (natural logarithm) coordinates allowed us to determine the exponent of the equation Hollomon [9]: $s = Ke^n$, where s - true stress; ϵ - true strain; n - parabolic index; K - constant for a given material, defined as a value of true stress at true strain at zero value from the experimental data. In this case, the index takes the value of the power function of the slope of the strain diagram in logarithmic scale, Fig. 3.b.

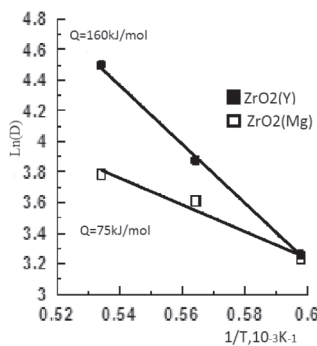


Fig. 4. The activation energy calculated from dependence of the crystallites size vs sintering temperature of porous ceramics ZrO₂

4. ábra Porózus ZrO₂ kerámiák számított aktiválási energiája a kristályméret és a szinterelési hőmérséklet alapján

The dependences of maximum stress σ_{max} and the stress corresponding to emergence of micro-damages in material σ_d from porosity were presented in Fig. 4.a. It can be seen that during decreasing the porosity in the ceramics from 80 to 30 % - the maximum stress and the stress corresponding to emergence of micro-damages in material increased from 50 to 400 MPa and from 50 to 250 MPa accordingly. With the increase in the quantity of pores in the ceramics difference between the maximum stress and the stress corresponding to emergence of micro-damages decreased. When the volume fraction of pores in the samples was more than 60 % σ_{max} and σ_d were identical. Rising and descending branches of stress-strain diagrams became gentler.

The dependence of strain corresponding to the end of the parabolic section on the rising branches of the stress-strain diagrams ϵ_1 (1) and the strain corresponding to the maximum value of stress in ceramic samples ϵ_{max} (2) from porosity were presented on Fig. 4.b. When porosity was about 30 % ϵ_{max} and ϵ_1 were identical. The increase of porosity from 30 to 80 % caused the increase of ϵ_{max} from 1.5 to 4 %. The obtained values of relative strain (up to ≈ 4 %) were significantly higher than values for nonporous ceramics.

With the increase of porosity from 30 to 50 % there was an intensive decrease of the strain corresponding to the end of the parabolic section on the rising branches of the stress-strain diagrams from 1.5 to 0.5 %. Further increase of porosity up to 80 % did not change the strain value which was 0.5 %. The character of the received dependence was probably a result of change of porosity type. When the value of porosity was from 30 to 50 % both isolated pores and interconnecting pore clusters were presented in the material.

The stress-strain diagrams for ceramics with porosity higher than 50 % has a remarkable features on initial stage of deformation, Fig. 5.a, which is denoted ϵ_1 value. This is absolutely atypical for the loading curves of sintered materials. Such dependences can be described by a power function of the type $Y=bX^n$ and n -values can be obtain by re-plotting "stress-strain" curves in "log-log" coordinates, this is shown in Fig. 5.b. As one can see the experimental values of n fit well into the two lines, i.e. there is a critical porosity value at which the deformation pattern of the porous body changes drastically - an exponent of the power function arises which is much higher than in the initial state. This is most likely associated with a change in the pore distribution pattern - from isolated pores to continuous porous structure. Experimental data are shown that no displacement of material volumes to the pore space has been found and we may thus assume that no compaction but only elastic deformation, i.e. elastic interaction of elementary volumes in the porous structure, takes place. However, the presence of so high values of $n \sim 2-4$ under deformation without residual strain is absolutely unexpected, which points to the fact that highly nonlinear mechanisms of deformation response to the applied load are implemented in specimen structures. Particularly, we may attribute to them a mechanism based on the known solution of the Hertz problem about the contact of two homogeneous bodies [10]. By extending the problem solution [10] for the case of contact between arbitrarily shaped bodies, we will have, passing on to engineering stresses: $s \sim A_c E e^{3/2}$

where A_c is the constant depending on the packing density of contacting grains and their size ratio, E is the modulus of elasticity. Thus, for grain systems having lamellar or cell structure reverse bending that disappears after unloading is possible. The deformation response of such structures after stability loss (in the subcritical state the response is described by Hooke's law) can be estimated with the application of the known Euler's elastic problem [2]. In this case, for post-critical strain one can find corresponding sizes of rods or cells and grain sizes of porous structure, in which the material is deformed without fracture but with stability loss [2]. According to these estimates, even at stability loss in rod-shaped structures with a small number of elements they may undergo noticeable macroscopic deformation in the elastic region as structural elements, which are observed experimentally.

4. Conclusions

It was shown that the structure of ZrO₂(Me_xO_y) ceramics, obtained from powders consisting of hollow spherical particles with a porosity more 30 % is represented as a cellular carcass with a bimodal porosity, formed of a large pore close to a

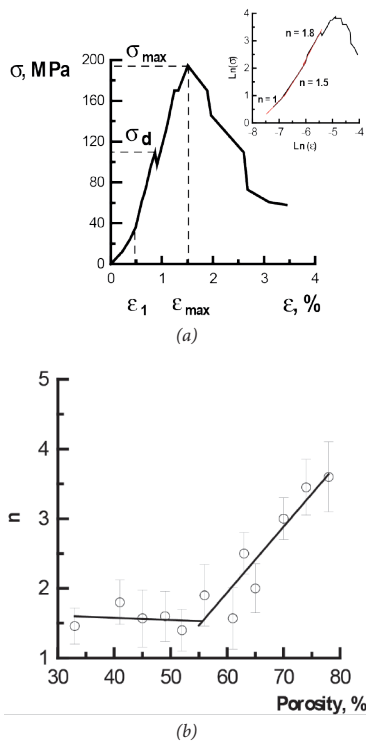


Fig. 5. a) Stress-strain diagrams of ceramics compression with porosity 50 %;
 5. b) The dependence of parabolic index from porosity.
 5. a) ábra Kerámiák nyomófeszültség-összenyomódás ábrája 50% porozitás esetén
 5. b) ábra A hatványkitevő függése a porozitástól

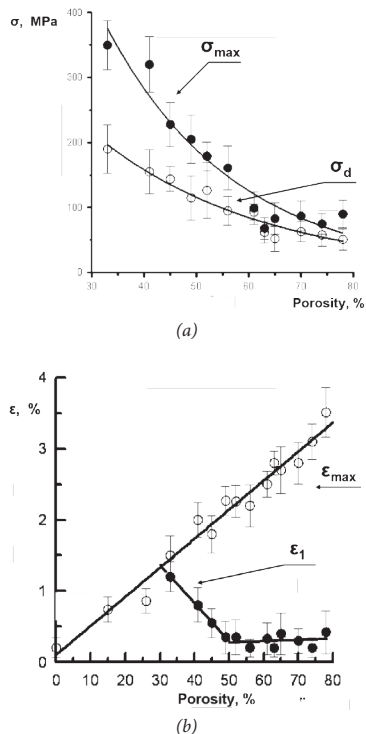


Fig. 6. a) The dependence of maximum stress σ_{max} and the stress corresponding to emergence of microdamages in material σ_d from porosity;
 6. b) The dependence of strain corresponding to the end of the parabolic section on the rising branches of the stress-strain diagrams ϵ_1 , and the strain corresponding to the maximum value of stress in ceramic samples ϵ_{max} from porosity.
 6. a) ábra A legnagyobb nyomófeszültség és a mikro-tönkremenetel megjelenéséhez tartozó feszültség függése a porozitástól
 6. b) ábra A feszültség-alakváltozás ábra felszálló, parabolikus ágának végéhez tartozó fajlagos alakváltozás és a legnagyobb feszültséghez tartozó fajlagos alakváltozás függése a porozitástól

spherical shape and the pores that were not filled with the powder particles during the compaction.

It has been shown that the most intensive densification of studied materials took place during heating stage. In the stress-strain diagrams the nonlinearity occurred due to the elastic deformation of ceramics with cellular structure. The character of the received strain-porosity dependences was probably a result of porosity type change.

It was shown that the stress-strain diagrams on the initial stage of deformation has a nonlinear behavior with high parabolic factor of strain-stress curves. It has been shown that fracture of the materials was observed from the elastic area and has rod-like and cellular-like parts in its structure.

It was found that in the range of sintering temperatures 0.56-0.63 ceramic ZrO₂(MgO) activation energy of crystallite growth of 75 kJ/mol, which corresponds to the surface diffusion, and for ceramic ZrO₂(Y₂O₃), 160 kJ/mole, which corresponds to the bulk diffusion.

5. Acknowledgments

This work has partial financial support by the Tomsk State University Competitiveness Improvement Program and Grant No 14.607.21.0069-RFMEFI60714X0069 of Ministry of Sciences and Education of RF.

References

- [1] Gömze, L. A. – Gömze, L. N. (2013): Ceramic based lightweight composites with extreme dynamic strength. *IOP Conf. Series: Materials Science and Engineering*, Vol. 47, <http://dx.doi.org/10.1088/1757-899X/47/1/012033>
- [2] Kulkov, S. – Maslovskii, V. – Buyakova, S. – Nikitin, D. S. (2002): The non-Hooke's behavior of porous zirconia subjected to high-rate compressive deformation. *Technical Physics*, The Russian Journal of Applied Physics, Vol. 47, No. 3, pp. 320-324. <http://dx.doi.org/10.1134/1.1463121>
- [3] Kalatur, E. – Kozlova, A. – Buyakova, S. – Kulkov, S. (2013): Deformation behavior of zirconia-based porous ceramics. *IOP Conf. Series: Materials Science and Engineering*, Vol. 47, <http://dx.doi.org/10.1088/1757-899X/47/1/012004>
- [4] Will, J. – Melcher, R. – Treul, C. – Travitzyk, N. – Kneser, U. – Polykandriotis, E. – Horch, R. – Greil, P. (2008): Porous ceramic bone scaffolds for vascularized bone tissue regeneration. *Journal of Materials Science Materials in Medicine*, Vol. 19, pp. 2781-2790. <http://dx.doi.org/10.1007/s10856-007-3346-5>
- [5] Fedorchenko, I. M. – Ivanova, I. I. (1974): About influence of particle size and specific surface on densification during the sintering. Theory and technology of sintering, *Naukova Dumka*, Kiev, pp. 193-199.
- [6] Gusev, A. I. – Rempel, A. I. (2001): Nanocrystalline materials. *Physmathlit*, Moscow, 224 p.
- [7] Kulkov, S. N. – Buyakova, S. P. (2007): Structure, phase composition and technologies features of zirconia-based nanosystems. *Russian nanotechnology*, Vol. 2, No 1, pp. 119 – 132. <http://dx.doi.org/10.1109/IFOST.2008.4603011>
- [8] Kofstad, P. (1972): Nonstoichiometry diffusion and electrical conductivity in binary metal oxides. *Wiley*, 379 p.
- [9] Hertzberg, R. W. (1989): Deformation and fracture mechanics of engineering materials. *John Wiley and Sons*, 576 p.
- [10] Landau, L. D. – Lifshitz, E. M. (1986): Theory of Elasticity. *Pergamon Press*, Oxford – New York, 1986.

Ref.:

Kulkov, Sergey N. – Buyakova, Svetlana P. – Chatzinikolaidou, Maria – Kocserha, István: Rheology and porosity effect on mechanical properties of zirconia ceramics
 Építőanyag – Journal of Silicate Based and Composite Materials, Vol. 67, No. 4 (2015), 155–158. p.
<http://dx.doi.org/10.14382/epitoanyag-jsbcm.2015.26>

Thermodynamic modelling of phase-chemical transformations as the method for study of rheological properties of substances

ALEXANDER SLOBODOV ▪ St. Petersburg State Institute of Technology, Physical Chemistry Department and ITMO University (St. Petersburg), Energetics Information Technology Department ▪ aslobd@gmail.com

ANDREY USPENSKIY ▪ ITMO University (St. Petersburg), Energetics Information Technology Department ▪ andreyuspensky@rambler.ru

RICARDAS RALYS ▪ ITMO University (St. Petersburg), Energetics Information Technology Department ▪ ricardas.ralys@gmail.com

DMITRIY KREMNEV ▪ St. Petersburg State Institute of Technology, Physical Chemistry Department ▪ spbscout@narod.ru

Érkezett: 2015. 08. 15. ▪ Received: 15. 08. 2015. ▪ <http://dx.doi.org/10.14382/epitoanyag-jsbcm.2015.27>

Abstract

Theoretical methods for describing, modelling and calculation of phase-chemical transformations without limitations on numbers of components and phases has been developed with the aim of predicting, evaluating and optimizing the rheological properties of substances and materials, based on extreme thermodynamic functions principle (maximum entropy, minimum free energy, etc.). These methods and databases were implemented in the software-information complex ASTICS for thermodynamic simulation and calculation of phase-chemical transformations in multi-component engineering systems of different nature. The high effectiveness of the approach is illustrated by results obtained for various natural and engineering systems and processes – mineral, rock, geochemical, silicate, glass, etc.

Keywords: rheology, thermodynamics, geochemistry, transformation, modelling, optimization, databases, multi-component system, mineral, silicate, glass

Kulcsszavak: reológia, termodinamika, geokémia, átalakulás, modellezés, optimalizálás, adatbázisok, többkomponensű rendszer, ásvány, szilikát, üveg

1. Formulation of the problem

The rheological properties of any substance and material depend not only on the composition and properties of its constituent components. These properties are determined, first of all, by the nature of chemical bonds between components, general characteristics and peculiarities of formation (composition) of the phase association, composing the substance (material) and conditions of these processes proceed. In other words, the rheology (structural-mechanical) properties of a substance are uniquely determined by its phase-chemical state, peculiarities of its formation, the nature of the interparticle phase and chemical interactions in the bulk material, etc. [1, 2].

Experimental investigation of simultaneous chemical and phase transformations is still too difficult in modern science and technology and therefore has incomplete solution. The major reason for high complexity of this problem underlies in multitude of simultaneous processes occurring in the wide range of temperatures and compositions. If one considers silicate systems, ceramics, glasses, firebreaks synthesis, it can be noticed that properties of final products are too different from those of the initial materials. These properties are resulted primarily from phase and chemical transformations, which proceed during the course of reaction.

In some cases, particularly in liquid and gaseous solutions, processes result in a complete transformation, meaning that such systems reach the equilibrium state. For such systems the justified and the most efficient way to investigate them is to use thermodynamic modelling, rather than conducting elaborate and expensive experiments to gather the information needed. In principle, thermodynamic modelling has the major advantage of being highly rigorous, and thus, more informative and detailed than direct experiments [2, 3].

It is specifically true if the investigators meet the following criteria when they take advantage of thermodynamic computations: use properties of substances involved in the reaction of interest of high reliability; and correctly interpret the results of modelling.

2. Methodology

2.1 General idea

Let us elaborate the method starting from basic ideas as general as possible. First, the system is considered consisting of m basic or Gibbs components. It is assumed that these components form n species because of all chemical reactions possible. The number of all species n is not less than the number of components m . The difference $n-m$ is the number of dependent substances in all forms available, e.g., gases

Alexander SLOBODOV

is Professor at St. Petersburg State Institute of Technology, Physical Chemistry Department and at ITMO University (St. Petersburg), Energetics Information Technology Department; Doctor of Science; Member of the New York Academy of Sciences; main fields of interest: thermodynamic physico-chemical research and modeling of multi-component natural and technological systems, mathematics methods in physical chemistry, thermodynamic databases, material science.

Andrey USPENSKIY

is a Post-graduate in Physical Chemistry at ITMO University (St. Petersburg), Energetics Information Technology Department; main fields of interest: Thermodynamic physico-chemical modeling of technological processes (polymers, silicates, glasses, etc.).

Ricardas RALYS

is a Post-graduate in Physical Chemistry at ITMO University (St. Petersburg), Energetics Information Technology Department; main fields of interest: experimental thermal analysis, thermodynamic modeling and calculation of physico-chemical processes.

Dmitriy KREMNEV

is a Post-graduate in Physical Chemistry at St. Petersburg State Institute of Technology, Physical Chemistry Department; main fields of interest: thermodynamic physico-chemical modeling of inorganic systems (silicate, ceramics, etc.).

dissolved in liquid solutions, ions, precipitated solids, etc. The total quantity of components across all species in the reacting system always remains same independent of which transformations take place. This reflects natural constraint imposed on the system and is the so-called material balance condition.

The system is in equilibrium when a function characteristic to external conditions is in its global minimum point and satisfies the material balance constraint [4]. In case of constant pressure and temperature, the total Gibbs energy of the system is minimized in the following form:

$$\left\{ \begin{array}{l} G = \sum_{i=1}^n \mu_i y_i \equiv \sum_{i=1}^n (\mu_i^0 + RT \ln \gamma_i x_i) y_i \rightarrow \min_{\{y_i\}} \\ \sum_{i=1}^n a_{ij} y_i = y_j^0, \quad j \in 1 : m \\ y_i \geq 0, \quad i \in 1 : n \end{array} \right. \quad (1)$$

where y_i^0 is the number of moles of basic components of the system; a_{ij} is the stoichiometric matrix of the system; y_i is the number of moles of all species in equilibrated system; μ_i is the chemical potential of the species i ; μ_i^0 is the standard chemical potential of the species i ; x_i is the molar fraction of the species i ; γ_i is the coefficient of activity of the species i .

Coefficients of activity depend on the model of excessive functions describing non-ideality of the system. In systems with pure substances, one should consider ideal conditions and, thus, phase transitions.

The problem described in a system given by Eq. (1) consists of three major parts:

1. Condition of minimum of the function of n variables – the total Gibbs energy;
2. Condition of basic components preservation;
3. Condition of non-negativity of the quantity of any species presented in the system.

One shall notice that the system given by Eq. (1) is not a model of equilibrium. It is a rigorous description of any real system in equilibrium. Any uncertainty associated with the solution of a problem given by Eq. (1) arises only from uncertainties of excessive function models and/or incomplete standard thermodynamic properties. The need to assess missing or unreliable data causes the need to model these data, which is only an auxiliary task, and the formulation of Eq. (1) still remains certain, however.

In this way, the level of reliability of the modelling results – the main investigation quality criterion – is defined via the level of problem description reliability, the quality of raw data, and the efficiency of the solution to the problem given by Eq. (1).

It is also worth noting, that Eq. (1) is only one from the set of possible formulations. Different objective functions can be used depending on what the external conditions are. For example, constant overall composition y^0 , volume V , and entropy S correspond to internal energy U ; constant overall composition y^0 , temperature T , and volume V correspond to

Helmholtz free energy A ; constant overall composition y^0 , temperature T , and pressure P correspond to Gibbs energy G .

One can use Lagrange function instead of characteristic function, when seeking for equilibrium solution. For example, for internal energy U the problem given by Eq. (1) transforms into the following expression:

$$\left(L \left\{ V^{(k)}, S^{(k)}, y_1^{(k)}, \dots, y_n^{(k)} \right\}, \lambda_r, \lambda_s, \{ \lambda_j \} \right) = U \left(\left\{ V^{(k)}, S^{(k)}, y_1^{(k)}, \dots, y_n^{(k)} \right\}_{k=1}^r \right) + \lambda_r \left(-V^0 + \sum_{k=1}^r V^{(k)} \right) + \lambda_s \left(-S^0 + \sum_{k=1}^r S^{(k)} \right) + \sum_{j=1}^m \lambda_j \left(-y_j^0 + \sum_{k=1}^r \sum_{i=1}^n a_{ij} y_i^{(k)} \right) \rightarrow \min \quad (2)$$

Problem in the form of Eq. (2) excludes the need to consider material balance and external constraints, only the “natural requirement” of substances quantities non-negativity remains. If only this “natural requirement” remains as the constraint, then the original problem is divided into the two separate tasks: the first one is the “core” task related to only internal state variables, which are species and phase composition. This “core” problem may be written as follows:

$$\mu_i^{(k)} = \sum_{j=1}^m a_{ij} \mu_j, \quad (i, k) \in I^0 : y_i^{(k)} > 0 \quad (3)$$

$$\mu_i^{(k)} \geq \sum_{j=1}^m a_{ij} \mu_j, \quad (i, k) \notin I^0 : y_i^{(k)} = 0 \quad (4)$$

$$\sum_{k=1}^r \left(\sum_{i=1}^n a_{ij} y_i^{(k)} \right) = y_j^0, \quad j \in 1 : m \quad (5)$$

where $\{y, \dots, y\}$, $k = 1..r$ is the composition of k -th phase, r is the number of phases, n is the number of chemical species in the system which are defined by stoichiometric matrix $\{a_{ij}\}$ and basic components with number of m .

2.2 Practical challenges

One shall notice that in the most practical cases minimization problem may be reduced to a much simpler one. In fact, most of the time, in real systems one observes either chemical transformation, or phase transition.

Problems involving only phase transitions require just to find set of phases, whilst chemical reactions are simple (or even non-existent). Such processes may be readily observed when dealing with natural geological or geophysical phenomena, or when processing materials in industry. For such systems, it is needed to find phase composition, and chemical equilibrium solution often turns to be trivial or even not requiring any actions at all.

Problems related to chemical transformations with the *a priori* known phases and their compositions do not need complicated solutions, too. For such systems it is just needed to find quantitative composition of each phase without the need to involve virtual species from non-existing phases.

The conditions given by Eqs. (1)-(3) reflect the material balance, and Lagrange function L minimum which is the generalized law of reacting masses. It is shown that specific constraints posed to the system, such as P , V , or S , are readily taken into account without loss of method generality described by Eqs. (1)-(3).

When seeking for the solution, one can divide the iterative solving into two sub-tasks: “phase” sub-task, and “chemical” sub-task. In the “phase” sub-task one can find the qualitative phase composition I^0 , i.e. which compounds actually form the phase. In the “chemical” sub-task implementation one can find the quantitative phase composition, which means in quantities the found compounds are present in the phase. Convergence criterion showing in which direction we need to move is the direction of L function descent. Sub-routines solving each sub-task and the whole problem could be formulated as well.

Despite the fact that one deals with problems either only of the first type, or only of the second type in most cases, it is evident that one may face much more complex processes in some cases, which involve both chemical transformations and phase transitions. Attempt to solve such problems takes lots of tedious calculations and high quality input data. Up to the date existing packages and software applications allow to solve only either of the problems, and, thus, it is a great and unsatisfied demand to solve simultaneous phase-chemical equilibrium problems.

3. Results and Discussion

3.1 Thermodynamic modelling procedure

During the solution of the problem either in the form of Eq. (1) or in the form of Eqs. (2)-(5), the need to find roots to non-linear equations always emerges. In fact, a closed form solution cannot be found to such equations, and, thus, iterative methods are needed to be involved.

Most of the iterative methods require in their turn to find the convergence region and to find the path with the highest convergence rate possible. In addition, specific requirements should be incorporated arising from the chemical nature of the system of interest.

Analysis of available literature [1-6] shows that both of the convergence problems are far from a good solution, despite the variety of methods being offered to date.

Before proceeding to the essence of the solution presented in this work, it must be noted that the problem is naturally divided into two interrelated parts: “qualitative” part and “quantitative” part. These parts are distinguished by the different role, which plays the equilibrium phase composition I^0 .

When dealing with “qualitative” problem, one should seek for the phase composition. This means that all possible phases are needed to be found that are in equilibrium. After this task is accomplished, one should move to the “quantitative” problem. In this stage, the calculation of quantitative composition of each phase in equilibrium is needed.

Therefore, bearing in mind these two interrelated tasks, the following strategy has been developed in seeking the simultaneous phase-chemical equilibrium solution. It starts from the initial point corresponding to the feed composition. Species with zero quantities are excluded from consideration and turn the non-equalities of Eqs. (3)-(5) into the following equations:

$$\mu_i^{(k)} = \sum_{j=1}^m a_{ij} \mu_j, \quad (i, k) \in I_t^0 \quad (6)$$

$$\sum_{(i,k) \in I_t^0} a_{ij} y_i^{(k)} = y_j^0, \quad j \in 1 : m \quad (7)$$

Then the problem given by Eqs. (6) and (7) is solved only for components with non-zero concentration (in the phases in interest). After finding that solution, it should be checked against the non-equalities given by Eqs. (3) and (4):

$$y_i^{(k)} > 0, \quad (i, k) \in I_t^0 \quad (8)$$

$$\mu_i^{(k)} \geq \sum_{j=1}^m a_{ij} \mu_j, \quad (i, k) \notin I_t^0 \quad (9)$$

If the solution meets these non-equalities, the computation is halted and the last results are stated as the result that satisfies the equilibrium condition. If the inequalities given by Eqs. (8) and (9) are not satisfied, then the “quantitative” phase composition is recalculated. When doing so, it should be considered which phases are needed to be included to the first task solution, and which phases have to be dismissed. After the new phase composition is evaluated, the calculation is continued with the second “quantitative” task until the solution converges to all inequalities given by Eqs. (8) and (9) being satisfied.

Modern state of optimization methods are of the great avail when applying them to the above-described two steps iteration procedure.

Despite high thermodynamic and mathematical rigor of the proposed methodology, we still may face pitfalls. Those pitfalls are mainly attributed to the quality of thermodynamic data available in the literature. The following requirements are need to be addressed to overcome data quality issues: the data should be complete in regard of which substances are available; thermodynamic properties accompanying the substances should allow the complete description of those; the data on properties should be of high reliability.

When considering the requirements, the necessary and sufficient properties that allow describing the system of inters must be defined in order to get accurate result.

To do so, the transformed equation of the Gibbs energy is considered as follows:

$$\begin{aligned} \bar{G}^0(P, T) = & \Delta_j G^0(P_0, T_0) - S^0(P_0, T_0)(T - T_0) + \\ & + \sum_{j=1}^k \left[T \int_{T_{j-1}}^{T_j} \frac{C_j^0(P_0, t)}{t} dt - \int_{T_{j-1}}^{T_j} C_j^0(P_0, t) dt + \left(\frac{T}{T_j} - 1 \right) \Delta H_j^0(P_0, T_j) \right] + \int_{P_0}^P V^0(p, T) dp \end{aligned} \quad (10)$$

It may be noticed that the requirements stated above are still not satisfied when taking a close look at the data on thermodynamic properties available in the literature [7-11]. This brings in another issue to solve. Testing of thermodynamic properties data against self-consistency, and finding the way to calculate correctly the missing data is needed.

Applying the strategy described above systematically, the set of high quality data for numerous substances have been created. These data are stored in the ASTIB database. Together with the package to solve phase-chemical equilibriums (ASCAT) based on the procedure that has been described earlier, this database forms the ASTICS application.

3.2 Application of the developed methods

A few real life cases are described in the followings in order to illustrate possibilities of the methodology offered in this work.

In Fig. 1 it can be seen how temperature influences the ceramics synthesis process in a silicate system – made of fourteen elements. Phase and phase-chemical transitions shown in Fig. 1 give the answers on which phases and in which quantities are formed, how their composition depends on gas composition and properties, which gaseous products are evolving during the synthesis.

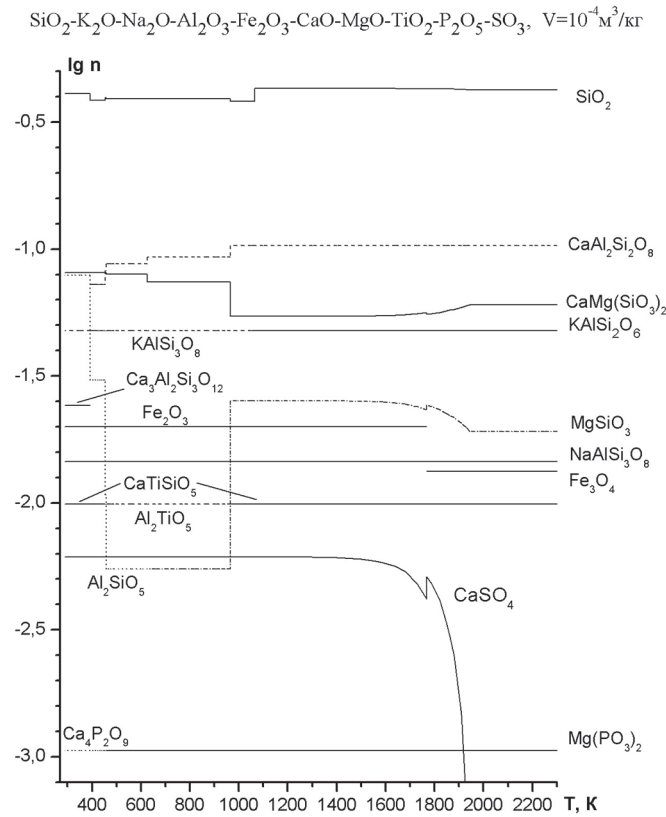


Fig. 1. Modelling and computation results in silicate system – influence of temperature on phase and chemical transformations for ceramics synthesis
1. ábra Szilikát rendszer modellezése – a hőmérséklet hatása a fázisokra és a kémiai átalakulásokra kerámia szintézis során

In Fig. 2 the result of modelling another important system is presented. The process of cleansing an atomic power station from corrosion products is shown. It can be readily seen, how the phases are transformed, which complexes are present in the aqueous solution, how pH value changes across the temperature range. This modelling gives the result on the overall solubility, which is in the excellent agreement with practically observed values.

As a result of these thermodynamic models and phase-chemical compositions, not only rheological properties of the materials can be explained but optimization of technological conditions of their synthesis (temperature regime, initial composition) is also possible.

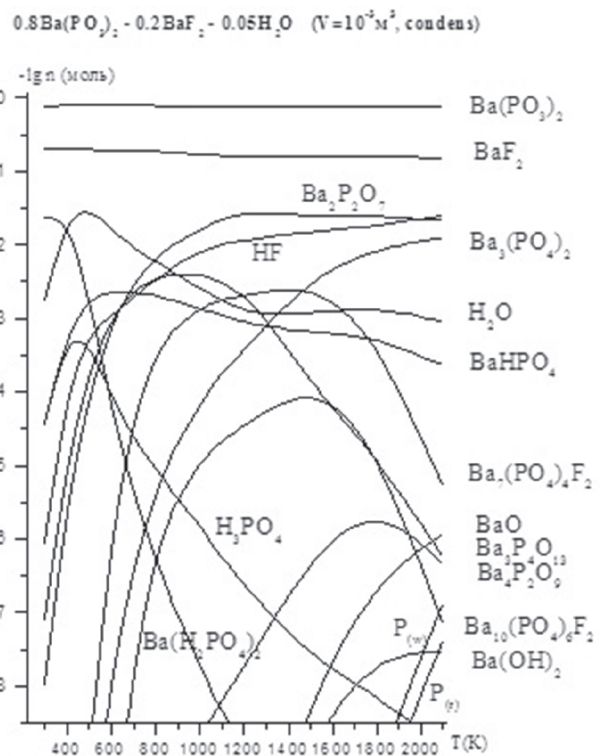


Fig. 2. Modelling and computation results for the phosphate-fluoride barium glasses synthesis – influence of temperature on physicochemical transformations
2. ábra Foszfát-fluorid-bárium üveg szintézis modellezése – a hőmérséklet hatása a fiziko-kémiai átalakulásokra

4. Conclusions

In the presented work, the general formulation on how to solve simultaneous phase-chemical equilibrium problems with use of strict and rigorous thermodynamic evaluations (without limitations on numbers of components and phases) has been shown. Based on these evaluations, a package has been developed to treat data on initial system composition in order to get equilibrium composition.

This treatment also uses database with revised, consistent, and reliable data on thermodynamic properties of numerous substances. The application including both the database and computation routines, allowed us to model and optimize the variety of systems, and to gather rich information on mechanisms of processes occurring in these systems [12-14]. Evaluated data was demonstrated to be in excellent agreement with experimentally observed data.

The data obtained by modelling and computation with the help of the developed software, showed not only good coherence with well known experimental data (which in most cases tend to be scarce and incomplete), but also provided more qualitative and quantitative information about mechanisms of processes taking place in the systems of interest, rheological properties, opportunities of natural and technological process optimization.

References

[1] Smith, W. R. (1980): Computational aspects of chemical equilibrium in complex systems. Theoretical Chemistry: Advances and Perspectives, Academic Press, pp. 185–259.

- [2] Slobodov, A. A. – Kritskii, V. G. – Zaremba, V. I. – Puchkov, L. V. (1988): Solubility products of steel corrosion in conditions simulating water chemistry reactors. *Russian Journal of Applied Chemistry*. Vol. 61, No. 10. pp. 2661-2667.
- [3] Suvorov, S. A. – Slobodov, A. A. – Bocharov, S. V. – Borzov, D. N. – Matuzenko, M. Yu. (2003): Thermodynamic simulation of the behavior of a carbonized refractory. *Refractories and Industrial Ceramics*. Vol. 44, No. 2, pp. 84-88. <http://dx.doi.org/10.1023/A:1024706909341>
- [4] Gibbs, J. W. (1928): The collected works. Thermodynamics: Vol. 1, *Longmans, Green and Co.*, 434 p.
- [5] Vasilenko, G. V. – Zaremba, V. I. – Slobodov, A. A. – Dooley, R. B. (1995): Relationship between the distribution coefficients of boiler water impurities and dissociation constants. *Thermal Engineering*. No. 7, p.64.
- [6] Ball, J. W. – Nordstrom, D. K. (1991): User's manual for WATEQ4F with revised thermodynamic data base and test cases for calculating speciation of major, trace and redox elements in natural waters. *U.S. Geological Survey*, 189 p.
- [7] Smith, R. M. – Martell, A. E. (1976): Critical stability constants. *Plenum Press*, 256 p.
- [8] Wagman, D. D. – Evans, W. H. – Parker, V. B. – Schumm, V. B. – Halow, I. – Bailey, S. M. – Churney, K. L. – Nuttall, R. L. (1982): The NBS table of chemical thermodynamic properties. Selected values for inorganic and C1 and C2 organic substances in SI units. *J. Phys. Chem. Ref. Data*. V.11, Suppl. 2. – 394 p.
- [9] Chase, M. W. (Ed.) (1998): NIST-JANAF Thermochemical Tables: Part I, II. (4th Ed.), *Journal of Physical and Chemical Reference Data*, Monograph No. 9, NSRDS-AChS-AIPh, 1151 p.
- [10] Glushko, V. P. (Ed.) (1981): Thermal Constants of Substances: Guide, Vol. 1-10. *USSR Academy of Sciences*
- [11] Mohr, P. J. – Taylor, B. N. – Newell, D. B. (2007): CODATA Recommended Values of the Fundamental Physical Constants: 2006. *NIST*, 105 p.
- [12] Kritskii, V. G. – Slobodov, A. A. (2009): Predicting Growth of Deposits on Fuel Assemblies of VVER-440 Reactors. *Thermal Engineering*, Vol. 56, No. 5, pp. 387-389. <http://dx.doi.org/10.1134/S004060150905005X>
- [13] Veiko, V. P. – Slobodov, A. A. – Odintsova, G. V. (2013): Availability of Methods of Chemical Thermodynamics and Kinetics for the Analysis of Chemical Transformations on Metal Surfaces under Pulsed Laser Action. *Laser Physics*, Vol. 23. No. 6, p. 066001. <http://dx.doi.org/10.1088/1054-660X/23/6/066001>
- [14] Slobodov, A. A. – Uspenskiy, A. B. – Kuznetsova, Z. G. – Shinkarenko, A. V. (2015): The Efficiency Problem of Thermodynamic Modeling and Calculation of Phase-Chemical Transformations in Multicomponent Systems. *13th Joint European Thermodynamics Conference, JETC-2015, Book of Abstracts*. ENSIC Nancy – May 20-22, 2015. pp. 183-184.

Ref.:

Slobodov, Alexander – Uspenskiy, Andrey – Ralys, Ricardas – Kremnev, Dmitriy: *Thermodynamic modelling of phase-chemical transformations as the method for study of rheological properties of substances*
 Építőanyag – Journal of Silicate Based and Composite Materials, Vol. 67, No. 4 (2015), 159–163. p.
<http://dx.doi.org/10.14382/epitoanyag-jsbcm.2015.27>



International Workshop on the Environmental Damage in Structural Materials Under Static Load/Cyclic Loads at Ambient Temperatures
 An ECI Conference Series
 May 29–June 3, 2016 • The Imperial Hotel, Cork, Ireland

Overview: Environmentally-assisted cracking, EAC, of engineering materials has been known for at least 50 years. The sensitivity of engineering alloys to environmental exposure is well known from an engineering perspective. What is not known with certainty at this stage is the mechanism by which the many manifestations of EAC occur. This understanding is fundamental to the development of strategies for control and predict failures of EAC is of great importance to the failure communities.

While significant progress in our understanding of EAC has been achieved in recent years, important fundamental questions like “how environment affects the crack driving force”, and “why do ordinarily ductile materials fail in a brittle manner when exposed to certain environments” remain unanswered. Our objective is to congregate a group of “skilled in the field” researchers in metallic materials for a workshop style conference that will endeavor to help clarify our current understanding of EAC and identify approaches to improve the current semi-quantitative understanding of the mechanisms.

The emphasis of the presentations will be on:

- Systematic evaluation of the governing parameters such as thresholds stress intensity factors, crack growth rates, steady state behavior, effects of yield stress, microstructure, and concentration of the aggressive environment (aqueous, gaseous, LME), and load-history on static/cyclic corrosion crack growth;
- Papers including experimental data for crack initiation and/or growth and those exploring unifying principles governing these time-static/cyclic stress dependent crack growth phenomena are particularly welcome;
- Analysis of crack tip microscopy, chemistry;
- New techniques for measuring crack initiation in aqueous environment;
- Emphasis is on understanding and quantifying rather than reporting the data of some material response;
- All topics are to be at room temperature; no high temperature work is accepted

<http://www.engconf.org/conferences/civil-and-environmental-engineering/international-workshop-on-the-environmental-damage-in-structural-materials-under-static-loadcyclic-loads-at-ambient-temperatures/>



Scope

The scope of symposium includes the fundamental understanding of EAC from the initiation stage to growth and final failure in engineering alloys.

Preliminary Technical Topics:

- Systematic variation of threshold K_{Isc} and steady state (da/dt) in aqueous and gaseous environments
- Role of internal/external hydrogen on threshold K and crack growth
- Crack tip chemistry and microscopy
- Modeling of the governing mechanisms-atomistic and continuum

Applicability of thermodynamic modelling of phase-chemical composition and rheological properties for multi-component natural and technological objects

ALEXANDER SLOBODOV ▪ St. Petersburg State Institute of Technology, Physical Chemistry Department and ITMO University (St. Petersburg), Energetics Information Technology Department ▪ aslobd@gmail.com

ALEXANDER USPENSKIY ▪ ITMO University (St. Petersburg), Energetics Information Technology Department ▪ alexander_uspensky@mail.ru

SERGEY YAVSHITS ▪ V. G. Khlopin Radium Institute (St. Petersburg), Nuclear Energy Laboratory ▪ syavshits@gmail.com

ALEXEY MISCHENKO ▪ St. Petersburg State Institute of Technology, Physical Chemistry Department ▪ spbaleksey@yandex.ru

Érkezett: 2015. 08. 15. ▪ Received: 15. 08. 2015. ▪ <http://dx.doi.org/10.14382/epitoanyag-jsbcm.2015.28>

Abstract

Thermodynamic methods and databases have been developed in this work that allow to model and calculate simultaneous phase-chemical equilibria of advanced materials with taking into account dispersion. The developed methods are unlimited with regard to number of species, components, phases, and composition of modelled system. Efficiency of the methods proposed is proved by good agreement with practically observed industrial processes along with properties of numerous synthetic and natural materials such as catalysts, silicate systems, oceanic concretes, etc.

Keywords: rheology, thermodynamics, modelling, databases, phase transformations, catalysts, silicate, radionuclides, concretes

Kulcsszavak: reológia, termodinamika, modellezés, adatbázisok, fázisátalakulások, katalizátor, szilikát, radionukleidek, betonok

1. Formulation of the problem

The problem of determining the phase-chemical composition of various substances and materials, the influence of state parameters on them (component composition, temperature, pressure, etc.) is fundamental task to identify and predict the rheological properties of substances and materials [1, 2].

This problem is particularly relevant for a wide class of rather complex composition substances (materials) obtained by various natural or technological processes (formation of rocks, mineral systems, silicate materials, glasses, etc.). In these cases external conditions (e.g. temperature, the contribution of any component, etc.) often significantly influence the direction and completeness of these processes. The determination of unknown phase-chemical composition of the substance or material (i.e. its rheological characteristics too), and optimization is very complex for both scientific and practical problems.

Thermodynamic approach (being predictive whether processes of interest are possible or not, and which are the optimal conditions to conduct them) is of use in a variety of scientific fields and industrial applications. Processes and transformations occurring in real life, e.g. in synthesis of advanced materials on industrial scale, or in natural phenomena, tend to be more complicated. In those complex processes kinetic inhibitions may occur restraining the whole process or its different stages. In such a case, factual efficiency of thermodynamic method is considerably reduced [2-4].

Kinetic limitations emerging in real phenomena may be overcome with the help of catalysts. Catalysts introduced into reactive systems withdraw the kinetic constraints, and allow reaching the maximal outcome possible. Systems with added catalysts and the retracted barriers therefore can be fully described with the efficiency and rigor characteristic to thermodynamic methods. In brief, modelling of the systems involving catalytic reactions is the most justified by thermodynamic analysis.

Large part of scientific investigations devoted to catalysis and catalytic systems covers kinetic aspects in first turn. Essentially, the kinetic efficiency of catalysts, i.e. how faster processes occur with the catalyst added to the system, is studied in the works on the subject. Practical use of catalysts, despite being helpful to achieve better yield, raises new issues that pose additional constraints, which require excessive study.

In first and foremost, catalysts are active in very definite temperature ranges at high temperature regions. This range might turn to be sub-optimal in terms of outcome of the process of interest. Therefore, the need emerges to refine the optimal reaction conditions which meet the requirements of catalytic activity. In this case, the target of modelling turns into a pure thermodynamic problem, rather than a kinetic one.

In second, catalysts are lacking selectivity. This means that these additives may involve into side interactions with reagents and products. The reason for that is thermodynamic as well.

Alexander SLOBODOV

is Professor at St. Petersburg State Institute of Technology, Physical Chemistry Department and at ITMO University (St. Petersburg), Energetics Information Technology Department; Doctor of Science; Member of the New York Academy of Sciences; main fields of interest: thermodynamic physico-chemical research and modeling of multi-component natural and technological systems, mathematics methods in physical chemistry, thermodynamic databases, material science.

Alexander USPENSKIY

is a Post-graduate in Physical Chemistry at ITMO University (St. Petersburg), Energetics Information Technology Department; main fields of interest: Thermodynamic physico-chemical calculation of technological processes (polymers, glasses, etc.).

Sergey YAVSHITS

is Head of Laboratory at V. G. Khlopin Radium Institute (St. Petersburg), Nuclear Energy Laboratory; Doctor of Science; main fields of interest: research of physical processes in nuclear reactors.

Alexey MISCHENKO

is a Post-graduate in Physical Chemistry at St. Petersburg State Institute of Technology, Physical Chemistry Department; main fields of interest: thermodynamic physico-chemical modeling of water-inorganic systems (electrolyte solutions, water chemistry in energetics, etc.).

This raises the need to account for such effects by expanding the original system “reagents-products” into a more complex system “reagents-products-catalyst”, which includes all the possible transitions and reactions. The optimal conditions should be found again in the expanded system [5-7].

In this way, adding catalysts significantly reduces kinetic barriers and gives the maximal yield, thus making modelling problem as being the most effectively solved by thermodynamic calculations. Thermodynamics applied to various computation challenges shows undeniable power in finding sought solutions.

2. Methodology

In this work, a methodology is offered to describe, model, and calculate physical and chemical processes occurring in multi-component arbitrary systems. The approach takes into account surface phenomena as well by considering dispersion surface properties (e.g. specific surface, surface energy, etc.) of system constituents. Such considerations are of great importance specifically to catalytic, especially heterogeneous systems and processes.

The suggested methodology considers systems as solutions (solid, liquid, or super cooled) consisting of all species which present in the system. This means that all possible conversions and transitions are taken into consideration that might occur during the process. Evolution of the methodology includes multiphase equilibrium between condensed, dispersed, and gaseous phases of the known composition and volume (or pressure).

The systems under study are treated not only as solutions, which correspond to temperatures of synthesis, but also as equilibrium heterogeneous mixtures made of individual substances, matching systems state at initial temperatures.

The developed methods are represented as an application written in Pascal, FORTRAN and PL/1. This application is unlimited with regard to number of species, components, phases, and composition of modelled system. An important feature of the application is its ability to correctly predict and evaluate both phase states, including metastable phases, and processes under changing conditions, e.g., feed composition, temperature, pressure, etc.

The basis of the approach is to take advantage of minimizing the characteristic function, corresponding to the imposed conditions. Conditions ubiquitously define this function: constant overall composition y^0 , volume V , and entropy S correspond to internal energy U ; constant overall composition y^0 , temperature T , and pressure P correspond to Gibbs energy G . All these characteristic functions can be turned into each other by Legendre transformation. This transformation makes all these functions, and thus, computation problems equivalent.

The computation of equilibria under different sets of constraints is easily reduced to minimization of Lagrange L , that allows excluding the constraints and considering only natural limitations, such as non-negativity of substances quantities in the resulting system. The minimization problem mainly consists of solving the system of equations and inequalities. The core of this system is independent of the minimized characteristic function and is defined only by internal parameters of state:

$$\mu_i^{(k)} = \sum_{j=1}^m a_{ij} \mu_j, \quad (i,k) \in I^0 : y_i^{(k)} > 0 \quad (1)$$

$$\mu_i^{(k)} \geq \sum_{j=1}^m a_{ij} \mu_j, \quad (i,k) \notin I^0 : y_i^{(k)} = 0 \quad (2)$$

$$\sum_{k=1}^r \sum_{i=1}^n a_{ij} y_i^{(k)} = y_j^0 \quad j = 1..m \quad (3)$$

where $\{y_1^{(k)}, \dots, y_n^{(k)}\}$, $k = 1..r$ is the composition of k -th phase, r is the number of phases, n is the number of chemical species in the system which are defined by stoichiometric matrix $\{a_{ij}\}$ and original substances with number of m .

The conditions given by Eqs. (1) to (3) reflect the material balance, and Lagrange function L minimum which is the generalized law of reacting masses. It is shown that specific constraints posed to the system, such as P , V , or S , are readily taken into account without loss of method generality described by Eqs. (1) to (3).

The iterative solving is divided into the two sub-tasks during seeking for solution: “phase” sub-task, and “chemical” sub-task. In the “phase” sub-task, the qualitative phase composition I^0 is found, which gives the compounds that actually form the phase. In the “chemical” sub-task implementation, the quantitative phase composition is found, which gives the quantities of the found compounds present in the phase. Convergence criterion shows the direction to move for the direction of L function descent. Sub-routines were developed to solve each sub-task and the whole problem as well.

The application developed in this work is lacking any limits either in regard of number of component, or in regard of substances nature. All the standard and high-temperature quantities necessary to evaluate system equilibrium are taken from expertise databases. These databases include the data extracted from reliable and mutually consistent sources. Also, insufficient data were computed with the most rigorous thermodynamic methods whenever it was possible.

3. Results and discussion

Thermodynamic modelling and optimization of the process of ammonium chloride synthesis in gaseous phase was performed with help of the application developed. It was defined how the salt dispersion, gas phase composition, partial pressures, and temperature affected the yield of the product. These evaluations allow finding the optimal synthesis conditions.

Another important issue was solved by the offered method in finding optimal conditions to produce manganese concentrate from shelf ferromanganese nodules. Upon seeking for solution, it was examined how nodules dispersion, surface properties, temperature, solution compositions, and gaseous compositions changed the yield of concentrate. This examination gave the optimal conditions to produce the concentrate depending on properties of ferromanganese nodules.

Mechanisms of phase and chemical conversions observed in carbo-thermally azotizing kaoline clay to synthesize sialons $\text{Si}_x\text{Al}_y\text{O}_z\text{N}_t$ were also successfully found. The influence of

reagents on properties and quantities of impurities, the region of thermal stability of sialons, and their chemical and thermochemical stability were evaluated. The conditions of phases recrystallization have been found as well, and it was discovered that the process occurs mainly in the gaseous phase.

Investigation of the process of composite cobalt-titanium-tantalum-tungsten carbonitride synthesis proceeds turned to be a challenging task, too. With help of the methodology, this system was studied in a large temperature range of 298-3000 K. This analysis revealed how temperature and components ratio quantitatively affected the phase transformations under the synthesis, which reactions take place in homo- and heterogeneous phases, and which intermediate and by-products are formed. The most important result of this investigation is that conditions were found that make impossible to form hazardous product – W_2C , which makes the composite fragile by forming the compound $(W,Co)_3C$.

The developed method resulted in rigorous, correct and efficient evaluation of numerous catalyst synthesis problems. In particular, it was modelled what is happening when ferromanganese catalysts are synthesized. Results obtained upon this computation allowed finding which phase transitions and reactions take place under conditions of agglomeration of hydrated metal nitrates. Also, it was successfully found which processes occur both in bulk phase of catalysts and in porous media over a wide range of temperature. Regions of stability of basic components of the catalyst were found by analyzing the influence of temperature and feed composition on simultaneous phase- and chemical transformations. Effectiveness of promoters and modifiers on synthesis yield has also been studied over a wide range of temperature.

Fig. 1 shows important data on phase transitions upon ferromanganese catalyst synthesis against temperature:

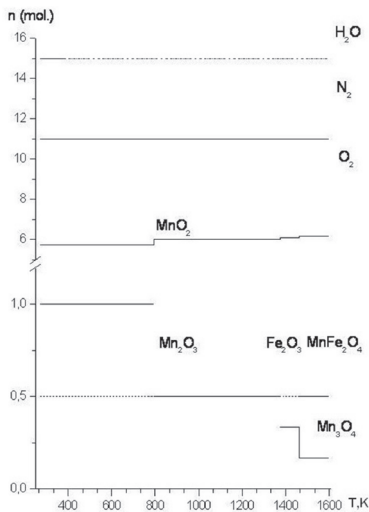
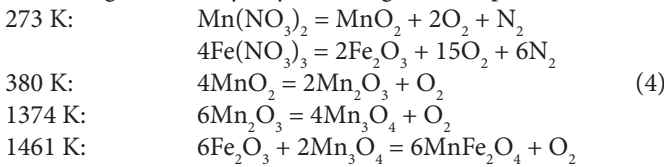


Fig. 1. Influence of temperature on phase-chemical transformations in Fe-Mn catalysis system

1. ábra A hőmérséklet hatása a fázis-kémiai átalakulásokra Fe-Mn katalízis rendszerben

Some of the data reflecting modelling results for Al-Cu-Cr-O catalyst synthesis are present in Fig. 2. These data illustrate how temperature influences the phase- and chemical transformations when synthesizing Al-Cu-Cr-O catalyst: phase transitions points and chemical transformations of the components can be seen in the mixture:

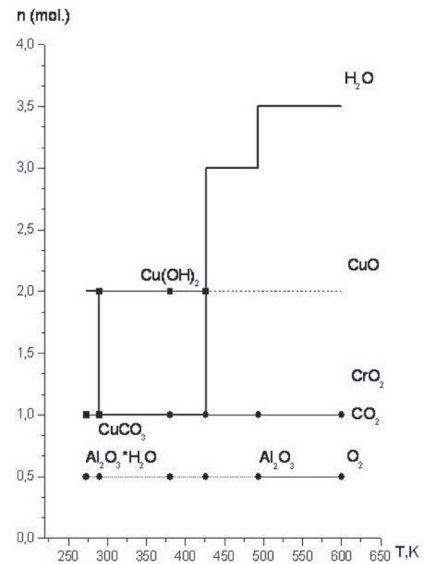
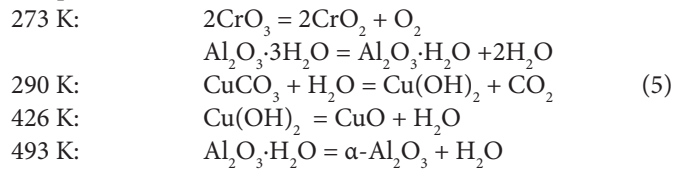


Fig. 2. Influence of temperature on phase-chemical transformations in Al-Cu-Cr-O catalysis system

2. ábra A hőmérséklet hatása a fázis-kémiai átalakulásokra Al-Cu-Cr-O katalízis rendszerben

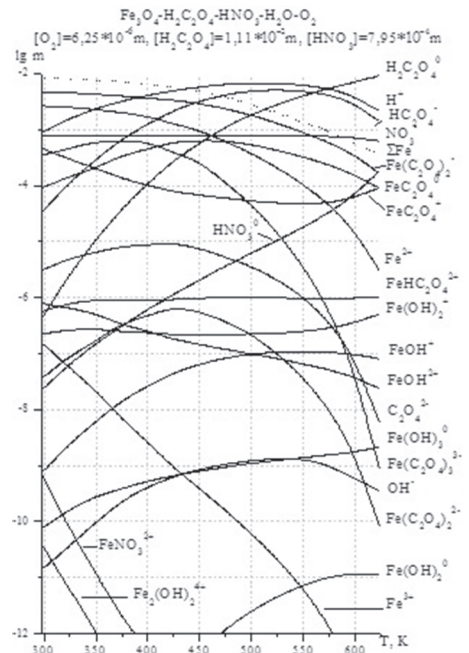


Fig. 3. Influence of temperature on water-chemical transformations – chemical washing of corrosion products sediments

3. ábra A hőmérséklet hatása víz-kémiai átalakulásokra – korróziós üledék termékek kémiai kimosódása

GUIDELINE FOR AUTHORS

The manuscript must contain the followings: **title; author's name, workplace, e-mail address; abstract, keywords; main text; acknowledgement** (optional); **references; figures, photos with notes; tables with notes; short biography** (information on the scientific works of the authors).

The full manuscript should not be more than **6 pages including figures, photos and tables**. Settings of the word document are: 3 cm margin up and down, 2,5 cm margin left and right. Paper size: A4. Letter size 10 pt, type: Times New Roman. Lines: simple, justified.

TITLE, AUTHOR

The title of the article should be short and objective.

Under the title the name of the author(s), workplace, e-mail address.

If the text originally was a presentation or poster at a conference, it should be marked.

ABSTRACT, KEYWORDS

The abstract is a short summary of the manuscript, about a half page size. The author should give keywords to the text, which are the most important elements of the article.

MAIN TEXT

Contains: materials and experimental procedure (or something similar), results and discussion (or something similar), conclusions.

REFERENCES

References are marked with numbers, e.g. [6], and a bibliography is made by the reference's order. References should be provided together with the DOI if available.

Examples:

Journals:

[6] Mohamed, K. R. – El-Rashidy, Z. M. – Salama, A. A.: In vitro properties of nano-hydroxyapatite/chitosan biocomposites. *Ceramics International*. 37(8), December 2011, pp. 3265–3271, <http://dx.doi.org/10.1016/j.ceramint.2011.05.121>

Books:

[6] Mehta, P. K. – Monteiro, P. J. M.: Concrete. Microstructure, properties, and materials. *McGraw-Hill*, 2006, 659 p.

FIGURES, TABLES

All drawings, diagrams and photos are figures. The **text should contain references to all figures and tables**. This shows the place of the figure in the text. Please send all the figures in attached files, and not as a part of the text. **All figures and tables should have a title.**

Authors are asked to submit color figures by submission. Black and white figures are suggested to be avoided, however, acceptable.

The figures should be: tiff, jpg or eps files, 300 dpi at least, photos are 600 dpi at least.

BIOGRAPHY

Max. 500 character size professional biography of the author(s).

CHECKING

The editing board checks the articles and informs the authors about suggested modifications. Since the author is responsible for the content of the article, the author is not liable to accept them.

CONTACT

Please send the manuscript in electronic format to the following e-mail address: femgomze@uni-miskolc.hu and epitoanyag@szte.org.hu or by post: Scientific Society of the Silicate Industry, Budapest, Bécsi út 122–124., H-1034, HUNGARY

We kindly ask the authors to give their e-mail address and phone number on behalf of the quick conciliation.

Copyright

Authors must sign the Copyright Transfer Agreement before the paper is published. The Copyright Transfer Agreement enables SZTE to protect the copyrighted material for the authors, but does not relinquish the author's proprietary rights. Authors are responsible for obtaining permission to reproduce any figure for which copyright exists from the copyright holder.

Építőanyag – *Journal of Silicate Based and Composite Materials* allows authors to make copies of their published papers in institutional or open access repositories (where Creative Commons Licence Attribution-NonCommercial, CC BY-NC applies) either with:

- placing a link to the PDF file at **Építőanyag** – *Journal of Silicate Based and Composite Materials* homepage or
- placing the PDF file of the final print.



Építőanyag – *Journal of Silicate Based and Composite Materials*, Quarterly peer-reviewed periodical of the Hungarian Scientific Society of the Silicate Industry, SZTE.
<http://epitoanyag.org.hu>

We are pleased to announce the organization of

ic-cmtp4

THE 4th INTERNATIONAL CONFERENCE ON COMPETITIVE MATERIALS AND TECHNOLOGY PROCESSES

to be held at Hunguest Hotel Palota Lillafüred in Miskolc, Hungary, October 3-7, 2016.

The 2nd International Conference on Competitive Materials and Technology Processes was also held in this wonderful palace hotel in the exceptionally beautiful Bükk Mountains and together with coauthors have participated on it more than 550 scientists from 36 countries of Asia, Europe, America and Africa.

The peer reviewed and accepted papers of **ic-cmtp4** conference will be published in periodicals of IOP Conference Series: Materials Science and Engineering (MSE) which are referred by Scopus, EI Compendex, Inspec, INIS, Chemical Abstracts, NASA Astrophysics Data System and many others. As organizers we hope you will submit your abstract and will attend on **ic-cmtp4** conference and we are looking forward to welcome you in **Miskolc, Hungary in October 3-7, 2016**.

The objectives

The event based more to academia than to industry and all papers will be peer reviewed before publication in **IOP Conference Series Materials Sciences and Engineering**, which is refereed by SCOPUS and many others. The international conference **ic-cmtp4** provides a platform among leading international scientists, researchers, engineers, students and PhD students for discussing recent achievements in research and development of material structures and properties of competitive materials like nanomaterials, ceramics, glasses, films and coatings, metals, alloys, biomaterials, composites, hetero-modulus and hybrid-materials, ... etc.

Among the major fields of interest are materials with extreme physical, chemical, thermal, mechanical properties and dynamic strengths; including their crystalline and nano-structures, phase-transformations as well as methods of their technological processes, tests and measurements.

Promote new methods and results of scientific researches and multidisciplinary applications of material science and technological problems encountered in sectors like ceramics, glasses, metal alloys, thin films, aerospace, automotive and marine industry, electronics, energy, security, safety and construction materials, chemistry, medicine, cosmetics, biosciences, environmental sciences are of particular interests.

Sessions

Session 1: Advanced Materials for Bio- and Medical Applications
Session 2: Advanced Materials for Extreme Applications
Session 3: Advanced Nanomaterials with Predesigned Properties
Session 4: Biomaterial Derived Ceramics and Composites
Session 5: Glasses, Coatings and Related Materials
Session 6: Hetero-Modulus, Hetero-Viscous and Hybrid Materials
Session 7: Light-Weight Metals and Alloys
Session 8: Materials with Extreme Dynamic Strength for Safety and Security

Session 9: Membranes and Catalysts
Session 10: Minerals for Environmental and Medical Applications
Session 11: Nanomaterials for Environment and Health
Session 12: Novel Synthesis and Processing Technology
Session 13: Phase Diagram as a Tool of Materials Science
Session 14: Polymer Derived Ceramics
Session 15: Processing and Properties of Silicate Ceramics
Session 16: Refractory and Fireproof Materials

The peer reviewed and accepted papers of **ic-cmtp4** conference will be published in periodicals of IOP Conference Series: Materials Science and Engineering (MSE) which are referred by Scopus, EI Compendex, Inspec, INIS, Chemical Abstracts, NASA Astrophysics Data System and many others.

The organizers hope that you will attend on **ic-cmtp4** conference and can welcome you in **Miskolc, Hungary in October 3-7, 2016**.



Further information can be obtained from Prof. Dr. László A. Gömze by e-mail femgomze@uni-miskolc.hu



EFCA – European Federation of Concrete Admixtures Associations

EFCA Aims

- To act as the official representative of the admixture industry when approaching authorities, institutions or other competent bodies in European and at International level
- To coordinate the activities of National Admixture Associations where these relate to European or International matters
- To advance and encourage the use of admixtures by means of lectures, publications and other activities including presentations at conferences
- To improve the technical and environmental profile of the industry including development of European Standards prepared under the aegis of CEN and development and sale of environmentally friendly and sustainable admixtures
- To work closely with other European organisations in the field of concrete, constituents and supply, in order to promote the use of concrete as the premier construction material of choice
- To collect and disseminate information and market surveillance on matters related to admixtures and concrete to the advantage of the EFCA Partner